University of Bath

UNIVERSITY OF
BATH

PHD

Distributed antenna system study

Tong, Fei

Award date:
2005

Awarding institution:
University of Bath

Link to publication

Distributed Antenna System Study

Fei Tong

September 26, 2005

PHD

LINIVERSITY of BATH

Submitted by

for the degree of

Doctor of Philosophy

of the University of Bath

2005

UMI Number: U196538

UMI

Dissertation Publishing

UMI U196538

ProQuest

Contents

List of Figures

List of Tables

Summary

The distributed antenna system (DAS) is a potential base station antenna structure for the future cellular networks. Having widely separated antenna units and jointly processing of signals received at all antenna units, DAS has many advantages on improving the propagation characteristics, especially in the urban area.

We evaluate the coverage of DAS in two types of environments. To characterize the propagation, in the outdoor environment, we use 2-D ray tracing technique and in the indoor environment we use wide-band measurement. The study of mean and CD of received power shows that DAS improves the radio coverage dramatically. After studying the measured channel response, we propose a co-phasing transmission diversity for downlink diversity in wide-band system. The simulation using the measured data shows that it can achieve better coverage than power-wise summation diversity scheme.

In a narrow-band network environment, the deployment of DAS has an impact on the inter-cell interference. Because of the off-centre antenna position, the DAS incurs marginally greater interference than the single central antenna assuming constant total transmitted power. When combines with the power control, the lower transmission power of DAS results in a reduced interference. When DAS is deployed in contiguous cells, DAS can improve spectral efficiency significantly.

In the uplink of CDMA system, combining reception of DAS achieve greater SIR than single antenna when adopting a new power control algorithm. 90% exceedance SIR against user numbers curves show that the uplink user capacity is increased in linearly proportional to the number of the antenna units. In the downlink, for the power-wise transmission diversity, it is proved that selective transmission is an optimal power allocation. 90% exceedance SIR against user number curves show the capacity gain. Co-phased transmission diversity can obtain greater capacity gain than selective diversity.

The study in this thesis shows that using a distributed antenna can improve the radio coverage in the urban area. This advantage can be translated into the capacity gain if used with proper power control and power allocation techniques. This system can combat the fading and at the same time improve the system capacity, which enable it to be a good candidate technique to further expand the network capacity in hot spots and even the whole service area.

Abbreviations

ARQ	Automatic-Repeat-reQuest
BTS	Base station Transmission System
CD	Cumulative Distribution
CDF	Cumulative Distribution Function
CDMA	Code Division Multiple Access
CIR	Complex Impulse Responses
CPT	Co-Phasing transmission diversity
CT	Cordless Telephony
DAS	Distributed Antenna System
EAM	Electron Absorption Modulator
EGC	Equal Gain Combining
FDD	Frequency Division Duplex
FDMA	Frequency Division Multiple Access
FDSU	Fast Data Storage Unit
FTH	Fibre-To-House
GPS	Global Positioning System
GSM	Global System for Mobile communications
HiFi	High Fidelity
IC	Interference Cancelation
i.i.d	independently and identically distributed
ISI	Inter-Symbol Interference
LMDS	Local Multi-point Distribution System
LOS	Line-Of-Sight
MAI	Multiple Access Interference
MA	Multiple Access
MIMO	Multiple Input and Multiple Output
MMF	Multi-Mode Fibre
MPA	MultiPath Antenna diversity
MPEG	Moving Picture Experts Group
MRC	Maximal Ratio Combining
MSC	Mobile Switching Centre
MUD	Multiple User Detection

NLOS	Non-LOS
OF	Orthogonal Factor
PDC	Personal Digital Cellular
PN	Pseudo-Noise
QoS	Quality-of-Service
ROF	Radio Over Fibre
SIMO	Single Input Multiple Output
SIR	Signal-to-Interference Ratio
SNR	Signal-to-Noise Ratio
TDD	Time Division Duplex
TDMA	Time Division Multiple Access
TETRA	TErrestrial Trunked RAdio
WCDMA	Wideband Code Division Multiple Access
WDM	Wavelength Division Multiplexing
Wi-Fi	Wireless-Fidelity
WI	Walfisch-Ikegami
W-LAN	Wireless Local Access Network
WLL	Wireless Local Loop

Acknowledgements

Chapter 1

CHALLENGES OF CELLULAR NETWORK DESIGN

Since the introduction of wireless technology, there have been designed many wireless systems for a variety of applications. For fixed wireless access application, there are Wireless Local Loop (WLL) and Local Multi-point Distribution System (LMDS). For local nomadic wireless access, there is Wireless Local Access Network (W-LAN) including different standards, such as Wi-Fi, Wi-MAX and HiperLan. Also there are cellular network for telecommunication application and TErrestrial Trunked RAdio (TETRA) for professional mobile radio users.

Among these systems, cellular network has received wide acceptance and achieved unprecedent growth, which requires a rapid expansion of the network not only of the services offered, but also in quality and capacity. But some inherent characteristics of the cellular network, for example performance degradation due to the self-interference caused by frequency reuse, limit its own ability to satisfy the demands of the market. This contradiction drives research activity to seek new techniques and new architectures to satisfy demand, resulting in evolution of the cellular network. In this thesis, we are going to study a distributed antenna base station structure, which can be used to tackle some restrictions on the expansion of cellular network. Indeed, in addition to cellular network, distributed antenna can benefit W-LAN as well. But considering the network scale and the benefit from deploying distributed antenna, the cellular network is the best target application.

First in this chapter, we first restrict the target systems to the terrestrial cellular network by highlighting the system features which distinguish it from other wireless systems. We also discuss the requirements of the trend for increasing demand. Then

we review this self-limiting issue and present the challenges inherent in the design of the future generation cellular network. We then propose a solution, or at least a method of finding a solution, to these challenges using clues from the past evolution of cellular network. This solution direction also defines the project presented in this thesis.

1.1 Terrestrial cellular networks

1.1.1 System features

There are, coexisting, various wireless communication systems, each of which is designed and optimized for a specific application. Because these applications may have a wide range of special requirements on data rate, mobility and geographic coverage, using one type of system to accommodate all of them is neither effective nor feasible.

The cellular mobile network is the most sophisticated wireless system, which provides for the largest subscriber population and the widest service area. It is in the extreme of the spectrum of wireless communication.

First, it provides wide and continuous service coverage. Different from other systems which provide fixed access, such as WLL and LMDS, or are restricted to small non-contiguous areas, such as W-LAN, this system provides coverage over an extended geographical area. Normally, the coverage area is continuous from city to city, and even from country to country.

Secondly, it provides full mobility, while the W-LAN can only provide mobility (strictly nomadicity) within a small service area. The ultimate goal is to provide subscribers fully mobile communication at all times no matter where they are. The range can be over the whole service area, while the velocity range can be from zero to that of high speed vehicles (including train around 300Km/h).

Although there are other solutions to this wide area wireless network such as satellite personal communication systems, operators use these as a supplemental means for coverage e.g. for remote and difficult to reach area. Our discussion here is restricted to the terrestrial cellular system.

1.1.2 The mobile radio channel

Although using of radio waves to carry the signal enables the communication parties to be free of the restriction of cables the mobile radio channel makes the signal vulnerable to many types of distortion, attenuation and interference.

First, in contrast to wired communication, in which the cable has a uniform electrical character and no significant scatterers (not considering the flaws in the medium), the terrestrial propagation environment consists of many natural and man-made objects with a wide range of size from centimetres to many tens of metres. The radio wave transmitted through this environment will interact with the surrounding objects in various ways, such as reflection, diffraction and refraction. All of these interactions tend to diffuse the radio energy which reduces the E-field magnitude along the intended propagation path and increases the E-field magnitude in other directions. The fields originally scattered in various directions may eventually arrive at the same location and add together.

One of the consequences can be a very large propagation loss between the transmitter and receiver. Also as the field strength is determined by the composite signal, this makes the local fields strength at a position not only determined by the propagation distance but also the surrounding environment. Because of the irregularity of the environment, the local field strength may differ greatly from position to position even though they have the same Transmitter-Receiver distance.

Superposition of waves will set up a standing wave like pattern in the environment so that in some positions the superposition is constructive and in others it is destructive. When the mobile station moves in the environment, it will traverse through this pattern, which results in variation of the instantaneous signal. This variation is called fast fading which is on a scale comparable to the wave-length. The other consequence of superposition is time dispersion depending the relative bandwidth of the signal and the mobile channel. When time dispersion becomes too large it produces Inter-Symbol Interference (ISI). This represents a major restriction on the bandwidth of data transmission.

1.1.3 Multiple-access cellular network

The mobile radio channel is unshielded in contrast to the wired channel in which the signal is effectively constrained. This unshielded nature makes it especially appropriate as a broadcast medium. Thus, a radio wave radiated to the environment can be

expected to reach nearly all receivers in the covered area. Therefore, in the wireless medium, signals of the same frequency from different users will interfere with each other. Signals transmitted via a wireless channel must be separated in a some way, otherwise they will interfere with each other; this is called co-channel interference.

A multiple access scheme is needed to enable multiple users to access the service at the same time without interfering each other. The access channels can be separated using different frequency slots, i.e. Frequency Division Multiple Access (FDMA), or time slot, i.e. Time Division Multiple Access (TDMA), or in code space, i.e. Code Division Multiple Access (CDMA). Indeed, no matter what kind of form is used for multiple-access, implicitly or explicitly a segment of spectrum is divided into a number of channels to be shared among a number of users. If each channel in the system is used exclusively by one user, therefore, the spectrum resource can only accommodate a fixed number of users.

Utilizing the propagation path loss between two geographic areas, the same channel can be reused at disjointed areas, i.e. cells. Therefore, the concept of frequency reuse is integrated with the cellular [46] scheme to build up the cellular network system. The frequency reuse inevitably causes the co-channel interference. To ensure adequate service quality, the reuse density, i.e. the distance between two cells using the same group of channels, has to be large enough.

Due to the cellular structure, when the mobile users move across cell boundary, the system has to perform hand-off to ensure a seamless service. A higher hand-off rate may cause the disturbance to the cell load and outage in the case of overloaded cells.

1.2 Trends of cellular network

1.2.1 Explosion of subscription

As the mobile phone becomes a tool for the mass population, subscriptions are exploding placing pressure on network design. Table 1.1 of the subscription to various cellular system [73] shows the popularity of this service.

Predicting from the past (shown in the Table 1.1) gives some indication of the explosion in the subscriber numbers. This process does not show any signs of slowing down. Intuition suggests that the penetration rate must have some saturation point, but there are some factors that suggest such intuition is simplistic. First, potential mobile

Table 1.1: Subscription increment (in Millions)

Technology	2000	2001	2002	2003	2004	2005
Analogue	91	84	81	75	67	55
GSM	384	497	596	690	783	891
CDMA	83	115	151	182	217	252
TDMA (U.S.)	61	93	129	161	192	222
PDC (Japan)	49	56	60	63	64	65
3G	0	1	6	23	46	83
Total	669	849	1,026	1,195	1,371	1,569

users expand from professionals or business users to young people and children as the use of cellular phones changes from convenience to entertainment. Due to increasing mobility in the factory, supermarket and office, mobile phones are increasingly used in those areas. People find it more convenient to use a mobile phone rather than a land-line phone even in the office environment. This contributes greatly to the increasing subscription as well.

The application of the cellular network is also increasing because not only the people, but some machines are using this service as well. Devices go on-line through wireless links e.g. in fleet control applications vehicles are becoming equipped with wireless terminal for their more efficient deployment and control.

1.2.2 Requirement for new applications

The success of cellular networks has triggered the development of new applications. The driving force also comes from the operators, who naturally wish to pursue higher and higher average revenues per user.

The traditional voice and short message service may be enhanced by image transmission. Internet access, especially access to the multimedia content, is another important new service. Multimedia applications such as, but not limited to, interactive conferences, distance learning and conference broadcasts [26] are also becoming popular.

New applications often involve the transmission of multimedia content. Some entertainment applications, such as video-on-demand and streamed media distribution, require real-time high quality video transmission. This results in even more requirement for bandwidth. The following Table 1.2 shows the data rate requirement of some typical application [32].

New types of applications also exert different Quality-of-Service (QoS) requirements on

Table 1.2: Transmission bandwidth

Application	Required Data Rate
Voice	4 - 25 kbps
HiFi-audio	32 - 128 kbps
Video, VCR-quality	1.5 Mbps
Video, TV-quality MPEG-2 compression	4 Mbps
Web-browsing	28+ kbps

the cellular network. Important quality indexes are error rate and delay. In real-time services, the requirements for small delay is actually transferred into a requirement for small error rate because the retransmission protocol – Automatic-Repeat-reQuest (ARQ) is not suitable.

1.3 Challenges for system design

1.3.1 Capacity requirement vs. limited spectrum resource

A major requirement created by the evolution of the cellular network service is the growing demand on the capacity, in terms of both subscription level and bandwidth. The implication of the growth of subscriber number is that more channels are needed in a given area. With increasing subscribers, the density of active users in a cell inevitably increases. This requires that the system provide more communication channels. Because of the nature of the cellular network as a multiple-access system, the spectrum resource must be divided among active users. But the available spectrum is limited.

Both increased subscriber capacity and data rate will force the carrier frequency moving towards the upper band. This trend has been shown during the past evolution process, i.e. from 800/900 MHz for the first- and second-generation systems to 2 GHz for third-generation. Therefore, it is expected that in the next 20 years, wide area cellular system will move to the range 3-5 GHz [73]. Although moving higher and higher in the spectrum can always release new capacity, this can not be an ultimate and sole solution because of two concerns. First, the propagation condition becomes so severe that a reasonable coverage can be very difficult to ensure when the carrier frequency moving extreme high. Secondly the implementation of high frequency electronics becomes difficult and expensive.

Besides moving the frequency higher in the radio spectrum, the network layer design is

also changed to accommodate new capacity demands, i.e. cell-splitting. By decreasing the cell size, each unit frequency is used to serve a smaller geographic area. In a unit area, therefore the number of cells is increased such that more users can be served providing they are distributed in that area evenly. Through a increasingly dense spatially reuse of the spectrum resource, the system can accommodate more users. This leads to the deployment of smaller and smaller cells, until we reach the stage where a micro-cell is mounted on every lamppost, covering around 100 m of the street, and a pico-cell is located in every room. But this capacity expanding solution relies on an assumption that the users geographical distribution is uniform, which is justified when the area is large enough. It does not hold however when the cell size shrinks to a level of tens of meters. Another disadvantage of this solution is that very small cell size may result in an unrealistic high rate of handoff between cells. Hierarchy cell structure can solve this problem [47] by overlaying a macro cell over the pico-cell layer. When the frequent hand-off mobile users increase, the higher layer cell needs more channels to serve these mobile users, which will sacrifice the spectral efficiency gain achieved by pico-cell layer. A more frequent hand-off also causes the extra exchanging of signalling, which obviously will take channel resource.

Secondly, the capacity expansion from geographic frequency reuse depends on an assumption that the mobile users distribute in the area evenly so that as every cell deployed in the area contains a similar number of mobile users. But as the size of the cell shrinking, the number of users contained in each cell may become disparate. A consequence is that some cells have more user load than other cells. Many users will therefore suffer from the channel shortage no matter how many more cells have been deployed in the area.

New approaches are therefore needed to solve capacity limitations in the face of ever increasing demand.

1.3.2 Demands on QoS in a hostile environment

Demand is not the only issue to be considered, but also quality. New wireless applications demand higher service quality from the network. Some applications, for example, require high reliability and low jitter of the information stream.

This quality requirement has two aspects: coverage – which is the spatial availability and reliability – which is the temporal availability (bit error rate).

The wireless channel generally hinders these requirements. The complexity of the

propagation environment brings shadowing effects so that coverage holes exist in the service area. Fast fading due to multipath propagation, makes the instantaneous signal strength vary so that link quality might not always be constantly acceptable.

As carrier frequency rises, transmission loss and the interaction with surrounding objects increases. This causes coverage range to shrink. Also, the radio wave is easily blocked by buildings. Scattering also becomes more severe. The penetration of the radio wave into the interior through the outdoor-indoor interface is weak and penetration loss at high frequency is very large. All these effects contribute to the formation of coverage holes within the service area.

A second cause of outage is co-channel interference. As increasing dense frequency reuse is required to solve the capacity demand problem, decreased co-channel distance will increase interference.

1.4 Finding the solutions

1.4.1 Clues from the past

Although it is a dilemma to expand the cellular network, there are some clues as to possible solutions from the past. By looking at the evolution of the network, we find that one important trend is the shrinking of the coverage area provided by a single base station.

When the first land mobile radio was introduced in 1921, all users in the whole service area divide the available spectrum them. In this system, the total user capacity is limited solely by the spectrum allocated. In 1970, a cellular structure was introduced into mobile communications. In this structure, only the active users in a smaller geographical area share the spectrum. This same spectrum is reused again in other geographical areas.

In second generation cellular network, sectorized cells were introduced, in which the base station antenna uses radiation beams with 120° to cover only one third of the cell (originally covered by an omni-directional antenna). When the service area is overloaded, cell splitting is used to accommodate subscriber population, increasing the system capacity [46, 39].

All these measures reduce the coverage of the base station antenna, which suggests

a better frequency reuse utilizing the spatial separation of radio signal. Moreover, as the size of cell is decreased, the chance that path is blocked is reduced and coverage is improved.

1.4.2 Recent research advances

Multiple antennas at base station represent a research frontier to boost system performance both in terms of quality and capacity. Closely placed antennas can provide micro antenna diversity. When different combining schemes are adopted, this can benefit link quality by either combating channel fading or reducing co-channel interference, or both. It can also provide MIMO channel, which achieves higher channel capacity [81, 52]. Widely separated antennas provide macro antenna diversity. This technique can combat outage caused by shadowing. When it is implemented as base station diversity, such as soft hand-off, it can improve the network capacity.

1.4.3 Approach in this thesis

We believe that one of the most promising approaches to improve future cellular network performance and spectral efficiency lies in area of new base station antenna structures. In this thesis, we are going to investigate a distributed base station antenna. We will demonstrate the ability of this structure to improve communication quality and achieve denser channel reuse. We will also address companion techniques to exploit the advantage of this antenna structure.

The outline of the thesis is as follows. In the next chapter, we review some base station multiple antenna techniques, which has been reported. In chapter 3, the distributed antenna system is introduced in details and qualitatively analyzed. Before studying the distributed antenna, in the beginning of chapter 4, we first determine an optimum antenna locations to give a consistent performance evaluation base. Then we evaluate the coverage performance for indoor and outdoor environments. In chapter 5, the transmission diversity for the distributed antenna in a wide-band system is studied. In chapter 6, the inter-cell interference performance is studied by placing the distributed antenna in a network environment. Also in this chapter, the spectral efficiency when the distributed antenna is deployed in the network is evaluated using simulation. In chapter 7 and 8, the application of the distributed antenna in CDMA system is addressed. Power control algorithm and optimal power allocation schemes are studied. In the last chapter, conclusions are drawn as well as the suggestion of future works.

Chapter 2

BASE STATION ANTENNA TECHNIQUES

Engineering the base station antenna structure is a promising solution direction to improve the performance of cellular networks. This chapter is dedicated to a literature review of various base station antenna structures and associated diversity schemes.

The base station antenna subsystem discussed here consists of an antenna module and a modem module with some enabling diversity schemes and signal processing techniques. First, we discuss a layered view of the base station antenna. According to the antenna structure, we categorize base station antenna techniques into several types and discuss each of them in detail. The distributed antenna, as an extension of macro antenna diversity, is the focus of this thesis.

2.1   Overview

2.1.1   Layered view of base station antenna

As shown in Figure 2.1, the base station antenna can be viewed as a layered structure, each layer of which can have a variety of implementations. The view comprises two planes: the link plane and the control plan. The link plan contains the signal transmission and reception related modules, such as the antenna, modem, combining module and other possible signal processing modules. For the combining module, combining can be performed after or before detection, corresponding post- and pre-detction com-
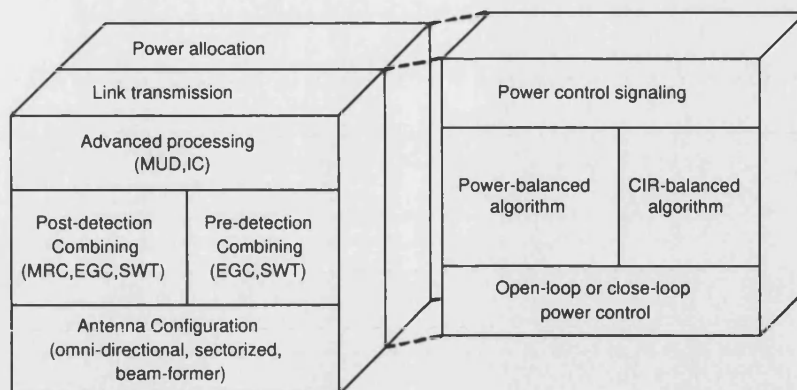
Figure 2.1: Layered view of base station antenna technique

bining. For each type, the combining algorithms include switched combining (SWT), equal gain combining (EGC) and maximal ratio combining (MRC). In the control plane, based on the monitored channel condition, decisions are made and delivered to the link plane to adjust the power or modulation parameters that make the link adaptive to radio channel conditions. In the layered structure, some upper layer algorithms, such as Multiple User Detection (MUD) and Interference Cancellation (IC), are general techniques, which can improve the overall performance, but some are optimized for specific lower layer schemes.

2.1.2 Antenna array structure

The antenna array structure is the most important part of the base station antenna technique. The configuration of the antenna array distinguishes the techniques.

The antenna units can belong to different adjacent base stations or cells. In this scenario, signals received at multiple base stations are jointly processed to achieve the diversity. We use the term antenna array refering to this case here in a wide sense although the antenna units are not located in a regular array. Some macro antenna diversities are of this kind. Through diversity reception, the coverage of multiple base stations are partially overlapped.

When all antenna units belong to one base station, there are two categories. One is co-located antenna array, in which antenna units are placed closely at the same site with small spacing of at the most several wavelengths. The technique using this kind of antenna configuration is referred as micro antenna diversity. The geometry of the antenna array can be of any shape, depending on the application. Arrays can be placed in a plane. In this co-located configuration, the coverage of each antenna element can

be seen to overlap completely. The other one is distributed antenna array, in which case although the antenna units belong to the same cell, they are separately placed at different sites. This is another implementation of macro diversity.

2.1.3 Utilization of multiple antennas

Multiple antennas can be configured flexibly in different ways to provide diversified channels. Theoretically, all the normal diversity techniques can be combined with multiple antennas to achieve diversity capability. Each antenna unit can be configured to work in a different frequency, time slot or polarization. Even when all antenna units are working on the same frequency at all times, the multiple propagation paths can provide spatial diversity. This can achieve diversity gain to combat fading.

A properly arranged antenna array can also be used to generate radiation patterns. Multiple radiation patterns separated in azimuth can achieve spatial diversity.

Apart from diversity, the signals sampled at multiple antenna units can span a vector space, within which independent signals can be differentiated. Exploiting these features, the data rate of the wireless channel can be increased using spatial multiplexing (with space-time coding) [51]. Another application of this feature is the reduction of co-channel interference. Interference reduction allows more dense frequency reuse and as a consequence improves the spectral efficiency.

When the antenna units located at different sites serve one cell, because the propagation paths between a specific mobile station to all antenna units are diferent, the strengths of these channels may be unbalanced. This suggests that each antenna unit could efficiently serve a different group of users. As these antenna units are collaborating as one base station, an optimal resource allocation, either in terms of power, or spectrum jointly among all antenna units is feasible. This gives another way to enhance the spectral efficiency [47].

2.2 Microscopic antenna array

2.2.1 Antenna spatial diversity

This is the simplest diversity scheme using multiple antennas. The signal received at all antenna units are combined linearly using one of the three combining schemes, i.e.

selective combing, equal gain combining or maximal ratio combining. The combined output has an envelope with less fading taking advantage of the multiple uncorrelated fast fading signals from all antenna units. This diversity scheme can effectively combat fast fading to achieve diversity gain [37].

Its performance depends on the correlation of the signals received in the diversity branches, which depends in turn on the antenna spacing. This is because both the theoretical and experimental results shows the relationship between the angle of arrival and the correlation of fading between antennas [36]. When the signal arrives parallel to the antenna array, the correlation increases dramatically and so the diversity gain reduces significantly.

2.2.2 Phased array and beamforming

Multiple antenna units can be used as beamformers. In this scheme, antenna units are configured as a phased array of antenna elements. The antenna elements are of regular geometry, such as rectangular, circular or planar shape, usually with constant spacing (although the constant spacing is not necessary).

The signals received at all antenna units are weighted with a complex coefficient (steering vector) to form a spatial filter, which can separate signals arriving from different directions [69]. By adjusting the steering vector, the beamformer can create a radiation pattern with a required main beam, nulls or both. By pointing these main beams and nulls, the beamformer can improve coverage or reject interference.

2.2.3 Adaptive array

Multiple antennas can be also used to separate signals occupying the same frequency and time slot, but coming from different locations. Signals from all antenna units are optimally weighted and combined to explore the multiple dimension space spanned by the spatial sampling of the multiple antenna. This application is known as an adaptive array.

For the reception of a particular user, the optimal combination can be performed to suppress interference signals [79]. Therefore, each user can be isolated from the other users. With K antennas, $K-1$ interferences can be nulled out [76, 77]. The interfering users which can be suppressed can be in the same cell or in a different cell. This scheme can therefore improve the capacity of any wireless communication system.

In contrast to antenna diversity, when used for interference cancelation, independent fading between antenna units is not necessary. The cancelation can be achieved with even complete correlation [60].

One thing worth noting is the difference between the phased array and adaptive array. Since at the first glance, they look like the same scheme. Actually, the adaptive array is a more general form than the phased array. The application of phased array depends on the angle of arrival of interfering signals, while in the adaptive array it is not necessarily so.

2.2.4 Limitations

Schemes based on the microscopic antenna array may have different design aims; either mitigating fast fading or increasing system capacity by decreasing interference. Even in the antenna spatial diversity scheme where the spacing of elements is sufficiently large to ensure de-correlation of fast (multipath-induced) fading, the spacing between antennas is still very small compared to the dimensions of environmental features. The spacing in the phased array scheme is normally one half wave-length. The signals originating from one user and received by all elements have essentially traversed the same (gross) propagation path. The mean signal powers in all branches are of similar level and the correlation of slow fading (or shadowing) between antennas is high. The limitation of all these applications is, therefore, that microscopic diversity is inherently ineffective in mitigating outages caused by shadowing. When the path between the transmitter and antenna array is blocked, all diversity branches become very weak which is likely lead to link outage. This feature dictates that this antenna structure can only be used for the link level performance improvement or as an overlay technique combined with other diversity techniques.

2.3 Macroscopic antenna diversity

2.3.1 Frequency macro diversity

In [5], a macro diversity scheme is proposed, which could be used in a frequency reuse radio system. In each cell, antenna units (which [5] refer to as ports) are deployed in a grid of locations, each transmitting on a different frequency. Selective diversity is performed over all ports. For one specific user, the port receiving strongest signal is chosen to serve it. Therefore, when the mobile user transverses the cell, rapid switching

among the ports tracks the strongest branch.

The geometry of an individual diversity group could be different. The spectrum allocated to that cell is exclusively divided among these antenna ports. This scheme is like splitting the original cell to a number of pico-cells, each of which is covered by one port. Therefore, the distance between two ports using the same frequency in the two co-channel cells is not changed.

The coverage in the cell is improved by using this macro antenna diversity scheme. At each moment for a given user, only one antenna port is used, which means the coverage condition over the whole cell is dynamically defined by the instantaneous propagation condition between the mobile users and their serving ports. The gain is derived from the (switched) diversity reception. This scheme provides better coverage.

2.3.2 Simulcast cellular system

In [87], the authors propose a new network architecture, which essentially overlaps cells to achieve macroscopic diversity. We call this scheme simulcast cellular because multiple antenna units are transmitting simultaneously to the mobile users in its coverage area. Just as with the frequency reuse scheme, there are different ways to organize the network. In one scheme, shown in Figure 2.2, each cell is supplied by three sectorized base station antennas located at every other edge of the cell hexagon. Accordingly, each base station site requires six antennas with 120° azimuthal sectorized characteristics. The two neighboring antenna units have 60° overlap. Each of these six antennas are allocated one of six groups of channels or frequencies. Therefore, each point in the plane is covered by two sectorized antenna units and has two groups of channels available. Therefore, the effective reuse factor is 6/2. All combining schemes can be used on reception of the uplink signal. Due to diversity reception, this network architecture can achieve a better reuse factor than the traditional frequency reuse pattern given the same SIR requirement. It can therefore accommodate more users in concentrated hot spots.

2.3.3 Soft handoff or base station diversity

Soft handoff [59], also called base station diversity is proposed first in CDMA systems. When the handoff is happened between two sectors in the same cell, it is called softer handoff [35]. Here, we refer both them as soft handoff. In FDMA or TDMA system, different frequency bands are used in neighboring cells. The hand-off process involves
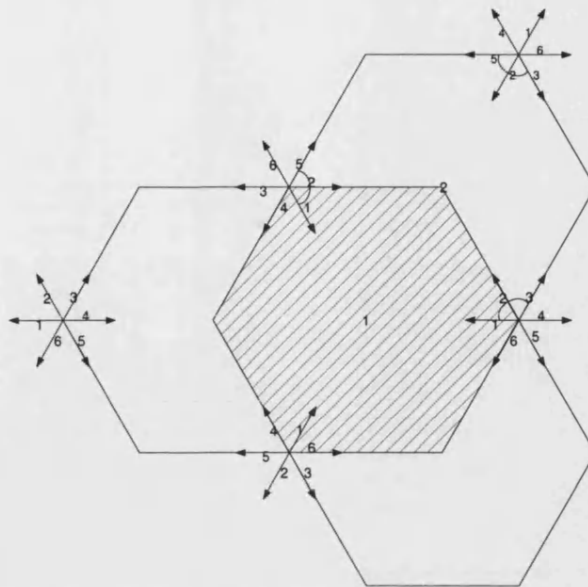
Figure 2.2: Geometry of simulcast macro diversity (adatpted from [87])

switching between two frequency bands as the user passes across the cell border. During the hand-off process, at any moment, the mobile user only communicates with only one base station. In a CDMA system, in which universal frequency reuse is feasible, the channel re-allocation does not involve frequency switching so it is possible that the mobile user can communicate with more than one base stations simultaneously.

Therefore, multiple radio links between the base station and mobile are possible. Macro diversity implemented during the soft hand-off process is different in the uplink and downlink. For the uplink, generally, the two base stations perform the reception independently. Then the received information streams are send to the Mobile Switching Centre (MSC) before one of them is chosen. Obviously, the base station which has the better channel condition is ultimately selected. The duration of one switch depends on the channel variation speed. In the downlink, both base stations send signals to the mobile station as if it is in their own cell. The mobile station de-spread both base stations' signals in the two RAKE fingers (de-spread with different PN codes corresponding to the different base stations) and combines them coherently.

The soft handoff can switch the mobile user from one base station to another in a smooth way as the redundant link is closed only if after the switched-to base station has a stable and strong link. In the hard handoff case, the random stroll of the mobile station may cross the irregular boundary between cells back and forth, which may incur several times of handoffs. The soft hand-off scheme also improves the link availability especially in the critical cell boundary area because when one link is completely blocked

there may be some others still alive. In addition, soft handoff increases cell coverage and decreases interference to other cells due to the reduced transmission power afforded by the macro diversity gain. It therefore also increases uplink capacity of a heavily loaded multi-cellular system [20, 70].

2.3.4 Limitation

The macroscopic diversities are all implemented at the base station level, either as cell splitting or cell overlapping (marginal overlapping as in the soft hand-off case). Although these schemes can improve coverage performance [2, 48], they do not make full use of available channels. In both the frequency macro diversity scheme and the uplink soft hand-off scheme, only selective diversity is used to receive signals at any one moment. Although in the downlink soft hand-off scheme the multiple antenna branches are involved in serving the mobile user, this is only restricted to the region of the cell borders.

The simulcast system provides the full advantage of macro diversity and covers the whole cell. This is the central topic of the rest of this thesis.

2.4   Distributed antenna systems

2.4.1 Leaky feeder distributed antenna for indoor environment

A primitive form of the distributed antenna is the leaky feeder, which consists of a transmission line enabling the wave propagating through it to radiate along its entire length. Originally, this scheme was used to provide coverage in tunnels and mines and was then adopted for indoor areas [8, 62, 3]. A leaky feeder winding its way through a building can provide relatively even coverage over a given service area. To control the radiation, a discrete form of leaky feeder is possible, which comprises cascaded lengths of low-loss coaxial cables and three-port directional couplers connected to an antenna [58].

Some indoor propagation measurements have been reported [58, 66, 85]. These measurements characterize attenuation and delay spread and it is shown that, compared to a single central antenna, propagation loss can be dramatically reduced.

2.4.2 Distributed antenna in indoor CDMA system

In a leaky feeder scheme, radiation from multiple points are summed with random phases at the receiver. Although it can improve radio coverage, performance is compromised due to the summation of multiple uncontrolled sources. When the leaky feeder is applied in an indoor CDMA system, due to its special spread-spectrum transmission, some simple modifications can enable it to be combined with multipath diversity [53] to achieve a better performance. To realize the multipath diversity, it is necessary to ensure sufficient delay between paths, i.e. the coherence bandwidth must be small with respect to the bandwidth of the transmitted signal. Artificial delay may therefore be required at each antenna unit.

In this scheme, a grid of antenna units together with delay elements is deployed to cover an indoor area. The key issue is to arrange these elements so that the signal sent from the antenna units have sufficient relative delay so that they can be resolved in the mobile users' RAKE receiver [82].
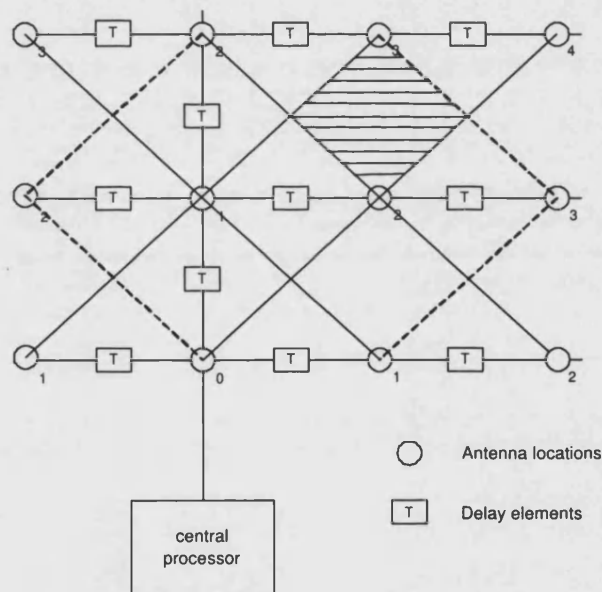
Figure 2.3: Geometry of the distributed antenna in indoor CDMA system

In this simple scheme as all antenna units are connected to a common cable, other users' signals will introduce Multiple Access Interference (MAI) via this common cable. An improved version is proposed in [83]. Simply, each antenna unit is connected to a processing center using a separate transmission line and the signals received at all these antennas can be optimally combined. Because each antenna unit is connected to the processing center separately, this prevents the accumulation of MAI. The MAI can

be reduced K times (K is the number of antenna units) compared to the single feeder scheme.

In this way, diversity using signals from multiple distributed antennas is achieved. This scheme can combat not only the shadowing, but also fast fading, because signals from multiple antennas are always available for reception and are subject to independent shadowing and fast fading. The coverage of the indoor service area is improved significantly. With a proper power control scheme, this architecture can achieve a SIR bound by:

$$\frac{NK}{M-1} \le \gamma \le \frac{NK}{M-K}, \; M > K \tag{2.4.1}$$

where N is the processing gain, K is the number of antenna units and M is the number of mobile users [83]. Compared to the signal central antenna case, the SIR gain is a factor of K.

2.4.3 Distributed terrestrial cellular system

It is well accepted that the distributed antenna is a good performance enhancing technology for the indoor area. This idea can be also applied to terrestrial networks, especially in the urban area where propagation through the environment involves a high penetration losses and the high subscriber density requires good spectral efficiency.

In the indoor area, as the transmission distance is limited, coaxial copper wire with low cable loss is good enough to connect antenna units and the processing center. In the terrestrial network, the transmission distance required is far greater, even in a micro cell. In this case, the loss of coaxial cable makes the implementation difficult.

The application of distributed antennas in the terrestrial network was enabled by fiber-optic micro-cellular radio [11, 23]. This system was proposed because micro-cell promises large capacity and ubiquitous coverage in the urban area with massive subscribers number.

The principle idea is to use an optical fiber network to connect antenna units to its serving station. No modulation, demodulation or base-band functions are performed at the antenna site at all. The RF signal is directly modulated onto an optical carrier. This scheme can improve coverage by illuminating dead spots in densely shadowed areas and accommodates more subscribers by reducing the radius of the cell. It should be pointed out that although in this scheme, all the antenna units are connected to the serving site, where the complete base station functionality resides, the processing of

the signals is still separate from base station to base station. There is no collaboration between two antenna units during the processing in the serving site.

With the RF signals all transmitted back to one site, it is easy to perform collaborative processing among antenna units. A fully distributed antenna network was first proposed for CDMA [25]. In a service area all base station antennas are connected together, the signals from one particular user received at all base station antennas are combined for reception. It is found that with proper power control and diversity reception, this structure can improve received SIR and therefore achieve a capacity gain linearly proportional to the total number of antenna units.

A conceptual distributed wireless communication system is proposed in [86], which is completely different from the traditional cellular network in that it contains no pre-defined cell. All base station antenna units, which have no processing functionalities, are connected over an optical network to a number of processing centers. These are responsible for reception and transmission. Each processing centre can collaborate using some subset of antenna units. The antenna units, whose signals are processed in the same processing center, effectively form a cell.

The essential idea of this architecture is the virtual cell, which is not base station centered, but processing centered. This architecture can achieve capacity gain by utilizing MIMO processing and dense channel reuse.

2.4.4   Contribution of this thesis

The review of the various base station antenna techniques suggests that the distributed antenna is a promising solution for the challenges faced by future network. But deploying distributed antennas over the whole PLMN as proposed in [86, 24] is neither practical nor necessary. Firstly, only those antenna units in the vicinity of the mobile user can contribute strong signal. Secondly, deploying multiple antennas with a fibre optic overlay network in an area with low user density is unlikely to be cost effective.

In this thesis, we study a more practical deployment scenario, i.e. using the distributed antenna in one, or several micro cells in the urban area, which co-exists with other traditional cells.

The propagation characteristics relevant to the distributed antenna are examined using ray tracing and measurements, coverage performance is evaluated. We also put the distributed antenna into a narrow-band (FDMA and TDMA) network context to examine

its performance in the presence of the co-channel interference and its influence on other (traditional) cells. By taking all these aspects into consideration, we also obtain the spectral efficiency.

Although in [24], the theoretical uplink performance of a distributed antenna is given for a spread-spectrum signaling system, the downlink case is left unaddressed. One problem in the downlink is the transmission diversity due to the single antenna of the mobile station. Utilizing wideband measurements, we studied possible transmission diversity techniques. The other problem is finding an approach to exploit the distributed antenna to improve capacity in the downlink. We propose a solution which optimizes the transmission power allocation between all base station antennas. Two transmission diversity schemes together with appropriate power allocation schemes are examined to give capacity performance curves.

We conclude that the distributed antenna is a promising base station antenna structure, which can improve both service quality and system capacity. It is also a flexible base station structure, which can be extended by combining it with many other techniques.

Chapter 3

DISTRIBUTED ANTENNA SYSTEM

The distributed antenna system is a new base station antenna structure. The three essential elements are widely separated antenna elements or units, an overlay network and a central processor. In the first part of this chapter, we will give a detailed view of this base station structure and some basic diversity techniques. We then qualitatively analyze the advantages it offers, i.e. the capability to improve coverage and the benefits that follow from this. We also identify its possible costs and disadvantages so as to justify its deployment.

3.1 DAS structure

3.1.1 Widely separated antenna units

In the distributed antenna system, multiple antennas are installed at different sites within one cell (see Figure 3.1). This is the main feature of this system while in the traditional base station, a single antenna or antenna array is typically located at the cell centre. As more antenna units are used, more regions within the service area will have a Line-Of-Sight (LOS) link to at least one unit. Even regions with only a Non-LOS (NLOS) link, the received signal is generally stronger due to the reduced separation between transmitter and receiver. An extreme approach would be to blanket the cell by deploying antenna units at every street intersection. This system could also be used to cover public indoor areas, such as shopping malls, theaters or metro stations etc.

The number of antennas and the positions of the antenna units are critical to the performance of this scheme. Performance essentially depends on the complexity of the environment. The spacing between antennas should be such that the distance is large enough to achieve de-correlation of the mean signal power between antennas. In the urban area, the spacing will be comparable to the dimension of the buildings or blocks of building. The antenna unit is a passive device, of small size, low cost, and is easy to deploy. Such units may be designed to be pole mounted.
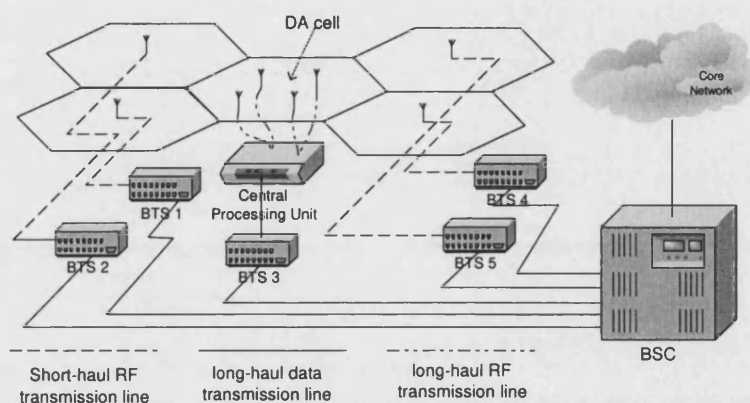
Figure 3.1: Distributed antenna system

3.1.2 Extension to the distributed antenna

A natural extension to the above scheme is to deploy directional antennas or even antenna phased arrays at each site. Diversity can be performed over the resulting multiple beams so that each mobile user is illuminated by several beams from different antenna unit sites.

Compared to single site beamforming, this scheme has two-dimensional resolution of the spatial position of the mobile user. Without further processing with delay information, single site beamforming can only easily differentiate users located at different azimuth. In an urban area the mobile users cluster in the street so that very likely, several mobile users lie at the same azimuth. In the multi-site beamforming scheme, two beams at two sites can differentiate users as shown in the Figure 3.2. (A single beam from site 1, represented by dashed line, cannot differentiate the users.)
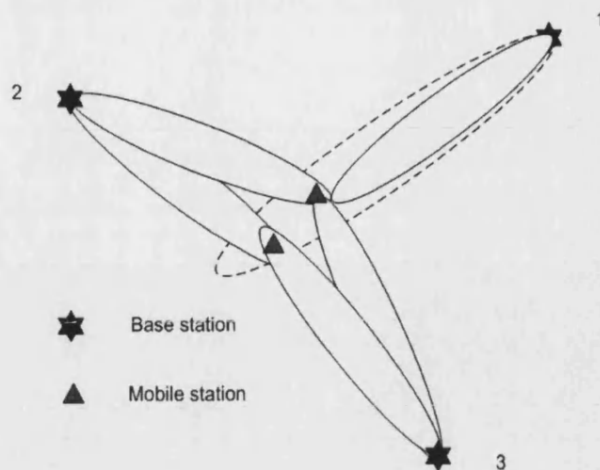
Figure 3.2: Two-dimensional beamforming

3.1.3 Overlay transmission network

An overlay network connects all antenna units to a central processing unit, forming a star topology. Little or no processing is implemented at the antenna unit and the RF signal or equivalent complex baseband modulated signals are transmitted through the overlay network to the central processing unit where all the significant signal processing is performed.

The bandwidth of the transmission network depends on the frequency bandwidth allocated for the air interface. The WCDMA baseband bandwidth is 1.6 MHz for the 1.28 Mchip/s option and 5 MHz for 3.84 Mchip/s option in TDD mode and 5 MHz for FDD mode [45]. To transmit this broadband signal in the overlay network, there are two obvious technologies: fibre-optic links and millimetre wave links.

Fibre-optic is a preferable approach for the transmission network due to its low attenuation properties. In [11, 68, 64], a Radio Over Fibre (ROF) network is proposed to connect remote micro/pico base station antenna. Single mode optical fibres can have very low loss, typically 0.2 dB/km and very large bandwidth-sufficient to carry the entire radio frequency spectrum (DC to 300 GHz). In some environment, the fibre length will be less than 1 km in which case Multi-Mode Fibre (MMF) can provide sufficient small loss. An advantage of using MMF where possible is that many buildings have pre-installed MMF infrastructures for data communications [34].

Another important issue is the implementation of the nodes, especially at remote sites, in a cost-effective and transparent way, such that they are not close coupled to the operating frequency. In [74], a bi-directional transceiver – Electron Absorption Modu-

lator (EAM) was introduced to connect the optic and electronic domain in an especially simple way (see Figure 3.3).
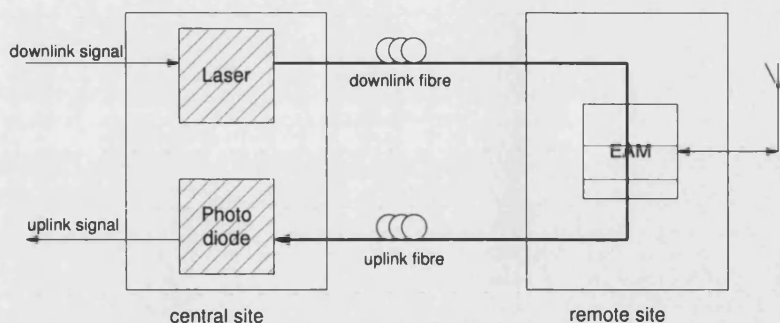
Figure 3.3: Application of EAM transceiver

An alternative is to use millimeter wave links for the overlay network. The advantage of millimeter wave links is their ease of deployment. It is vulnerable, however, to the weather, e.g. the fog and rain which may introduce large path loss. In the urban area, where the building density is high, it may be difficult to find locations high enough to realize LOS links to all the remote sites. Millimetre-wave technology could be used as a complementary solution to the ROF, however.

3.2   Signal processing

3.2.1   Combining techniques

Signal processing is an essential component for this antenna structure. In a practical system, this involves various functionalities, e.g. signal combining, channel estimation, interference cancelation and power control. Combining is one of the most important, however, and is critical to performance.

Although more sophisticated combining schemes exist, such as optimal combining and space-time coding, traditional combining techniques are both common and simple and are therefore used widely in practical system. In this section, we review these techniques. Here we assume each antenna branch suffers from the same thermal noise. The SNR of each branch is denoted by γ_i and we assume that γ_i represents independently and identically distributed (i.i.d.) random variables in all channels.

3.2.2 Selective and switched combining

Selective and switched combining are the most straightforward means to achieve diversity gain, in which the signal from only one branch is taken for reception or transmission. In selective combining, at any instant, the strongest branch in terms of signal strength or SNR is selected. This scheme is not always practical, however, considering the switching rate and the transients caused by switching. A more practical approach is switched combining, in which one branch is used as the active link until its signal strength falls below a preset threshold.

At any instant, the outage probability (defined by the fraction of time the resulting SNR γ_{sel} is less than the threshold x) for selective combining is:

$$
\begin{aligned}
\mathbf{P}(\gamma_{sel} < x) &= \mathbf{P}(\max(\gamma_1, \ldots, \gamma_K) < x) \\
&= \prod_{i=1}^{K} \mathbf{P}(\gamma_i < x)
\end{aligned}
\tag{3.2.1}
$$

For switched combining, the expression of the cumulative probability depends on the switching threshold γ_t and is more complicated than for the selective case. The cumulative probability for the switched combining case is always inferior to selective combining, i.e. $\mathbf{P}(\gamma_{sel} < x) \leq \mathbf{P}(\gamma_{swt} < x)$ [57]. For the particular cumulative probability when $x = \gamma_t$, the two combining schemes are equal, i.e.:

$$
\mathbf{P}(\gamma_{swt} < x | x = \gamma_t) = \mathbf{P}(\gamma_{sel} < x | x = \gamma_t)
\tag{3.2.2}
$$

Normally, the switching threshold is chosen to satisfy a required outage probability. Therefore, during the performance evaluation, these two schemes are interchangeable.

3.2.3 Equal gain and maximal ratio combining

Selective combining achieves improved outage, but does not exploit all signal branches. In a linear combining scheme every signal branch is weighted and summed after being co-phased. This achieves extra Signal-to-Noise Ratio (SNR) gain due to the incoherent summation of noise signals.

For Equal Gain Combining (EGC), the combined signal can be expressed as:

$$
\begin{aligned}
r(t) &= \sum_{i=1}^{K} s_i(t) + n_i(t) \\
u_i^2 &= E(s_i^2(t)) \\
\sigma^2 &= E(n_i^2(t))
\end{aligned}
\tag{3.2.3}
$$

The SNR of the EGC combined signal is:

$$
\gamma_{egc} = \frac{(\sum_{i=1}^{K} u_i(t))^2}{\sum_{i=1}^{K} \sigma^2}
\tag{3.2.4}
$$

For Maximal Ratio Combining (MRC), the combined signal can be expressed as:

$$
r(t) = \sum_{i=1}^{K} \alpha_i(s_i(t) + n_i(t))
\tag{3.2.5}
$$

By applying the Schwartz inequality, the weights can be optimized to achieve a maximum SNR, which is:

$$
\begin{aligned}
\gamma_{mrc} &= \sum_{i=1}^{K} \frac{u_i^2}{\sigma^2} \\
&= \sum_{i=1}^{K} \gamma_i \\
\alpha_i &= \frac{u_i}{\sigma^2}
\end{aligned}
\tag{3.2.6}
$$

It is difficult to get an analytic expression of the outage probability of an EGC combined signal. The result for MRC follows a χ^2 distribution and its probability density function and cumulative probability function have been obtain following [67]. It is easy to get a closed-form expression for MRC. It is worth noting, however, that a comparison of EGC and MRC reveals that EGC performance is only marginally worse than the MRC [37].

3.2.4 Pre-detection and post-detection combining

Linear combining can be implemented before demodulation (at RF or IF). This is called pre-detection combining. Alternatively, it can be implemented after demodulation. This is called post-detection combining. The modulated signal can be expressed as:

$$r_i(t) = a_i e^{j\phi_i} e^{j\omega_c t} + n(t) \tag{3.2.7}$$

where the $a_i e^{j\phi_i} + n(t)$ is the baseband equivalent signal and noise.

For linear detection, the result is exactly the same irrespective of post- or pre-detection combining. For non-linear detection (e.g. square-law detection), combining can only occur on a power level. The result SNR for equal gain combining is:

$$\gamma_{sqr} = \frac{\sum_{i=1}^{K} u_i^2}{K\sigma^2} \tag{3.2.8}$$

The equivalent result for linear detection is:

$$\gamma_{lin} = \frac{(\sum_{i=1}^{K} u_i)^2}{K\sigma^2} \tag{3.2.9}$$

The performance of post-detection combining is therefore inferior. Given equal strength branches, the gain of linear detection over square-law detection is $\gamma_{lin}/\gamma_{sqr} = K$.

3.3 Advantages of distributed antenna system

3.3.1 General analysis

The advantage of the distributed antenna system lies fundamentally in two types of matching.

The first is the matching of the radiation of multiple antennas to the environment. Streets have waveguiding effects [44]. The propagation across waveguides (from street to street) involves large penetration or diffraction loss, whilst propagation within a waveguide (along a street) experiences little loss. Using a single antenna to cover such an area is neither effective nor efficient. Increasing transmitted power to fill coverage holes will cause higher than necessary received power in other areas. Deploying antenna units in each major waveguide avoids propagation across streets so that less power is needed for adequate coverage. Natural barriers can also confine radiation leading to

reduction of interference.

The second is the matching of antenna units to the spatial distribution of the mobile users. As mobile users in an urban area are normally clustered, matching the antenna units to their spatial distribution ensures power is concentrated in those regions where it is needed. This further reduces the required transmitted power. The other benefit is that separating the signals to two user clusters at different antenna units can reduce in-cell interference in CDMA systems.

3.3.2 Improved coverage performance

The significant improvement realized using the distributed antenna system is a more appropriate spatial distribution of signal power over the cell compared to the single antenna case. Firstly, the "ubiquitous" presence of antenna units can reduce coverage holes. The multiple antenna units reduce mean access distance (i.e. the distance from mobile user to the base station antenna). Large access distance causes both higher path loss (dependant on the distance) and higher probability of blockage (shadowing). In the ideal case, when antenna units are installed at every main street intersection, service quality may be almost the same wherever the receiver is in the area. In the single antenna structure, coverage is typically diamond shaped, with the two orthogonal streets as the two diagonal lines [14, 21, 27].

In an urban area, because of the complexity and time varying nature of of the environment (due, for example, to moving vehicles) fast fading is another important cause of link outage. In the distributed antenna diversity scheme, several antenna units establish links with the mobile user, each of which is subject to independent fast fading allowing its normal diversity mitigation. It will also reduce the frequent switching between base station antennas which would be experienced in a pico-cell solution, as user move between streets or from the outdoor to indoor environment.

3.3.3 Increase the system capacity

Improving link quality and capacity simultaneously is a feature of the distributed antenna system. Link quality, which suffers from fading, is normally overcome by diversity techniques. But this inevitably involves sacrifice of spectral efficiency because, in principle, it uses channel resource to deliver redundant information. Even in the case of antenna diversity, which does not use extra frequency or time resources, the use of multiple antennas to combat fading sacrifices the ability to create more channel capacity

using the spatial resource as achieved, for example, by Multiple Input and Multiple Output (MIMO) configurations.

The distributed antenna system can achieve capacity gain through engineering the radiation. The increase of the capacity is in terms of the number of users can be accommodated per unit bandwidth in a unit area ($/Hz/m^2$). This represents an improvement in spectral efficiency whilst simultaneously combating shadowing and fading. The Multiple Access (MA) scheme influences the approach required to achieve this capacity gain.

In FDMA or TDMA systems, the mobile users inside a cell are allocated an exclusive channel. It is worth noting that although the deployment of the antenna units is the same as in a pico-cell scheme, each unit represent only one part of one base station. They share, therefore, only one group of frequencies. In the pico-cell scheme, each antenna uses a different group of frequencies. Since the distributed antenna can transmit the signal to the target mobile users more efficiently, the reduction in transmitted power compared to a single antenna scheme results in a denser channel reuse pattern. If we consider the separation between antenna units, it is possible to reuse channels even within a cell, which will increase spectral efficiency further. This would require a channel allocation scheme, however, which is not discussed in this thesis.

In CDMA systems the situation is different since all users use the same frequency. To ensure the link is available for communication, the self-interference level is carefully managed. In the uplink of a distributed antenna system, as multiple antenna units are involved in reception, diversity reception can increases the received SIR. This suggests that it can tolerate more interference, which means more in-cell users. On the downlink, the distributed antenna matches the mobile user clusters and the spatial separation can be utilized to reduce interference between users.

The capacity gain in CDMA systems is due to increased SIR. This is similar to the situation in FDMA or TDMA systems when considering interference due to co-channel cells. The difference is that in CDMA systems, SIR improvement can increase the number of users supported in one cell.

Other interference reduction techniques might be able to achieve better performance due to the separated antenna sites. Two-dimensional beamforming, for example, might give rise to a better spatial resolution.

3.3.4 Hand-off issues

The pico-cell scheme, which has a similar antenna configuration to the distributed antenna, can provide better coverage and capacity in terms of number of users per unit area. But pico-cell solutions have their own disadvantage, i.e. increased hand-off rate. Frequent handover will involve network disturbance because of the signaling needed to be exchanged during the process as well as the channel reallocation. This does not happen in case of the distributed antenna system. This is because all antenna units belong to one cell.

When reception diversity combining is employed the signals are tracked continuously and there is no need to switch between antenna units. Even when the switched diversity is used, the switching is at the level of the RF domain, when the user moving from the vicinity of one antenna to another. This will not incur channel re-allocation. For the distributed antenna system the mobile user therefore receives a more stable service.

3.3.5 Benefits to the mobile user

In the distributed antenna system, all diversity schemes are all implemented at the base station. This suggests that the complexity of the signal processing in the mobile station will not be increased. More importantly, the distributed antenna improves coverage performance, decreasing the transmitted power of not only the base station, but also the mobile stations. Both of these two facts will increase batter life.

As the mobile service becomes more popular, people are getting increasingly concerned about the possible biological effects of e/m radiation [1, 63]. Compared to a single antenna structure, the lower transmission power of both base station and mobile stations are advantages in this respect.

3.4 Disadvantages and cost

3.4.1 Overlay network

Deploying a distributed antenna system will inevitably incur extra costs, of which the major component is represented by the overlay network. To connect several antenna units to the processing center requires infrastructure, which involves a fibre-optic or

millimeter-wave network. In the traditional network, the data link between base stations and the MSC (in GSM system, Base station Transmission System (BTS) connected to BSC via A-bis interface) is for the transmission of digital voice-frequency signals, which can be fit into 64kbps PCM circuit. Voice circuits can be multiplexed into T1/E1 interface [38, 43].

Transmitting wideband signals over long distances is potentially difficult and/or expensive. The degree of difficulty depends on the scale of the distributed antenna cell, which in turn is determined by the target service area. If it is only used to cover a micro-cell area, the overlay network will comprise fibre links of a few hundreds metres at the longest. When the distributed antenna is used to cover a moderate to large area, link of several kilometers may be needed.

This problem may not be as serious as it first seems. First, the overlay network can be implemented using a hierarchical structure. The antenna units being connected to a local center first. This type of connection requires only short link length. Local centers are then connected to a higher layer concentration center using longer links. By concentrating end connections, fibre or cable can be saved.

Advances made in the data communication also relieves the problem. With Wavelength Division Multiplexing (WDM) techniques now widely used, optical networks especially Fibre-To-House (FTH), have become widely available in urban areas. Optical fibre has already been buried much of which is dark [34]. These resources could be utilized.

3.4.2 Complexity of implementation

Although the distributed antenna has inherently good radio coverage performance, a set of proper diversity schemes and companion techniques are necessary to realize its advantages. From implementation perspective, the processing unit is no different from that of a co-located antenna array. The difficulties come rather from the wide separation of the antenna units. This will be discussed in detail in the following chapters.

Another aspect of complexity lies in the management of both the antenna units and the overlay network. As the complexity increases, the probability of failure rises. Management functions will therefore be needed to comply with the high reliability required in the the telecommunications industry.

Chapter 4

RADIO COVERAGE IMPROVEMENT

By deploying multiple base station antenna units at different separated locations in urban areas, the distributed antenna can improve coverage dramatically. This chapter analyzes this coverage improvement. Because antenna unit location influences performance, we first present a method of optimizing the antenna unit positions. With the resulting optimum antenna position guideline, we examine its coverage performance in two environments, i.e. urban and indoor.

4.1 Study method

Although the BER depends on many aspects of the channel, such as the mean power, variation of instantaneous signal strength, time dispersion etc, the total received signal power is still a useful and straightforward measure of link quality.

The signal strength at all receiving positions is a snapshot of the coverage condition, which could give an idea of what fraction of the cell is well served and what fraction suffers outage. This spatial distribution of received signal strength over the service area reflects the overall coverage quality. Mean and variance of received signal strength reflect average link conditions. But these statistics are only of comparative significance. The cumulative distribution is clearly a more complete description. From it, we can obtain two useful coupled metrics: spatial service availability (the percentage of area where the local mean signal strength is greater than a given threshold) and exceeded signal strength (local mean signal strength exceeded in a given percentage area of the

cell). These two metrics are critical for service provision evaluating.

Estimation of path loss is another issue for performance evaluation. A statistical model of the distributed antenna involves a joint probability function, which is difficult to obtain. We therefore sample these multiple channels using a physical model, which is specific to the detailed environment configuration. Since different environments have distinct propagation characteristics, we study them separately as two types: indoor environment and outdoor micro/pico environment.

4.2 Access distance analysis

4.2.1 Optimize the antenna positions

To position the distributed antenna unit is an optimization problem. The ultimate objective is, of course, to provide a more even and better coverage in terms of the received signal strength over the whole area. To do this experimentally would require too much effort in terms of on-site measurements. We turn to a simpler metric - access distance. Access distance is the distance between the mobile user and base station antenna. It is well correlated to received signal strength.

Access distance for the distributed antenna is defined as the distance of the mobile station at location $M_j : (X_m(j), Y_m(j))$ to the nearest antenna unit. We define the antenna coordinate set C_b, and access distance $D_a(M_j, C_b)$ of location M_j as:

$$
\begin{aligned}
C_b &= \{(X_b(i), Y_b(i) \mid i = [1, K]\} \\
D_a(M_j, C_b) &= \min_{i \in [1,K]} \sqrt{(X_m(j) - X_b(i))^2 + (Y_m(j) - Y_b(i))^2}
\end{aligned}
\tag{4.2.1}
$$

Since the mobile user can be in any location within the cell, the access distance is a spatially distributed random variable. The average access distance over the whole area can be used to as a optimization objective:

$$
\overline{D}_a(C_b) = E(D_a(M_j, C_b))
\tag{4.2.2}
$$

The distribution of the mobile user in the area is assumed to be uniform. The optimal

antenna position is the one which gives the minimal mean access distance:

$$C_b^* = \arg \min_{C_b} \overline{D}_a(C_b) \tag{4.2.3}$$

4.2.2 Reducing dimensions of the optimization problem

The optimization is a multi-dimensional problem. The dimensionality depends on the number of antenna units used. As the access distance for one mobile station position is the shortest of the distances to all antenna units, then the whole area can be divided in to a number of circles centred on the antenna units positions. The access distance minimization problem is similar to a problem that place the largest possible number of equal size circles into a circumscribing circle, i.e. the circle packing problem [75]. The solution of this problem for less than six circles suggests that all circle centres lie on a circle concentric with the circumscribed circle.

The conjecture that radially symmetric antenna unit positions will be optimal suggests a circular antenna unit configuration, in which case we need only determine the radius of this circle. The optimization problem is thus reduced to one dimension. The antenna positions are expressed by:

$$(X_b(i), Y_b(i)) = (R_a \times \cos(\theta_i), R_a \times \sin(\theta_i)), \ \theta_i = \frac{2\pi i}{K} \tag{4.2.4}$$

where K denotes the number of antenna units deployed and R_a is the radius of the antenna ring (as shown in Figure 4.1).

In a discrete area integration, the optimization problem can be expressed as:

$$R_a^* = \arg \min_{R_a} \frac{1}{2\pi R_c} \sum_j D_a(M_j, C_b) \Delta s \tag{4.2.5}$$

where Δs is the discrete area.

4.2.3 Numerical results

We use a numerical approach to estimate the solution for this optimization problem. R_a is sampled discretely in the range from $0 \leq R_a \leq R_c$ and $R_c = 300\text{m}$. For each sample, the mean access distance is calculated numerically using equation (4.2.2). The functional dependence of mean access distance on ring radius is obtained. The five curves in Figure 4.2 correspond to diversity order from 1 to 5. For each curve the
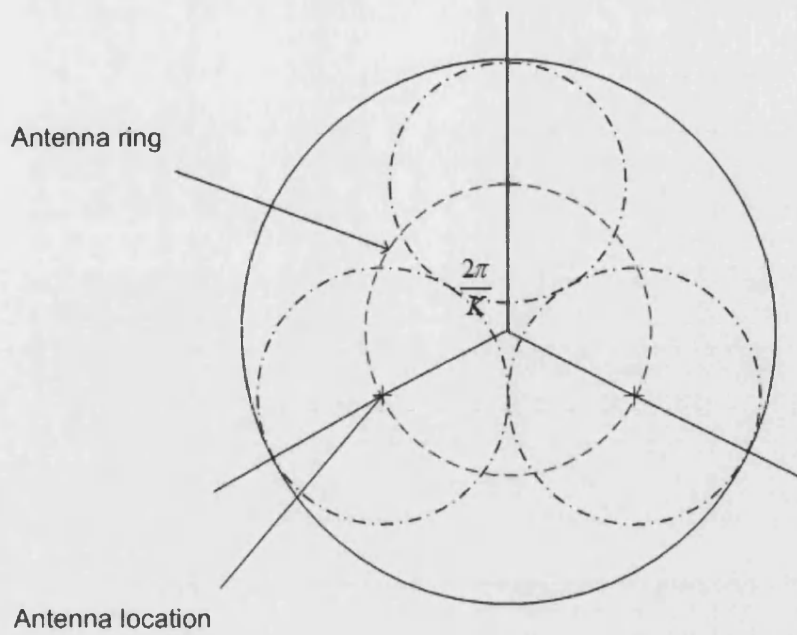
Figure 4.1: Antenna units positions

minimum represents the optimum ring radius.
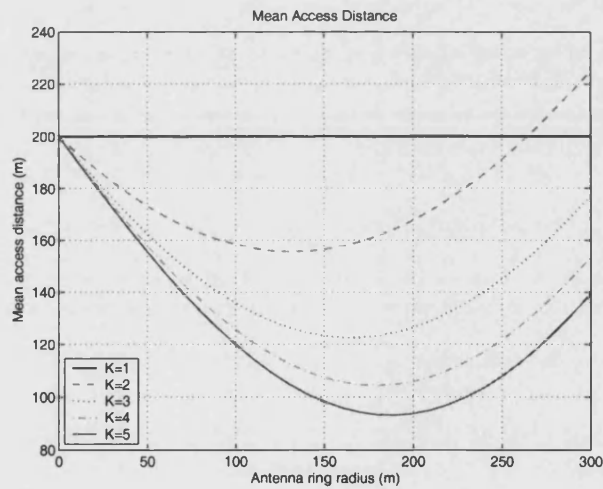
Figure 4.2: Mean access distance vs. antenna ring radius

The mean access distance only shows the first order statistics of the spatially distributed access distance. We also use the variance of the access distance as the objective of the optimization procedure as well. Similar curves are shown in Figure 4.3.

And from the numeric simulation results, we can observe the optimality of these antenna
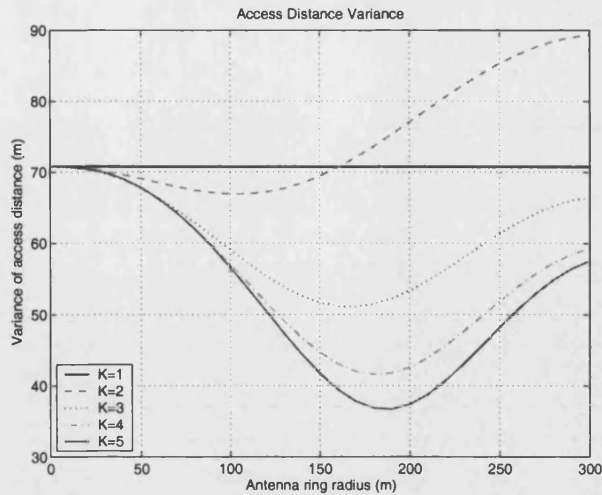
Figure 4.3: Access distance variance vs. antenna ring radius

position, which is observed in the mean and variance of access distance curves.

Due to the similarity to the circle packing problem, this optimum position can also be obtain geometrically [75]. For the less than 6 circles case, the best antenna position are equivalent to the center of circles of same radius inscribed by the circumscribing circle (see Figure 4.1). Using trigonometry, the optimum radius is given by:

$$R_a = \frac{R_c}{1 + \sin(\pi/K)} \qquad (4.2.6)$$

Table 4.1: Comparison of optimum radius between numerical and analytic results (m)

Num of Antennas	Min. mean	Min. variance	Analytical
2	130	100	150
3	170	170	161
4	180	180	176
5	190	190	189

In the table 4.1, the optimal positions calculated using minimal mean access distance, minimal access distance variance and the analytical optimal positions are compared. Reading the table, we can find that apart from the two antennas case, using either mean or variance of the access distance gives the similar result. When compared the optimal result from the numerical calculation with the analytical result, we can find that the difference is within the error introduced by the discrete sampling of the variable (step of 10). We can conclude that these results match fairly well. Hereafter, in all studies, this antenna configuration is used.

4.2.4 CDF of the access distance

We have also obtained the CDF of access distance for various orders of distributed antennas with units located in optimum positions. From the Figure 4.4, it can be
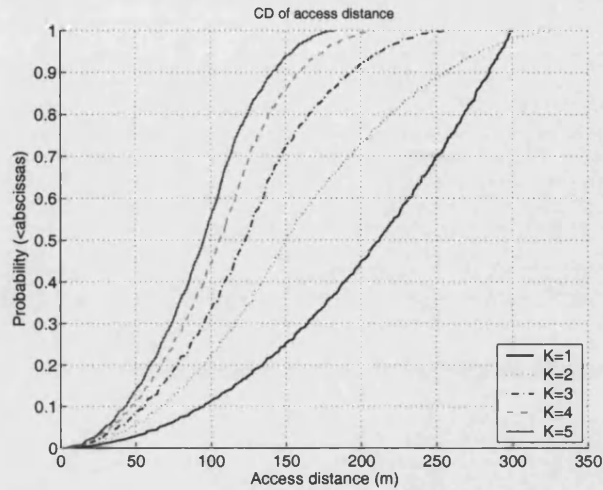
Figure 4.4: CD of access distances

seen that as more antenna units are deployed, access distance in the area is reduced dramatically. For 90% access distance exceedance, access distance for 5 antenna case has almost half the access distance of the single antenna.

4.3 Urban area coverage performance

4.3.1 Propagation characteristics

Propagation in urban areas has some special features. In built-up areas where antenna heights are lower than the surrounding buildings, the propagation paths are submerged in the environment. The propagation conditions are highly influenced in this case by the details of the environment, especially the planar features [40, 4, 6].

The coverage area comprises street canyons bounded by buildings and received signal strength when the mobile station is in the same street as the base station is around 10 dB higher than when they are in perpendicular streets. This loss is caused by blockage. The more rows of buildings there are between the two stations, the higher is the blockage loss. Blockage loss is investigated in the following sections.
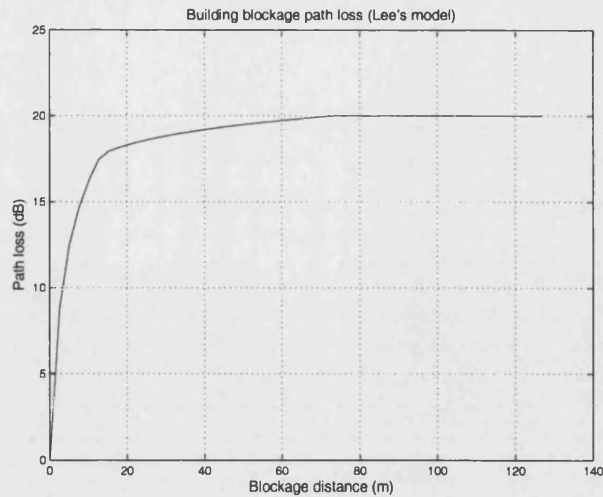
Figure 4.5: Path loss due to the building blockage (from Lee's model)

4.3.2 Two-dimensional ray tracing

Although on-site measurement gives highly accurate information, the effort to measure several outdoor environments is generally too great to be practiced. We therefore turn to ray tracing, another site-specific physical model.

The ray tracer works out the paths taken as radio waves travel through a complicated environment. As the radio frequency has longer wavelength than light, there are some significant differences between the implementation of optical ray tracing and radio wave ray tracing. Two-dimensional ray tracing [19] is used, which can give enough accuracy, but less CPU run time.

4.3.3 Parameterized artificial environments

Being a site-specific physical model, ray tracing only works on a digitized database of the propagation environment, which normally includes information of the topology, buildings and vegetation as well as electrical properties.

There is much evidence that urban environment features such as building widths, separations etc, fundamentally influence the radio propagation [33]. We have therefore modeled this type of environment by a grid of building blocks with parameterized building separation and building width.

We choose a micro-cell with the coverage area of 303 m×303 m. We assume a grid-

like floor plan of the buildings in the cell. This is similar to a typical urban area in a highly modern city. In a micro cell, the dimensions of the scatterers and the open area will influence the propagation characteristic greatly. We use building block size and street width to parameterize the environment. We perform the investigation using a catalogue of such environments. We select some typical parameters derived from statistics found in the open literature [33]. The typical value of these environment parameters in different type of environment is shown in the Table 4.2.

Table 4.2: Category of typical environments (after [33])

Land usage	Building width	Street width
Village	15 m	20 m
Open village	18 m	30 m
Small town	15 m	20 m
City suburbs	15 m	20 m
City	25 m	20 m
Satellite city	30 m	15 m
Industry	20 m	20 m

For the building width, we select the largest one 30 m, a typical one 15 m and a smallest one 6 m. For the street width, we select a largest one 30 m, a typical one 20 m, a small one 15 m. After combination, we get a catalogue of 9 environments. For each environment, a land-usage factor [5, 49] is derived from the two parameters, which gives a simple metric of the environment. The parameters for the environment are shown in the following Table 4.3.

Table 4.3: Parameterized artificial environments

Env. ID	Size of Blocks	Width of Street	Usage Factor
grid-1-1	6 m × 6 m	30 m	2.5%
grid-1-2	6 m × 6 m	21 m	4%
grid-1-3	6 m × 6 m	15 m	7.6%
grid-2-1	15 m × 15 m	30 m	9%
grid-2-2	15 m × 15 m	21 m	15%
grid-2-3	15 m × 15 m	15 m	25%
grid-3-1	30 m × 30 m	30 m	16%
grid-3-2	30 m × 30 m	21 m	36%
grid-3-3	30 m × 30 m	15 m	36%

One environment is shown in Figure 4.6. The antenna in the centered is for the single central antenna case. The guideline derived previously for placing antenna units is followed in all environment configurations.
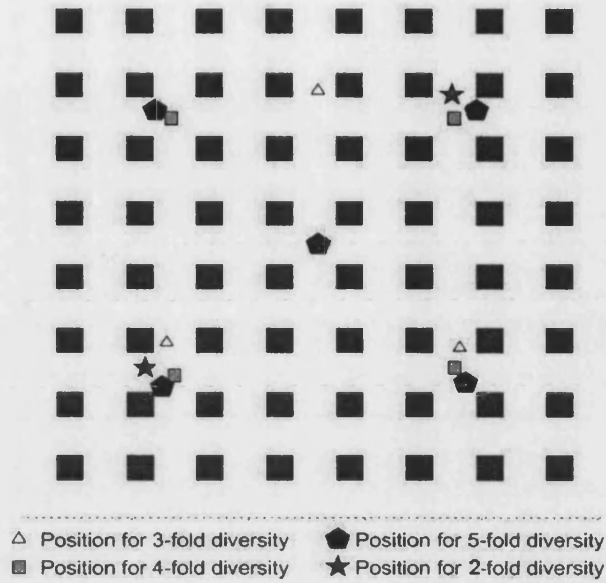
Figure 4.6: One environment example (grid-2-2)

4.3.4 Spatial resolution

The ray launching angular step is critical for the integrity of the resultant field strength. It also impacts dramatically on the run time of the ray tracing software. It depends on the spatial frequency of the environment. Before we start, we need to make sure the angular step is fine enough. For one environment (grid-3-1) in the environment category, we run the ray tracer several times with the angular step set to different values. We check the mean square difference (point-by-point over the whole area) as well as mean value and deviation, between two data sets from two consecutive iterations to find if they have converged.

Table 4.4: Spatial resolution test

Angle step	[min, max] (dBW)	[mean, median] (dBW)	Standard deviation (dB)	average rms difference
1°	[-120.1, 0]	[-105.4, -120.1]	20.5	
0.666°	[-120.1, 0]	[-105.5, -120.1]	20.6	0.9999
0.444°	[-120.1, 0]	[-105.5, -120.1]	20.6	0.2589
0.296°	[-120.1, 0]	[-105.5, -120.1]	20.6	0.0773
0.197°	[-120.1, 0]	[-105.4, -120.1]	20.6	0.0240
0.132°	[-120.1, 0]	[-105.4, -120.1]	20.6	0.0075
0.088°	[-120.1, 0]	[-105.4, -120.1]	20.6	0.0024

From Table 4.4, it is observed that from an angular step of 0.666° to 0.444°, the rms difference drops dramatically. An angular step of 0.5° was therefore chosen as a trade-off between good resolution and computational efficiency.

4.3.5   Statistics of received signal power

In each environment, the path loss from every mobile station to each antenna unit of the base station is estimated using the ray tracer. The signal strength from each branch is combined. After obtaining the signal strength for each antenna unit position, post-processing is performed to simulate the diversity combining. The signals are co-phased before combining so that the result represents an upper-bound. The combining algorithms simulated are: switched combining (SWT) and equal gain combining (EGC).

We first study some statistics of the combined signal power sampled in the coverage area, including the mean and variance. For each combining scheme, we examine the performance of a different number antenna units (the diversity order). The diversity order ranges from 1–5. Diversity order 1 represents the single antenna case. For different diversity orders, the total transmission power is the same. For switched combining, the best signal branch is chosen. In the following Tables 4.5 and 4.6, the mean signal powers for both schemes are compared. Each row corresponds to one environment.

Table 4.5: Mean signal power (dBW) (SWT)

ENV. ID	1 ant	2 ant	3 ant	4 ant	5 ant
1-1	-83.9	-78.3	-75.5	-74.4	-72.7
1-2	-87.3	-80.0	-76.7	-75.2	-73.6
1-3	-90.7	-83.0	-78.8	-76.4	-74.7
2-1	-86.0	-80.3	-76.7	-74.8	-73.1
2-2	-88.7	-82.6	-77.8	-74.8	-74.0
2-3	-92.0	-84.0	-79.6	-78.8	-73.8
3-1	-84.3	-79.7	-76.0	-74.7	-72.9
3-2	-88.8	-85.7	-79.1	-77.8	-73.5
3-3	-92.7	-88.0	-81.2	-80.3	-74.8

As more antennas are deployed, the mean signal power increases for all environments. For the same diversity order, using EGC achieves higher mean signal power than SWT. It is observed that the narrower the street, the higher gain the distributed antenna achieves. This trend is obvious when the diversity order is small (2–3). For the same building width, the gain for different street widths is more than 1 dB. In the case of diversity order 5, the gain is less than 1 dB. This gain improvement with increasing diversity order saturates.

Table 4.6: Mean signal power (dBW) (EGC)

ENV. ID	1 ant	2 ant	3 ant	4 ant	5
1-1	-83.9	-76.0	-71.5	-68.3	-66.7
1-2	-87.3	-78.2	-73.4	-70.0	-68.5
1-3	-90.7	-81.3	-76.0	-72.5	-70.8
2-1	-86.0	-78.6	-73.3	-69.5	-68.2
2-2	-88.7	-81.0	-75.0	-71.5	-69.9
2-3	-92.0	-82.4	-77.0	-75.0	-70.7
3-1	-84.3	-77.6	-72.6	-69.6	-67.4
3-2	-88.8	-84.1	-76.7	-73.6	-69.8
3-3	-92.7	-86.1	-78.6	-76.2	-71.0

Next, we examine the signal power variation over the cell in Tables 4.7 and 4.8. We observe that the diversity scheme also decreases signal fluctuation. The improvement in signal variation results in a standard deviation that is halved from the single antenna to the 2-antenna case.

Table 4.7: Variation of signal power (dB) (SWT)

ENV. ID	1 ant	2 ant	3 ant	4 ant	5 ant
1-1	12.2	7.6	6.4	6.0	5.8
1-2	14.5	8.8	7.4	7.1	6.9
1-3	16.5	13.0	10.3	9.0	7.7
2-1	13.7	9.3	8.0	9.0	6.5
2-2	15.8	13.3	9.6	7.9	7.5
2-3	17.7	15.3	12.1	11.4	7.7
3-1	11.9	10.2	7.3	7.1	6.3
3-2	17.2	16.7	12.0	10.6	9.1
3-3	19.1	18.9	14.6	13.0	10.9

Table 4.8: Variation of signal power (dB) (EGC)

ENV. ID	1 ant	2 ant	3 ant	4 ant	5 ant
1-1	12.2	6.9	5.6	4.9	4.5
1-2	14.5	8.1	6.7	6.3	5.6
1-3	16.5	11.9	9.5	8.4	6.5
2-1	13.7	8.5	7.1	6.1	5.0
2-2	15.8	12.1	8.9	7.4	6.6
2-3	17.7	13.9	11.1	10.3	7.0
3-1	11.9	9.4	6.6	6.4	5.2
3-2	17.2	15.0	10.9	9.9	7.9
3-3	19.1	16.8	12.7	11.6	9.5

4.3.6 CD of signal power

Mean and variation give us only first order statistics of the signal power. The CDF of the signal power is a better performance indicator and reveals the fraction of area in the cell that receives adequate service in terms of signal strength. The following two Figures 4.7 and 4.8 show the CDF of signal power for switched combining and equal gain combining for environment grid-2-2. The x-axis is signal power. The y-axis is the probability that received signal strength is less than the abscissa.
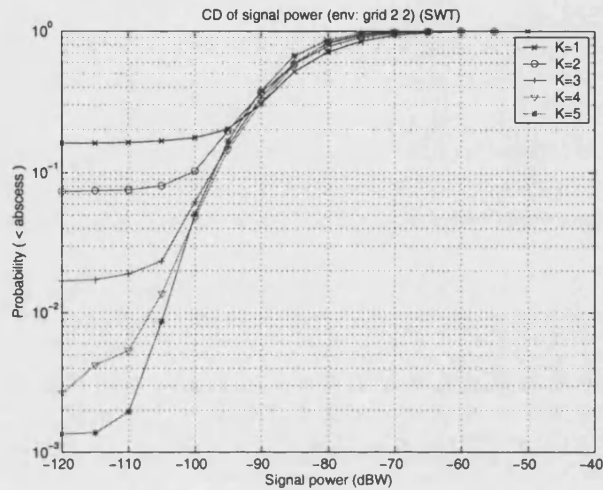
Figure 4.7: CD of signal power (SWT)
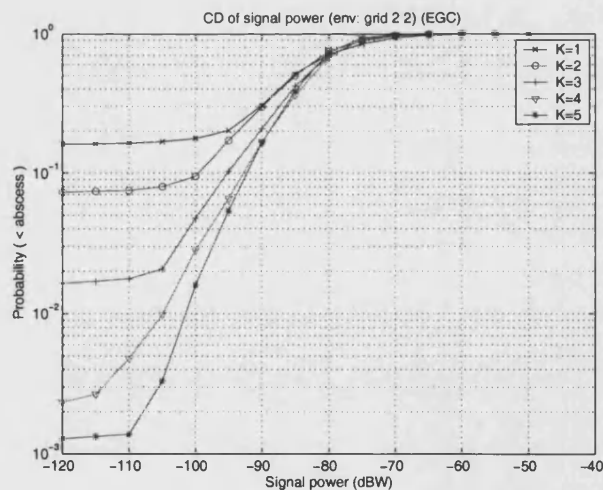
Figure 4.8: CD of signal power (EGC)

From the Figures 4.7 and 4.8, we see that the area suffering outage (signal power less than the abscissa) shrinks dramatically as more antennas are installed in the cell.

This can be explained by the following observation. When one antenna is installed (at the cell centre), there is a large area near the cell boundary which is shadowed by several building blocks. As more antennas are deployed, those areas could be served by a nearby antenna. In consequence, the blockage between the transmitter and receiver decreases. More area is thus served with higher signal power in the distributed antenna case.

4.4 Indoor coverage performance

4.4.1 On-site measurement and channel sounder

For the indoor area, we now turn to on-site measurements. The distributed antenna supports several simultaneous channels. To conserve the multiple channel structure, especially their time variation property, we need to measure these multiple channel simultaneously (or quasi-simultaneously). In the measurement, we use a wide-band MIMO channel sounder, which has the capability to obtain high resolution, quasi-simultaneous measurements.
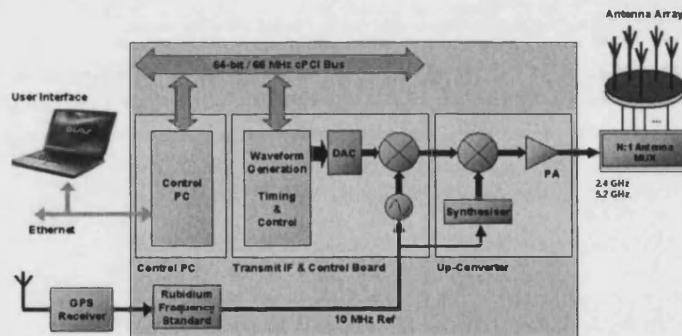
Figure 4.9: Diagram for channel sounder transmitter

This channel sounder, developed by QinetiQ, can be divided into transmit and receive subsystems, which are shown in Figures 4.9 and 4.10. Each subsystem comprises a primary transmit or receive unit, a 16-way antenna multiplexer (connected to the primary transmit/receive unit via 5 m of coaxial cable) and a laptop PC to provide a user control interface via Ethernet. The transmission loss of the cable is shown in the Table 4.10, which will be later used to compensate for the measurement result of each antenna. In the receive subsystem, a Fast Data Storage Unit (FDSU), comprising fourteen 73-GB hard-drives, is used to store raw Complex Impulse Responses (CIR). In order for data that is captured and stored by the receive subsystem to be post-processed for further analysis, an Ethernet interface allows stored data to be transferred from the FDSU to
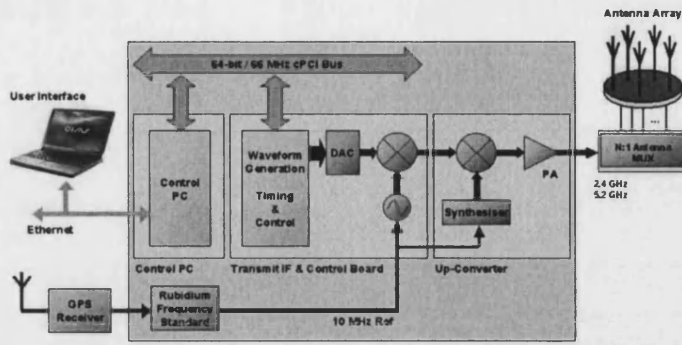
Figure 4.10: Diagram for channel sounder receiver

an auxiliary PC/network.

The sounder employs pulse compression. The default sounding waveform is a single-sideband BPSK modulated maximal length Pseudo-Noise (PN) sounding sequence with a maximum chip rate of 165 Mchip/s. Pulse shaping ensures that better than 50 dB peak-to-sidelobe ratio can be achieved following back-to-back calibration of the transmit and receive units. The PN sequences are chosen such that their length is equal to the required measurement delay time range (5 or 10 μs). Since implementation is software controlled, any desired sounding waveform (including FM chirps) can be realized. Tetherless operation is possible using Global Positioning System (GPS) disciplined rubidium frequency standards. The storage capacity allows approximately 50 minutes of data to be recorded at the maximum data acquisition speed. The sounder's principal operating parameters are listed in the Table 4.9.

Table 4.9: Parameters of channel sounder

Band centre frequencies	990 MHz, 2.442 GHz, 5.4375 GHz
Band tuning range	200 MHz
Maximum sounding band-width	500 MHz
Delay resolution	7 ns (for 250 MHz bandwidth, equal amplitude paths)
	15 ns (for 500 MHz bandwidth, 0 dB and -40 dB adjacent paths)
Maximum unambiguous delay	5 μs or 10 μs
Maximum transmitter power	30 dBm
Data acquisition modes	free-run, triggered Maximum free-run
Data acquisition rate	10,000 CIR/s in 5 μs mode
Maximum data storage	1 TB
MIMO capability	Any n × m ($n \leqslant 16$, $m \leqslant 16$)

The sounder measures the wideband, time-varying, CIR of the equivalent baseband channels between 16 transmitter output ports and 16 receiver input ports. It has been designed, primarily, to allow MIMO characterization of the radio channels. The capability to measure Single Input Multiple Output (SIMO) and MIMO channels is realized using a high-speed, digitally-controlled, 16-way antenna multiplexer at both the transmitter and receiver. Measurements are made on each receive antenna in turn before the transmit signal is switched to the next antenna in the series (to minimize RF switching transients). Power is not transmitted during the time that the antenna multiplexer is switched between channels. The multiplexer cycles between channels sufficiently quickly such that for practical engineering purposes the set of CIRs comprising a MIMO measurement can be assumed to be made simultaneously.

4.4.2   Measurement environment

The measurements were made on the fourth floor of the Department of Electronic and Electrical Engineering at the University of Bath. The measured area (approximately 27 m × 11 m), is bounded by the solid line in Figure 4.11). The area includes three laboratories and one corridor. The internal walls are constructed, principally, of plasterboard. In laboratory 4.15 and 4.13, there are desks separated by free-standing partitions. There are some small metal cabinets placed along the walls.

Three transmit antennas and one receive antenna are used in the measurements. All are sleeve dipoles tuned to the measurement frequency of 2.4 GHz. The antennas are mounted on tripods at a height above the ground of 1.5 m. One transmit antenna is located in each laboratory. The antenna in lab 4.13 is identified as 1, the antenna in lab 4.15 as 2 and the antenna in lab 4.1 as 3. All three transmit and one receiver antennas are connected, via low loss coaxial cable (see Table 4.10), to the channel sounder's transmit/receiver multiplexer.

Table 4.10: Cable Loss

@2.4GHz	Length (m)	Cable Loss (dB)
Cable RX	2.2	1.8
Cable Tx 1	2.2	1.8
Cable Tx 2	22.5	16.6
Cable Tx 3	22.5	12.8

There are two sets of transmit antenna locations (although in lab 4.13 the antenna location remains unchanged, see Figure 4.11). In set 1, the antenna units are placed in the far corner in the respective laboratory. In set 2 they are placed in the middle along

the wall. The receive antenna locations form a 1 m square grid (the black squares in Figure 4.11) within the measurement area.

The CIRs of the three channels are measured sequentially, at each receive location, in a period that is short enough to deem them simultaneous. After the measurement, two data sets have been acquired, each of which has three groups of CIR measurements corresponding to each transmit antenna unit.

×   **TX Antenna set 1**

◫   **TX Antenna set 2**

■   **RX Antenna Location**
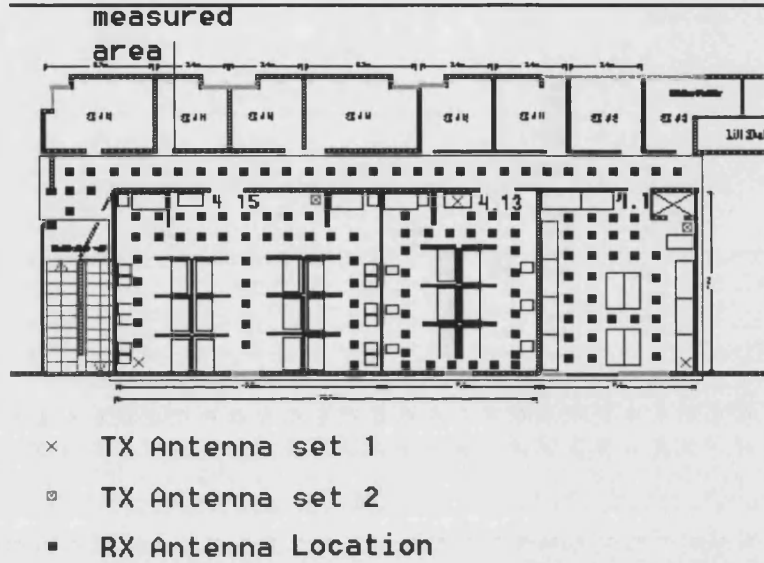
Figure 4.11: Floor plan of 4 floor in EE Department

4.4.3   Statistical analysis of the measurements

The channel response is expressed as a discrete power delay profile [55], where $\alpha(n)$ is the complex amplitude of each multipath component, i.e.:

$$h(t) = \sum_{n=-\infty}^{\infty} \alpha(n)\delta(t - \tau(n)) \tag{4.4.1}$$

For narrow-band signaling, the delay spread of the signal is relatively small compared to the width of the transmitted symbol. The equivalent narrow-band complex envelope is the vectorial summation of all multipath signals, i.e.:

$$r_c = \sum_{-\infty}^{\infty} \alpha(n) \tag{4.4.2}$$

We use equation (4.4.2) to process the measured CIR to obtain the complex envelope for each antenna at every receiving position. We then simulate the two diversity schemes: switched combining and equal gain combining. After processing the entire set of channel response we obtain a set of complex signal envelopes. In following Tables 4.11 and 4.12, we tabulate the mean and variance for each antenna configuration.

Table 4.11: Statistics for antenna set I

No. Ant	Mean (dB)		Variation (dB)	
	SWT	EGC	SWT	EGC
1 Ant	51.8	51.8	55.2	55.2
2 Ant	51.9	53.1	54.8	56.3
3 Ant	53.4	55.5	56.0	58.1

Table 4.12: Statistics for antenna set II

No. Ant	Mean (dB)		Variation (dB)	
	SWT	EGC	SWT	EGC
1 Ant	48.1	48.1	52.1	52.1
2 Ant	51.1	51.4	53.8	53.8
3 Ant	52.3	53.1	54.4	54.7

From Table 4.11 and 4.12, it is observed that the distributed antenna has greater mean signal strength. The gain is different, however, for different antenna positions. Antenna set 2 has greater gain compared to the single antenna. This is because the antenna units are moved from the edge of the "cell" towards the middle, which is closer to the optimal antenna positions derived previously.
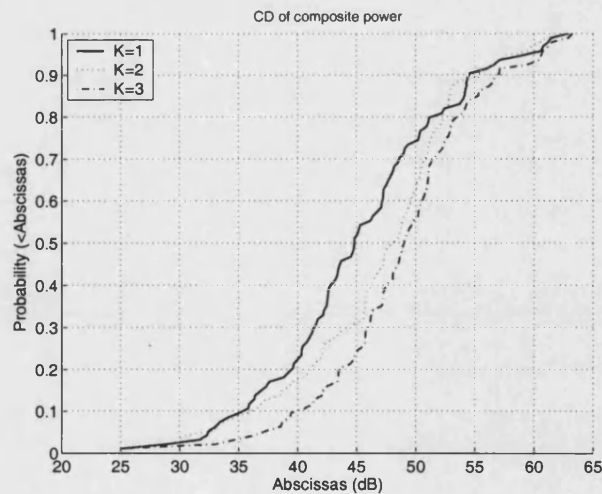
Figure 4.12: CD of signal power (SWT, set 1)
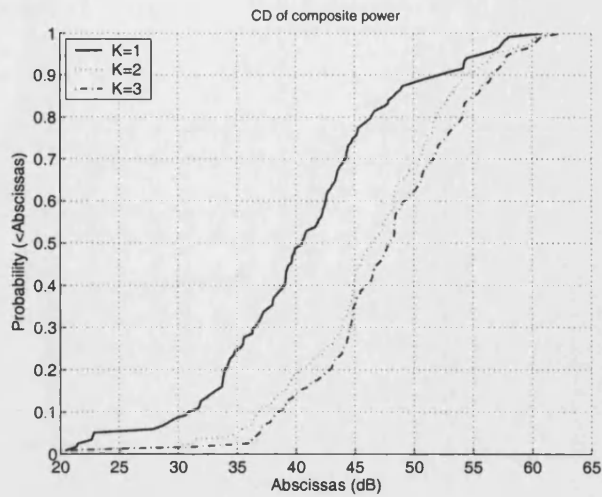
Figure 4.13: CD of signal power (SWT, set 2)
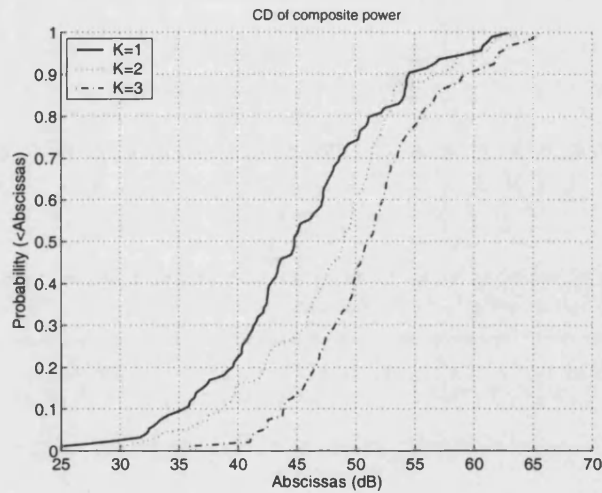
Figure 4.14: CD of signal power (EGC, set 1)

We compare here the CDF of the resulting signal strength for both diversity schemes. Figures 4.12 and 4.13 show the selective combining results for both antenna sets and Figures 4.14 and 4.15 for the equal gain combining. We notice that at 90% SIR exceedance, the distributed antenna with two and three antenna units achieves more than 5 dB gain in signal power. The EGC scheme has better gain than the SWT scheme by around 5 dB. Comparing the two data sets, we found that in data set 2, the gain achieved by using two and three antenna units for both diversity schemes is higher.

50
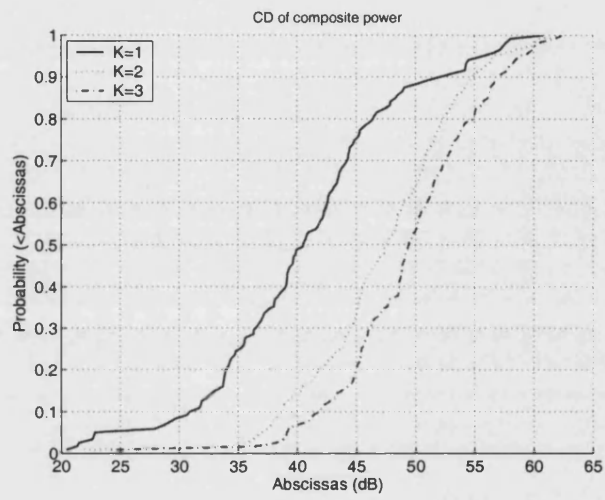
Figure 4.15: CD of signal power (EGC, set 2)

Chapter 5

WIDEBAND TRANSMISSION DIVERSITY

On the uplink, each antenna unit of a distributed antenna independently receives signals propagating via different paths, therefore benefitting from diversity gain. On the downlink, however, since all base station antenna units transmit the same signal simultaneously (as in a simulcast system [80]), signals sum at the antenna before the mobile station can separate them. The advantage of multiple propagation paths antenna cannot therefore be fully utilized, resulting in inferior performance than uplink.

Many services however have asymmetric traffic, with the downlink having higher data rate than the uplink. For a distributed antenna, the downlink could therefore be a system performance bottleneck .

In this chapter, we study wideband transmission diversity in an indoor environment using measurements. Firstly, we make some observations about measured CIRs. A detailed examination of the CIRs shows that phase variation between adjacent components is small, especially within a time window containing the majority of the CIR energy. Based on this observation, we propose a co-phasing transmission diversity technique which adjusts the timing and phase of the transmitted signal at each antenna unit such that the peak component of the CIR from each branch is aligned in time and phase. Then we use the measured CIRs at multiple antenna units to simulate a transmission diversity scheme and evaluate its performance.

5.1 Wideband channel model

5.1.1 CIR metrics

If we use a finite tapped delay line model, the CIR expressed in equation (4.4.1) can be expressed as:

$$h(t) = \sum_{n=1}^{L} \alpha(n)\delta(t - \tau(n)) \qquad (5.1.1)$$

There are two important metrics to describe the quality of a multipath channel: gross power and rms delay spread. Gross power reflects how much energy is delivered to the receiver and is related to the delay line model parameters by:

$$P_{tot} = \sum_{n=1}^{L} |\alpha(n)|^2 \qquad (5.1.2)$$

Rms delay spread summarizes the time dispersion introduced by the multipath propagation. It is related to the delay line model parameters by:

$$T_{rms} = \sum_{n=1}^{L} \frac{|\alpha(n)|^2}{P_{tot}} (\tau(n) - \bar{\tau}) \qquad (5.1.3)$$

where

$$\bar{\tau} = \frac{1}{P_{tot}} \sum_{n=1}^{L} |\alpha(n)|^2 \tau(n) \qquad (5.1.4)$$

In a wideband system, signal bandwidth is larger than the coherence bandwidth (approximately the reciprocal of the rms delay spread) and so that channel is frequency selective. The RAKE receiver performs optimal reception of frequency selective channel. Assuming perfect channel information, the output of the RAKE receiver represents the gross power of the channel response. Since the multipath components are spaced by more than the reciprocal of the bandwidth of the signal (wideband signaling), each of these paths can be resolved in RAKE receiver. Therefore, all the power P_{tot} can be collected.

5.1.2 CIR integrity check

COST 231 [12] has defined a way to verify the validity of measured CIR data. It states that a valid CIR must have a 15dB clearance between its peak value and the noise floor. When calculating the metrics from the measured CIR, only sample points above the noise floor is used (see Figure 5.1).
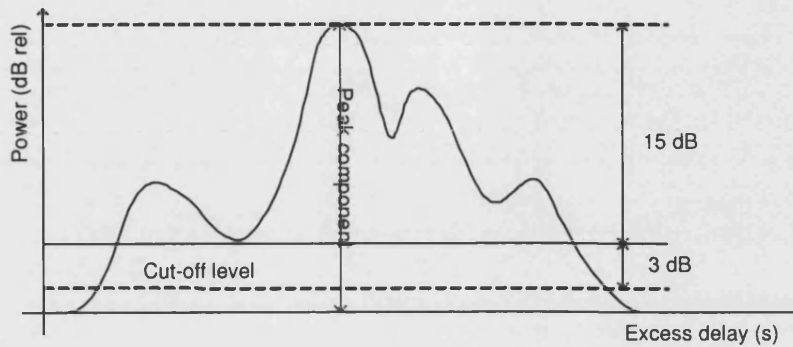
Figure 5.1: CIR integrity checking

5.1.3 X-dB peak window

We define an X-dB window with respect to the CIR peak value, in which most of the power concentrate. The window is delineated by two cut-off points, which are X dB from to the peak (see Figure 5.2). We denote the two cut-off points t_d and t_u, with the
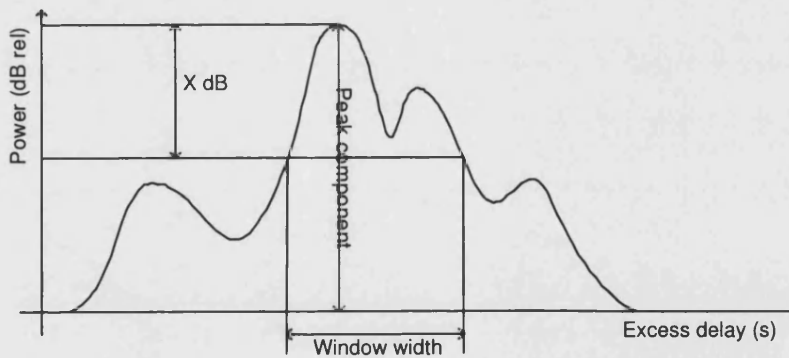
Figure 5.2: X-dB peak Window

peak as t_p. In the discrete form, they are n_d, n_u and n_p. The width of the first half window is T_f and second half as T_s. It is worth noting that these two width are not necessarily the same because the peak is not always symmetrical to the peak point.

5.1.4 Problem of transmission diversity

The channel response from each antenna unit is denoted by $h_i(t), i \in [1, K]$. We assume the signal from branch 1, $h_1(t)$, arrives first. We define the arrival time as that of the peak of the CIR rather than the earliest multipath component. If we use the peak of $h_1(t)$ as a reference, we can define the arrival time of other signal components with respect to this and denote them as T_i ($T_1 = 0$).

We assume that the initial phase and time delay of the signal transmitted from each antenna unit can be controlled separately. The time delay is denoted as ΔT_i and the initial phase as φ_i.

In contrast to the uplink, in which transmitted signal is received independently at the multiple antenna units, the transmitted downlink signals from the antenna units sum at the mobile station's single antenna. The signal at the mobile station is thus expressed by:

$$h_c(t) = \sum_{i=1}^{K} h_i(t - \Delta T_i)e^{j\varphi_i} \tag{5.1.5}$$

The object of transmission diversity is to determine ΔT_i and φ_i to achieve a maximum gross power of $h_c(t)$.

5.2 Multipath antenna diversity

5.2.1 Principles

In spread spectrum signaling, multipath components with sufficiently different time delay can be isolated by a RAKE receiver. Taking advantage of this feature, [82] proposes that delay is intentionally introduced between signal branches (i.e. different antenna units). These signals present themselves as multipath components in the RAKE receiver which can then be combined independently. We call this multipath antenna diversity.

The processing center can estimate the path length between a mobile station and each antenna unit and the time dispersion of each antenna unit branch. This information can be used to actively adjust downlink transmission timing so that the signals in all

branches do not overlap. The phase does not need adjustment.

5.2.2 Implementation
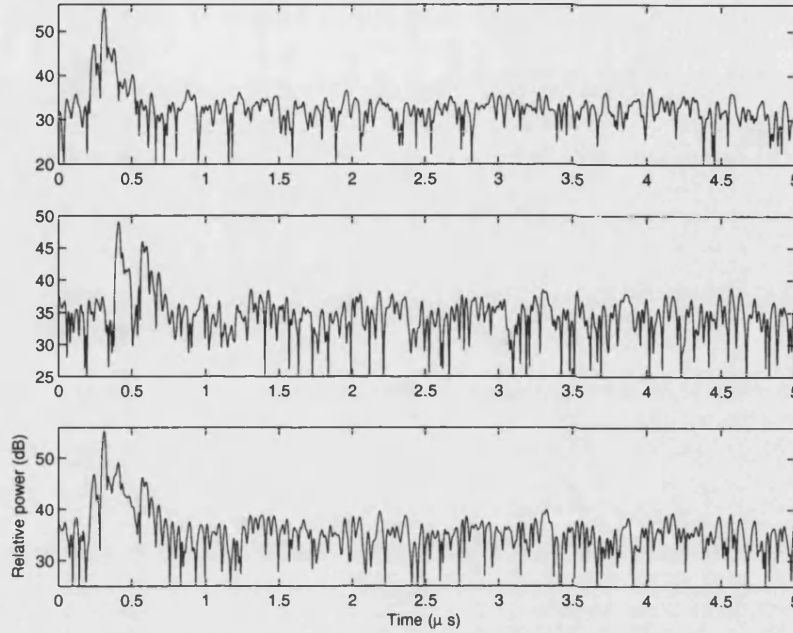
Figure 5.3: Multipath antenna diversity example

We use an X-dB window to determine the differential delay between at each units. Each branch channel (from one antenna unit to the mobile-station) has a different CIR and the X-dB window has different width. The delay is set such that signals from all branches arrive at the mobile station with their X dB windows closely adjacent to each other, but without any overlapping.

In iterative form, the time shift for each signal branch with increasing index is:

$$
\begin{aligned}
\Delta T_i &= t'_{p,i-1} + t_{u,i} - (t_{p,i} - t_{d,i}), \ i > 1 \\
t'_{p,i} &= t_{p,i} + \Delta T_i \\
\Delta T_1 &= 0
\end{aligned}
\tag{5.2.1}
$$

where t'_p is the new peak component position after time shifting. By using the X-dB window, it is assured that the powers within the windows from all antenna units will not sum with random phase. Inevitably, the signals overlap outside the window, but the power involved is small. The deeper the window (i.e. the larger is X), the less energy

5.2   56

overlaps but this results long delay and long tap delay lines in the RAKE receiver. Trade off between these two contradictory goals is realized by adjusting the depth of the window.

5.3 Co-phasing transmission diversity

5.3.1 Conjecture

Multipath antenna diversity sums the power from all antenna units by avoiding overlap of CIRs. If the components can be summed in-phase, greater gain will be achieved than power-wise addition since each multipath component has independent phase. This requires not only timing, but also the phase angle of the signal transmitted from each antenna unit to be adjusted. This may be a difficult requirement to implement practically.

5.3.2 Observation of CIR

Based on measured CIRs, we first study the phase variation between multipath components. In discrete form, we define differential phase angle to represent the phase angle difference between two adjacent components:

$$\Delta\phi(n) = \phi(n) - \phi(n-1) \tag{5.3.1}$$

Since the CIR sample period is approximately one tenth of the delay resolution every tenth sample may be considered to represent.

First, we examine the cumulative distribution of differential phase angle sampled at all time instants of all measured CIRs. Figure 5.4 shows that 80% of components have differential phase angle less than 60°.

When we narrow down the observation of differential phase with a 6-dB window, we find that the probability of small phase difference is higher. The analysis shows that 90% of maximum phase difference within the window is within 60°.

We also observe the maximum phase difference between peak components and around the peak components. The maximum phase shift ϕ_m within the 6-dB window is defined
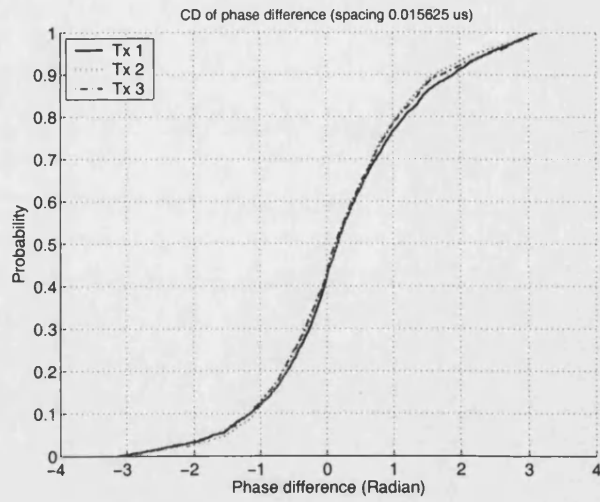
Figure 5.4: CD of differential phase angle
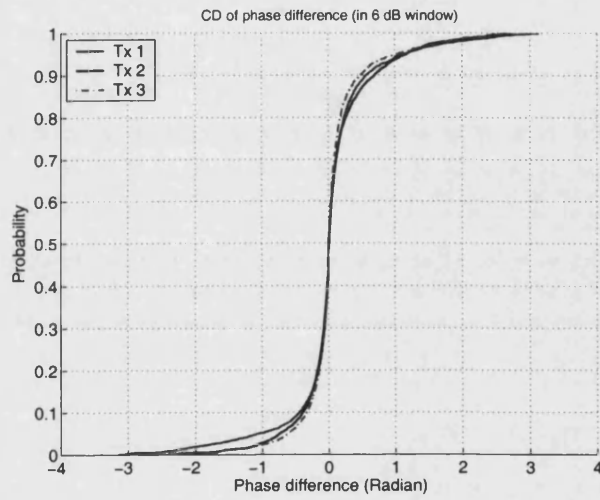
Figure 5.5: CD of differential phase angle inside 6-dB window

by:

$$\phi_m = \max_n \phi(n) - \phi(n_p) \qquad (5.3.2)$$

where:

$$n_p = \arg\max_n \alpha(n), n \in [n_d, n_u] \qquad (5.3.3)$$

The CDF of maximum phase difference, Figure 5.6, shows that approximately 90% of
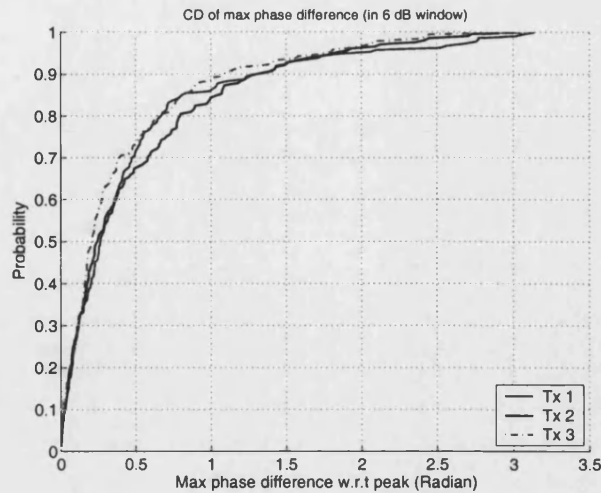
Figure 5.6: CD of maximal phase different w.r.t peak component

the samples have a maximum phase shift less than 60°.

The results suggest that the sequence of phase angles in a CIR vary slowly. The explanation of this is that two components arriving at close by spaced time instants tend to propagate via similar paths. They therefore undergo similar phase shifts during propagation. (Conversely the probability that two signals propagating over very different path arrive close spaced in time is small.)

It is appreciated that absolute phase angle follows a uniform distribution, but this does not contradict the observation described obtained above.

The observation of the maximum phase shift relative to the peak component suggests that if the peaks of two delay profiles are time aligned and co-phased then the component pairs within the 6 dB windows are likely to have less than 60° phase angle difference.

5.3.3   Co-phasing transmission diversity

The study of phase angle in a CIR suggests that a co-phasing transmission diversity scheme is possible. Assuming the downlink CIR is known at the base station, the timing and phase of the signal at each antenna unit can be adjusted so that all CIRs would be aligned with respect to their peak components and these peak components will be co-phased.

5.3   59

At each antenna unit therefore each signal is advanced by ΔT_i and adjusted in phase. This scheme is shown in Figure 5.7. The signal transmitted from each antenna is received as:

$$
\begin{aligned}
r_i &= s_i(t + \Delta T_i)e^{j\varphi_i} \\
\Delta T_i &= t_{p,i} - t_{p,1} \\
\varphi_i &= \phi_i(t_{p,i}) - \phi_1(t_{p,1})
\end{aligned}
\tag{5.3.4}
$$
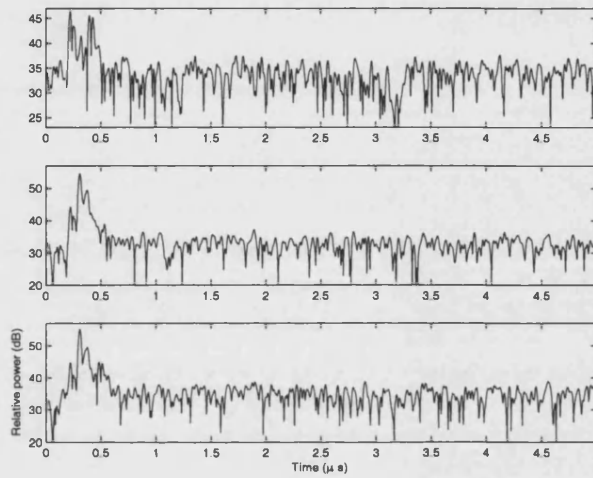
Figure 5.7: Co-phasing transmission diversity example

The scheme can only assure proper co-phasing of the CIR peak components. Since the phase angle of adjacent component changes only modestly within the 6 dB window, however the remaining components will, with high probability, sum approximately constructively.

The gain achieved by nearly co-phasing can be shown in a example. Given two complex signals A and B with phase angle θ, the signal power of the vectorial summation of A and B can be expressed as:

$$
|A + B|^2 = |A|^2 + |B|^2 + 2|A||B|\cos(\theta)
\tag{5.3.5}
$$

The gain G_r of the vectorial summation relative to the power-wise summation can be

expressed as:

$$G_r = \frac{|A+B|^2}{|A|^2 + |B|^2}$$
$$= 1 + \frac{2AB\cos(\theta)}{A^2 + B^2} \tag{5.3.6}$$

If the phase angle is less than $60°$ (as in equation (5.3.5)), the gain G_r will be lower bound by $G_r > 10\log(3/2) = 1.76\,\text{dB}$ provided $|A| = |B|$.

5.4 Performance evaluation

5.4.1 Gain bound

Compared to MultiPath Antenna (MPA) diversity, Co-Phasing Transmission (CPT) diversity will have larger received power because of close to constructive summation at each multipath component position.

If the multipath profile consist of L components, the gain of the distributed antenna relative to power-wise addition can be expressed by equation (5.4.1). If we assume the total power of the delay profile is constant, then L is trivial to this gain expression. The gain depends on phase difference at each location. The upper bound of this gain occurs when the phase difference is $0°$ at every multipath position.

$$G_r = \frac{\sum_{n=1}^{L}(\alpha_a^2(n) + \alpha_b^2(n) + 2\alpha_a(n)\alpha_b(n)\cos(\theta_n))}{\sum_{n=1}^{L}\alpha_a^2(n) + \sum_n \alpha_b^2(n)}$$
$$\leq 1 + \frac{\sum_{n=1}^{L}2\alpha_a(n)\alpha_b(n)}{\sum_{n=1}^{L}\alpha_a^2(i) + \alpha_b^2(i)} \tag{5.4.1}$$

If we assume that CIRs from both diversity branches have the same impulse response,

i.e. $h_l(n)$, but with different total power a and b. Then G_r can be expressed by:

$$G_r = \frac{\sum_{n=1}^{L}(\alpha^2(n)(a^2+b^2+2ab)}{(\sum_{n=1}^{L}\alpha^2(n))(a^2+b^2)} \qquad (5.4.2)$$

Applying the Schwartz inequality, we get:

$$1 \leq G_r \leq 2 \qquad (5.4.3)$$

The maximal gain is achieved when the two branches have equal total power, equivalently i.e. $a = b$.

5.4.2 Combining performance comparison

In the development of the gain bound, we assume the delay profiles are exactly the same and the phase difference at every instant is $0°$. We can use the measured CIRs to evaluate the actual performance of co-phasing transmission diversity and compare it against the MPA scheme. For the comparison, the total power of all CIRs has been normalized so that all combinations are realized using balanced power branches, i.e. the CIR from each branch has the same total power.

We also simulate an ideal scheme (that will give the upper bound performance), in which we assume that the phase angle of each individual multipath component is precisely co-phased at every instant. We use this as a reference point to investigate that the compromised gain due to imperfect co-phasing of all other but the peak multipath components.

In Figure 5.8, each curve shows the gross power of a different combining scheme at each receiving position. The performance of CPT is the curve labeled Pow Cpeak. The curve labeled Pow sum, which represents the performance of MPA scheme. The ideal combining result labeled Pow ceach, which represents an ideal upper bound.

It is shown that for the ideal case, the total power of the combined result is not constant for all samples. This is because the delay profiles of all branches are not the same. The delay profile determines the distribution of the total power between the multipath components, which in turn determines the combined result.

If we compare the MPA scheme and CPT scheme by examining the relative gain be-
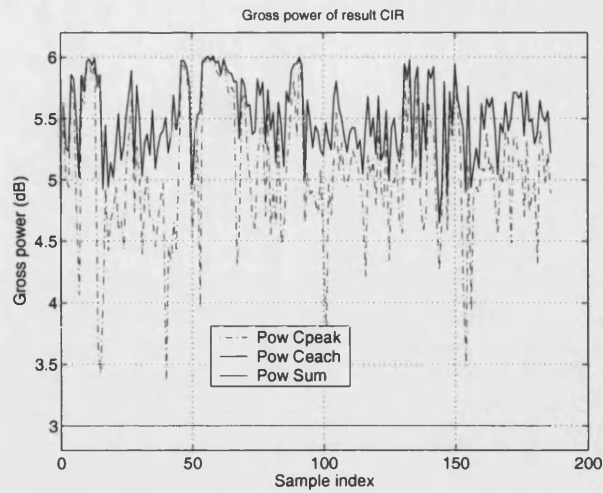
Figure 5.8: Comparison of combined signal power for all diversity schemes
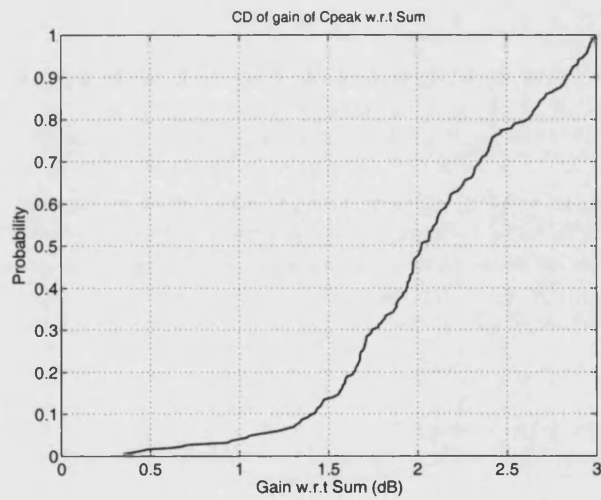
Figure 5.9: CD of relative diversity gain

tween them, we obtain the CDF in Figure 5.9. Approximately 90 % of samples have gain greater than 2.5 dB.

We also look at the negative gain of CPT with respect to the upper bound. By examining the CDF in Figure 5.10, we see that, due to imperfect phase alignment of components other than the peaks, in more than 90% of locations, the gain difference (loss) is less than 0.9 dB.

5.4   63
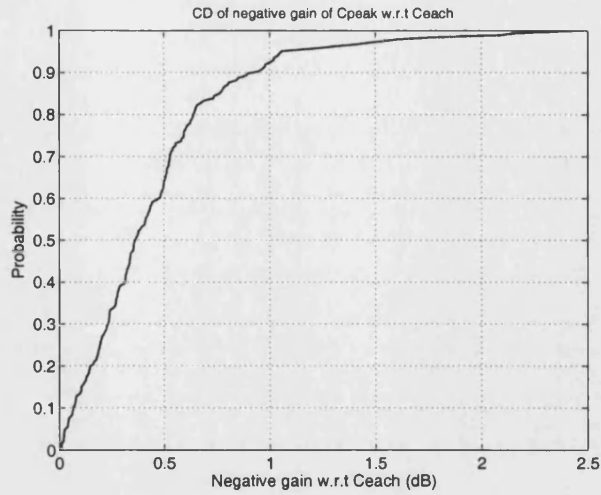
Figure 5.10: CD of negative gain w.r.t Ceach

5.4.3 Coverage performance

Now, we examine the coverage of diversity schemes using measured CIRs (without normalization). At every receiving location, this simulation generates a CIR using each different transmission diversity scheme.

We use the mean gross power of combined CIRs averaged over the whole measurement area as a coverage metric. To compare the various diversity schemes, we calculate the ratio between the mean gross powers of each diversity scheme and the single antenna scheme. These ratios are shown, along with the variance of received gross power, in Tables 5.1 and 5.2. The keys used in the tables are: $SEL(K) =$ Selective diversity order K; $MPA(K) =$ multipath antenna diversity order K; $CPT(K) =$ co-phasing transmit diversity order K.

Table 5.1: Mean gross power (data set I)

Diversity scheme	Mean power ratio w.r.t no diversity (dB)	Variance(dB)
None	0	42.4
SEL(2)	0.7	42.5
SEL(3)	1.9	43.5
MPA(2)	2.5	44.5
MPA(3)	4.7	46.2
CPT(2)	4.8	47.0
CPT(3)	8.2	50.0

Table 5.2: Mean gross power (data set II)

Diversity scheme	Mean power ratio w.r.t no diversity (dB)	Variance (dB)
None	0	38.4
SEL(2)	3.7	40.7
SEL(3)	4.6	41.0
MPA(2)	4.4	41.0
MPA(3)	5.9	41.7
CPT(2)	5.2	41.3
CPT(3)	8.1	44.1

It is observed that multipath antenna diversity and co-phase transmission diversity have the largest mean gross powers. This is because these two schemes make use of signals from all antenna units. The co-phasing transmission scheme has the best coverage. It achieves approximately a 3 dB advantage over multipath antenna diversity with the same number of antenna units. When comparing the results from the two data sets, it is found that the ratio of different schemes varies. This is due to the changing of the transmit antenna positions. In both data sets, the advantage of antenna diversity can be observed. Selective antenna diversity appears to be more sensitive to antenna position than co-phasing transmission diversity at least in the case of these limited measurements.

In addition to gross power, rms delay spread is another influential metric for channel quality. Even in CDMA systems which can isolate multipath components, a small delay spread means that fewer taps are required in the RAKE receiver. The statistics of rms delay spread are shown in Tables 5.3 and 5.4. Compared to selective diversity, multi-

Table 5.3: rms delay spread (data set I)

Diversity scheme	rms delay (ns)	Variance
None	25.0	7.50
SEL(2)	41.7	21.4
SEL(3)	29.6	12.2
MPA(2)	92.8	36.5
MPA(3)	128.9	38.8
CPT(2)	42.2	18.4
CPT(3)	30.0	9.5

path antenna diversity suffers longer delay spread. This is due to the delay introduced at the transmitter. Co-phasing transmit diversity has a similar delay spread to selective diversity. In contrast to multipath antenna diversity (in which delay spread increases with increasing number of antenna units) each additional signal in co-phasing transmit

Table 5.4: rms delay spread (data set II)

Diversity scheme	rms delay (ns)	Variance
None	25.0	7.9
SEL(2)	40.4	38.2
SEL(3)	28.4	35.4
MPA(2)	77.6	40.4
MPA(3)	109.7	49.0
CPT(2)	38.4	18.3
CPT(3)	28.1	10.9

diversity does not necessarily result in extra delay spread. In fact, order 3 co-phasing transmit diversity achieves reduced delay spread. It is thought that this is because the order 2 scheme employs antenna units located at the extreme ends of the measurement area. The order 3 scheme adds an antenna near the centre of the measurement area. This central antenna results in less delay spread because the propagation paths to it are more similar in length than the case for the antenna units at more extreme locations.

Chapter 6

PERFORMANCE IN A MULTIPLE-CELL ENVIRONMENT

In chapter 4, we evaluated link quality improvement of distributed antenna considering only signal strength. This could be looked on as single cell network performance. In real FDMA or TDMA systems, interference coming from other cells reusing the same frequency is a major constraint. Its degrading effects on the link quality restricts frequency reuse, therefore limits spectrum efficiency.

In this chapter, the performance of distributed antennas in a network environment is studied considering both propagation loss and inter-cell interference. This results in a more thorough evaluation of the distributed antenna system than examining it as a single cell. We also study the interference of the distributed antenna to other traditional cells which is appropriate if it is deployed in hot spots.

We will first analyze the possible influence on inter-cell interference of geometric changes in antenna position. The inter-cell interference level of the distributed antenna is then studied, isolated by observing a pair of interfering cells. Finally performance in a multi-cell network is simulated. We consider two network configurations: the distributed antenna single cell network and the distributed antenna multiple cell network. To simplify the study, we assume uniform cell radius and reuse factor in the network. We assume narrow-band signaling used in either an FDMA or TDMA system.

Although it is too ideal to be an entirely realistic environment, the comparative results

are still meaningful. The network is modeled by tessellating hexagons.

6.1 Distributed antenna position

6.1.1 Splitting transmission power

Each antenna unit transmits the same signal but only fraction of the total transmitted power. The more antenna units used, the lower the transmitted power of each antenna unit.

Interference in the victim cell thus arises from multiple sources. The received interference is the sum of the signals from all antenna units, i.e.

$$r(t) \;=\; \sum_{i=1}^{K} \sqrt{P_s} a_i e^{j\phi_i} s(t) \tag{6.1.1}$$

where $P = KP_s$. All antennas share the total power P equally. ϕ_k and a_k are the phase shift and amplitude of the received signal. If the antenna units are located at the same site but with antenna spacing larger than the coherence distance, a_k will be the same for all units and may be denoted by a_c. ϕ_k are independent and identical distributed random variables across all antenna units. We can safely say, therefore, that given a constant total power, the sum of the received signal power from the multiple antenna unit sources is less than that received from a conventional (single) source.

$$P a_c^2 \geq a_c^2 P_s \frac{1}{K} (\sum_i^{K} e^{j\phi_i})^2 \tag{6.1.2}$$

Splitting of the transmitted power leads to lower transmitted power from each antenna unit and dispersion of transmitted power at the receiver.

6.1.2 Proximity of co-channel cell

The distance between base station antenna and co-channel cell is another factor affecting interference level. In a single antenna system, the base station antenna is located at the cell centre. This gives the largest isolation distance between the interfering pair:

the base station antenna and the mobile station antenna. In the distributed antenna system, antenna units are shifted away from the cell centre toward the cell edge. Some antenna units are therefore closer to a specific co-channel cell. This reduces the isolation distance between antenna unit and mobile station in the co-channel cell so that the path loss of the interference reduces, resulting in more interference power leaking to the neighboring cell. This influences inter-cell interference, in the opposite way to reduced transmission power.

Here we compare the attenuation by considering both the reduced propagation distance and the reduction of transmitted power. We consider only that radiation from the antenna through which the line passes since it provides the greatest contribution to interference. We assume an inverse power law path loss model. To keep the total transmitted power constant, for the multiple (K) antenna units, we assume each distributed antenna unit radiates a fraction $1/K$ of the total power. For single antenna, the antenna is placed in the origin. For the distributed antenna case, the antennas are displaced from the origin by half radius (normalized cell radius). The powers received as a function of distance (d) from the cell origin, for the conventional and distributed antenna respectively, are then given, to within a constant of proportionality, by:

$$R_0(d) \quad \propto \quad \frac{1}{d^n} \tag{6.1.3}$$

$$R_K(d) \quad \propto \quad \frac{1}{K(d-1/2)^n}, K = 1,2,3,4 \tag{6.1.4}$$

n is the exponential path loss law in both cases. And in the calculation, the constant in equation (6.1.3) has been (arbitrarily) set to unity.

Figure 6.1 shows curves for these two cases (single antenna and distributed antenna with distance from the cell center measured in cell radii).

For the two antenna unit case, in the range up to three times cell radius, the change in distance is more significant than the lower transmission power, while in four antenna unit case, the range is twice the cell radius. In other words, for the two antenna case, even with half the transmitted power, within three times the cell radius, the shift away from the cell centre will cause an increase in inter-cell interference. (The distance between the centers of co-channel cells for a reuse factor of 7 is 4 times the cell radius).

Figure 6.1 is for a free space environment. In realistic environments, the path loss exponent is normally larger than 2. In Figure 6.2, we give the curves for a path loss exponent of 4. The turning point for the two antenna case becomes 6 and for the four
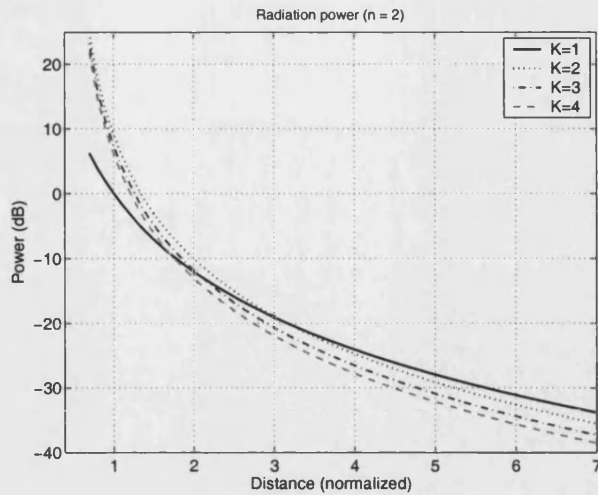
Figure 6.1: Power attenuation comparison (n=2)

antennas case becomes 3.
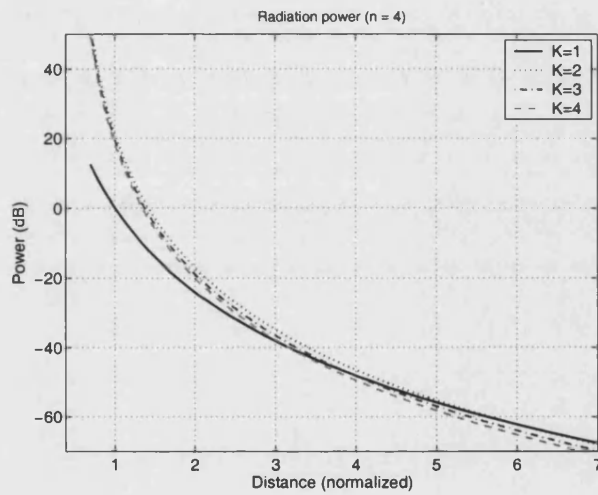
Figure 6.2: Power attenuation comparison (n=4)

6.1.3 Non-isotropy of interference

For a single central antenna a free space propagation environment results in a equal interference power in all azimuthal direction. In the distributed antenna case, considering that signals from all antenna units propagate via independent paths, their phases are independent and uniformly identical distributed. The total interference power is the sum of the individual interference powers. The constituent signals are of different power due to different propagation path distance. When the receiver has a different

relative location (azimuthally) with respect to the distributed antenna, the relative strengths of individual signal powers may vary. Thus received interference will vary with azimuth.

If we estimate the received power on a circular locus using a free space propagation model and sum interference power-wise (with normalized total transmission power), we obtain the power variation pattern shown in Figures 6.3 and 6.4.
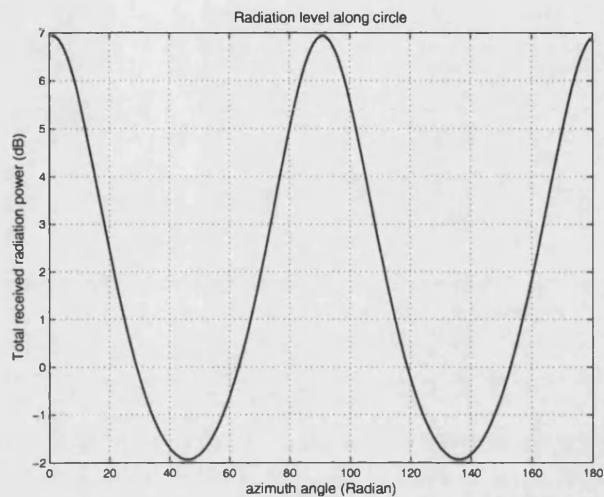
Figure 6.3: Interference variation pattern (two antenna units)
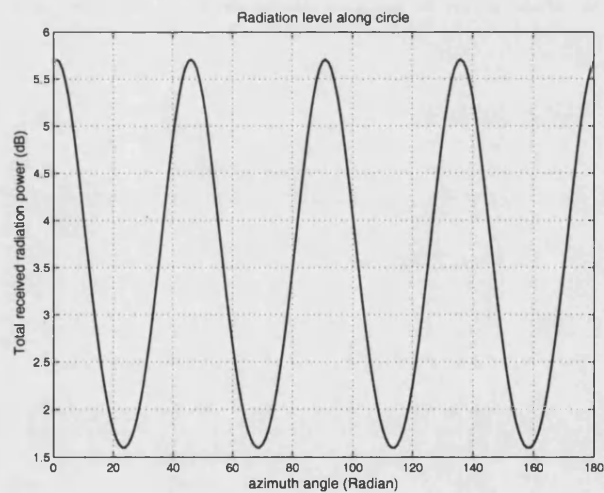
Figure 6.4: Interference variation pattern (four antenna units)

From the interference power variation pattern, it is observed that for two antenna units, the difference in power received at different position is up to 8 dB. As more antenna units are used, the power difference becomes smaller.

6.1.4 Meaning of the antenna position changes

From the above analysis, it is understood that the change of antenna position influences interference level in two opposing ways. When the co-channel distance is large enough, splitting the power between antenna units reduces interference to other cells. This allows reduced reuse distance. As the reuse factor gets smaller (co-channel distance decreases) the distributed antenna deteriorates inter-cell interference because the shorter distance dominates over the lower transmitted power.

From a system performance perspective, in victim cells around the distributed antenna cell, as a consequence of the shortened co-channel distance, the interference received at the mobile station experiences less loss than the single antenna case. The downlink of the victim cell clearly suffers from this phenomena. The uplink in the distributed antenna cell experiences the same level interference. The improved signal strength achieved by combining diversity will be compromised due to increased interference power.

6.2   Interference to other cell

6.2.1   One-cell-to-one-cell scenario

In the previous section, we have shown how the propagation distance and transmitted power collectively influence interference. To evaluate inter-cell interference for the distributed antenna, a pair of interfering cells are set up, with a distributed antenna cell as the interfering cell and a single antenna cell as the victim. The geometry is shown in Figure 6.5.

We consider interference at the two stations: the distributed antenna base station and the mobile station. We then simulate the SIR experienced by the mobile station at different positions, representing downlink quality in the victim cell. Because the interference channel is symmetric, this simulation also shows the deterioration of uplink reception for the distributed antenna. A uniform spatial distribution of the mobile station is assumed.

For the distributed antenna, we consider the transmission diversity scheme in which all antenna units transmit the same signal with time and phase adjustment. In a narrow-band system time dispersion can be neglected. The signal received at the mobile station in the victim cell consists of three parts: one is the intended signal (from the serving
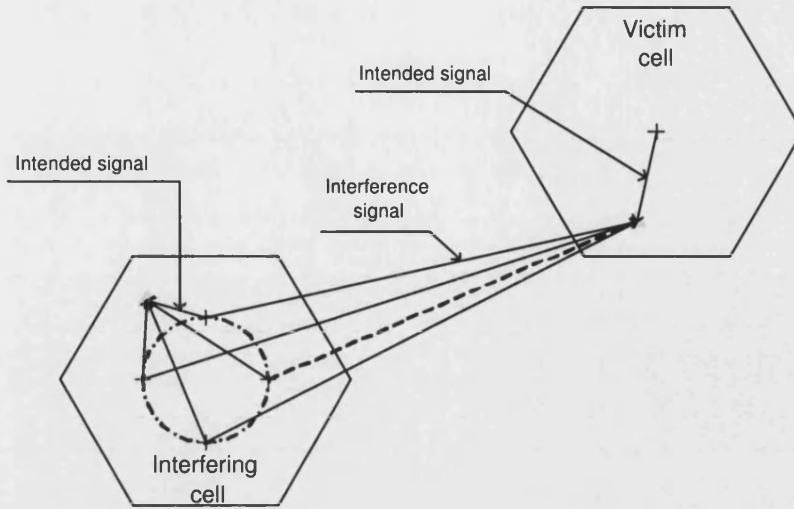
Figure 6.5: Geometry of a pair of interfering cell

base station); one is the interfering signal from the base station antenna units in the co-channel cell and the one is thermal noise. When the distributed antenna is deployed in the interfering cell (denote by the subscript 1), the signal can be expressed as:

$$r_0(t) = \sqrt{P_0} a_{01,0} e^{j\phi_{01,0}} s_0(t) + \sum_{i=1}^{K} \sqrt{P_1} a_{1i,0} e^{j\phi_{1i,0}} s_1(t) + n(t) \tag{6.2.1}$$

where $s_i(t)$ is the equivalent complex baseband signal with unit power intended for the in-cell mobile user. It is reasonable to assume independence of $s_0(t)$ and $s_1(t)$.

$a_{ji,m} e^{j\phi_{ji,m}}$ is the complex gain of the channel between i^{th} antenna in j^{th} cell and mobile user in m^{th} cell. Subscript i denotes the antenna unit (1 to K). P_0 and P_1 are the radiated power of each antenna unit in each individual cell. As the signal from every antenna unit propagates via different paths, the phase of interfering signal is independent and identical uniformly distributed at the victim mobile station. Neglecting thermal noise, the SIR is given by:

$$\gamma = \frac{P_0 |a_{01,0}|^2}{P_1 |\sum_{i=1}^{K} a_{1i,0} \exp(j\phi_{1i,0})|^2} \tag{6.2.2}$$

6.2.2 Constant transmission power

First, we study the situation when the distributed antenna keeps the total transmitted power the same as for single antenna with equal share $(1/K)$ among all antenna units. Therefore, it holds that $P_0 = KP_1$.
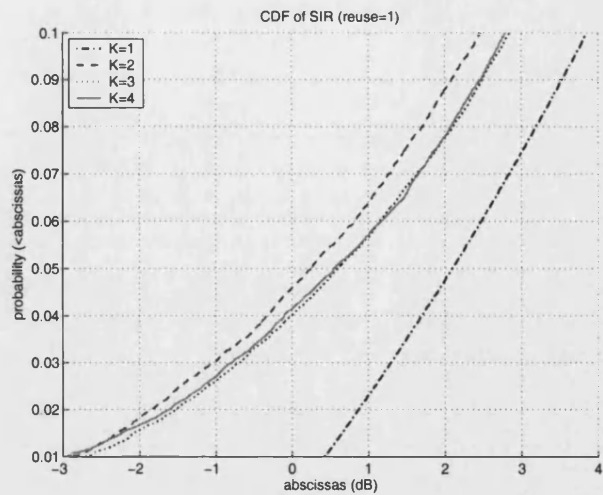
Figure 6.6: CDF of SIR with constant power (reuse=1)

Figure 6.6 shows the CDF of SIR in a free space propagation environment with reuse factor 1. By reading 10% exceeded SIR, it is observed that the 90% positions in signal antenna case has SIR about 1.5 dB better than the distributed antenna.
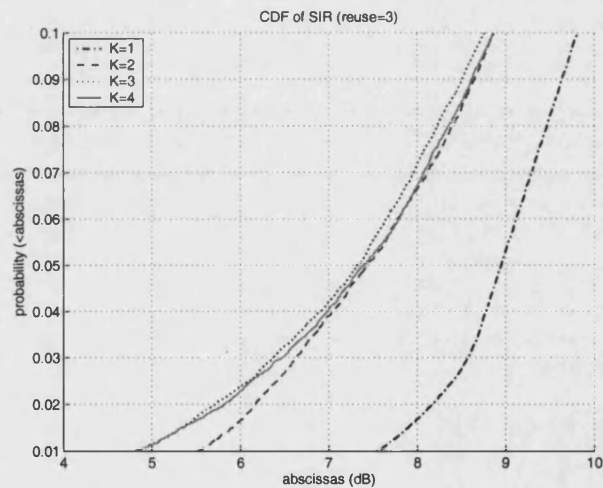
Figure 6.7: CDF of SIR with constant power (reuse=3)

Figure 6.7 shows the case for a reuse factor of 3. The gap between the single antenna and the distributed antenna shrinks to about 1 dB. The common feature in these two figures is that the multiple antenna unit cases have similar SIR CDF. This is because in the DA cell, antenna units are closer to the cell edge than in the central antenna cell. (Antenna units are located approximate half a cell radius closer to the co-channel cell.) This shows that the distributed antenna geometry change causes an increase of

6.2

74

the inter-cell interference power. We conclude that because the antenna shifts towards the cell edge, the distributed antenna compromises link quality in the victim cells.

The significance of the decreased isolation between interfering antennas depends on the reuse factor. For a location of the antenna units at half the radius of the cell and for a reuse factor 1, interference is increased by 6 dB in the worst case when the mobile user is on the edge of the co-channel cell.

Two links are affected by this change in geometry. The first is the compromised reception of mobile user's signal (the uplink in the DA cell). The second is the compromised reception of base station's signal (the downlink in the single antenna cell).

6.2.3 Effect of antenna array orientation

In our simple model the distributed antenna has a non-isotropy interference with azimuth periodicity. In some azimuth direction, the received radiation is higher than others. A co-channel cell center exists for every 60° azimuth. The relative angular position of the co-channel cells may therefore influence interference levels.

In the previous simulation, the influence on interference caused by the position of the distributed antenna is studied. Now we focus on the influence of the orientation of the distributed antenna. The antenna orientation is defined in Figure 6.8.
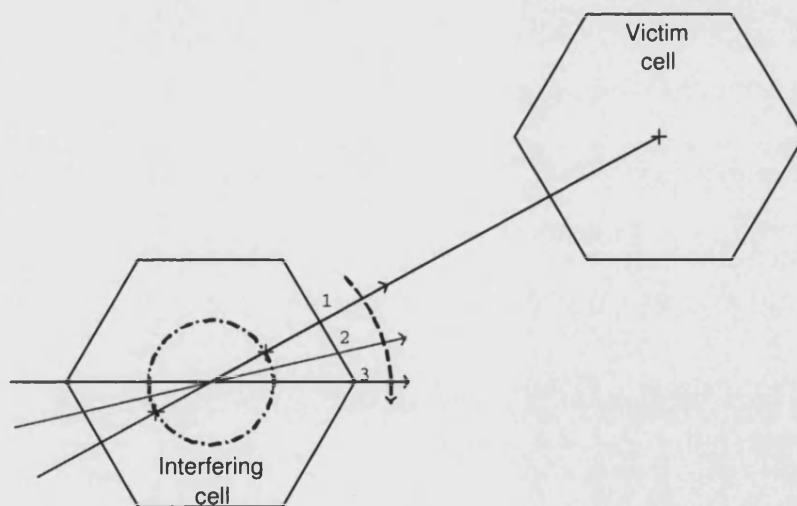
Figure 6.8: Geometry of the orientation of the distributed antenna

If a cell is assumed to be of an hexagonal shape, in the same tier, after every 60°

azimuth separation, there is a co-channel cell. Recognizing the symmetry, we only examines antenna orientation between 0°, 15° and 30°. For a given reuse factor and number of antenna units, the initial orientation is set to 0(indexed as a=1), i.e. one antenna unit "points" to the victim cell centre. The antenna array is then rotated in 15° steps till (indexed as a=3).
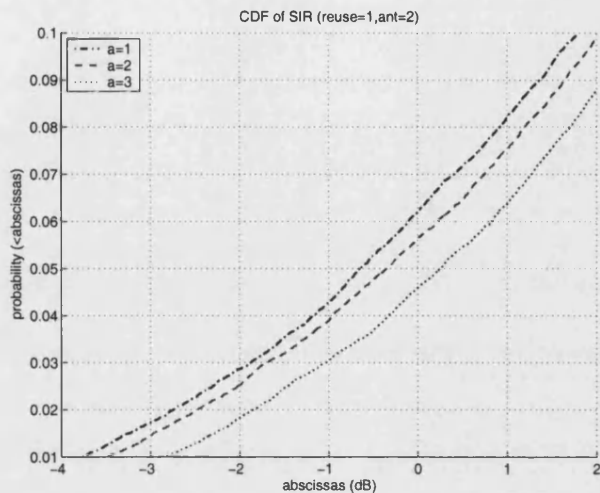
Figure 6.9: Impact of orientation (reuse=1, 2 antennas)

Figure 6.9 shows the influence of orientation on SIR in the victim cell with a reuse factor of one and two antenna units. The maximum difference in SIR caused by rotating the antenna 30° off the victim cell centre is 1 dB (for the two antenna unit case). This means the victim cells in the first tie will have unbalanced interference.
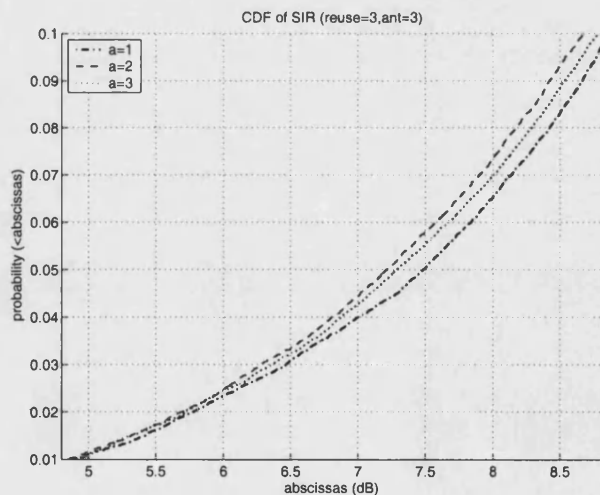
Figure 6.10: Impact of orientation (reuse=3, 3 antennas)

Figure 6.10 shows the case for a reuse factor of 3 and 3 antenna units. As the reuse factor and number of antenna units becomes larger, the influence of the orientation gets less. Compared to a reuse factor of one, the SIR difference between different orientation is insignificant.

Although, the analysis is made in a free space environment, it is still meaningful because the distance related path loss reflects the general situation in a real environment. Using objects in the environment to reduce the antenna unit illumination of neighbouring cells and avoid locating the antenna towards the base station antenna will reduce interference.

6.2.4 Dynamic power control

The advantage of the distributed antenna is that it decreases mean propagation distance and combats shadowing encountered in the urban areas. This could lead to a decrease in transmitted power while still maintaining acceptable link quality, when the power control is used.

In the two-cell scenario, since only interference from the base station is considered, then power control is applied to the downlink. For the distributed antenna, the total power is adjusted and transmitted power at all antenna units is controlled in a unified way. It is worth noting that the received power of the intended signal is the result of coherently combining the signals from the distributed antenna units. This is based on an assumption that perfect coherent transmission diversity is possible. The transmitted power for each in-cell mobile user is controlled to keep the received power constant. The received signal is given by:

$$r_1(t) = \sqrt{P_1} \sum_{i=1}^{K} a_{1i,1} e^{j\phi_{1i,1}} s_1(t) \tag{6.2.3}$$

$a_{1i,1}$ and $\phi_{1i,1}$ are the amplitude and phase received by the mobile user from each distributed antenna unit. The phase at each antenna unit is adjusted so that $\phi_{1i,1}$ is co-phased.

$$P_1 (\sum_{i=1}^{K} a_{1i,1})^2 = constant \tag{6.2.4}$$

In the corresponding simulation, two kinds of randomness must be accommodated. One is the mobile station position in the distributed antenna cell, which will result in

changing transmitted power. The other is the mobile station position in the victim cell, which will change the distance between the two stations interfering with each other. In each cell, a grid of mobile station positions is sampled. For each position in the distributed antenna, all grid positions in the victim cell are sampled to collect the instantaneous SIR. This process is applied to all mobile station locations in the distributed antenna cell. The CDF is obtained based on the resultant SIR samples.
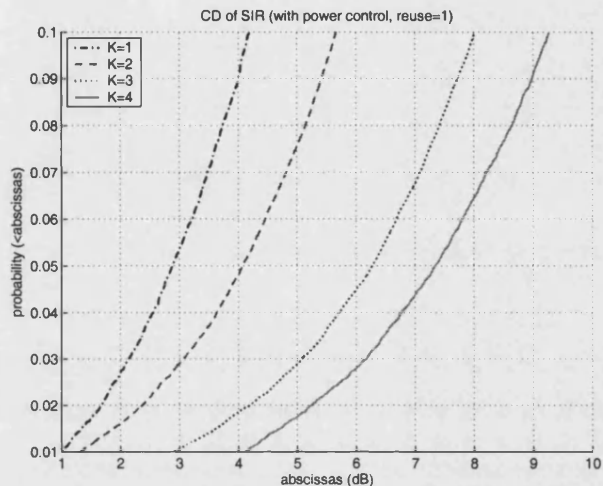
Figure 6.11: CDF of downlink SIR using power control (reuse=1)

Figure 6.11 shows the CDF of SIR when power control is used in both of the two cells with reuse factor of 1. It is observed that the distributed antenna produces a significant decrease in inter-cell interference. Reading the 90% exceedance SIR, the four antenna unit case achieves a maximum improvement of 5 dB. This is due to the decrease of transmitted power, especially in the edge region. In the distributed antenna case, mobile stations use nearby antenna units, which requires reduced power. The gain is dependant on diversity order. This is different from the trend shown in the constant power case. The gain achieved here is due to the multiple antenna, not just the antenna unit locations.

Figure 6.12 shows the case for a reuse factor of 3. As the reuse factor gets larger, this gain increases slightly (from 5 dB to 6 dB as reuse factor increases from one to three). This is because the penalty due to the antenna location closer to the cell edge decreases with reuse factor. A trend in both figures is that the extra gain due to one more antenna deployed is shrinking.
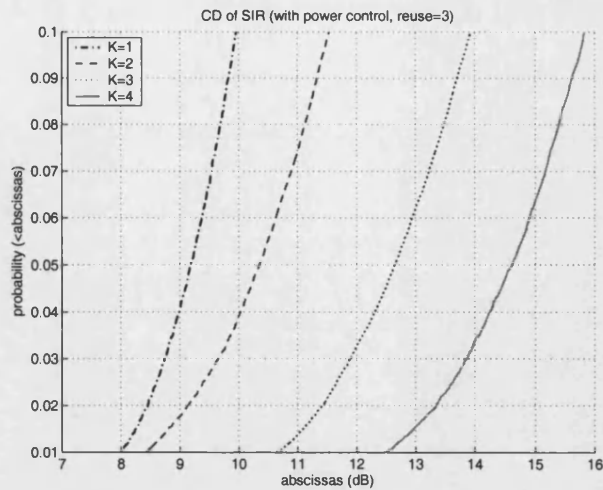
Figure 6.12: CDF of downlink SIR using power control (reuse=3)

6.3 In-cell performance

6.3.1 System and signal model

In the previous section, we have analyzed the inter-cell interference from a distributed antenna and shown that the antenna unit locations can cause increased interference. It follows from symmetry that the antenna unit will be subject to increased interference, which will degrade uplink quality. The isolation distance between in-cell mobile stations to a conventional central antenna in the co-channel cell is not changed and performance is not deteriorated by changing the antenna position. Therefore, we only simulate uplink.

When a distributed antenna cell is deployed in the cell, interference arises from six co-channel cells around it. We consider a single distributed antenna cell surrounded by traditional single (central) antenna cell. This is a likely configuration since only a relatively small area in a city center with high building and user densities may require a distributed antenna. The distributed antenna is the target cell, which receives interference from all co-channel cells around it. Although all co-channel cells contribute interference to the victim cell, those from the closest co-channel cell will dominate. We therefore consider only the co-channel cells located in the first tier.

Here, we assume uniform cell size and constant cell separation. Although the assumption makes the environment idealistic, the study is still of value, since it shows, for the same network and propagation conditions, the net gain achievable using a distributed

antenna in place of a traditional, centrally located antenna. Figure 6.13 shows the geometry of multiple co-channel cells.
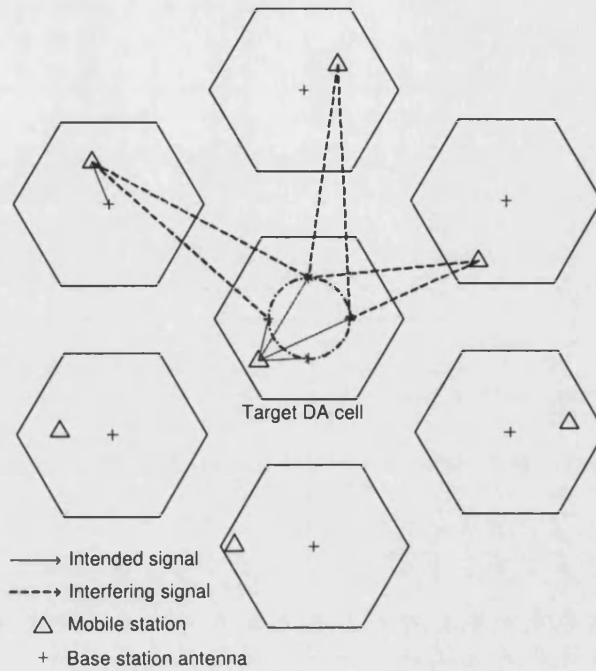
Figure 6.13: Network configuration

The signal received at the base station antenna has three components: the intended signal, the co-channel interference from mobile stations in the co-channel cells and thermal noise. At the ith antenna unit the received signal from a particular mobile user is:

$$r_i(t) = a_{0i,0}e^{j\phi_{0i,0}}s_0(t) + \sum_{m=1}^{6} a_{0i,m}e^{j\phi_{0i,m}}s_m(t) + n(t) \qquad (6.3.1)$$

where $s_0(t)$ is the (unit power) complex envelope of the signal from the intended user, $s_m(t)$ is the (unit power) complex envelope of interfering signal from the mobile user in the mth co-channel cell, $a_{0i,m}$is the amplitude of the received signal transmitted from the mobile station in m^{th} cell to the ith antenna unit in the target (0th cell. It is also reasonable to assume i.i.d noise in all antenna units, to neglect the thermal noise. It is reasonable to assume mutual independence between $s_m(t)$ for different m. The SIR at the output of the ith antenna unit is given by:

$$\gamma_i = \frac{a_{0i,0}^2}{\sum_{m=1}^{6} a_{0i,m}^2} \qquad (6.3.2)$$

The SIR after maximal ratio combining of all (K) signal branches is:

$$\gamma = \sum_{i=1}^{K} \gamma_i \tag{6.3.3}$$

6.3.2 CDF of uplink SIR

First, a simple environment with free space propagation is considered. In this model, the effect of the reduced isolation distance can be observed clearly. Figures 6.14 and 6.15 compare the SIR CDs for different numbers of antenna units for cell reuse factors of one and three.
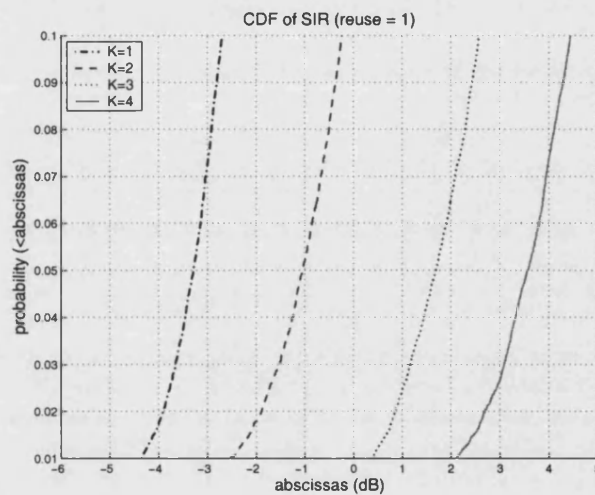
Figure 6.14: CDF of uplink SIR (reuse=1,free space)

It can be seen from the figure that the distributed antenna achieves up to around 6 dB (5 antenna units) better SIR for an availability of 99% for reuse factor of one . The performance improvement increases from a reuse factor of one to three. This is due to the influence of the antenna offset from the cell centre diminishing as the co-channel distance increases.

The simulations have been repeated using the more realistic Walfisch-Ikegami (WI) model [12], which parameterizes environment features, such as the street width, building height and antenna height. The shadowing is modeled as a log-normal random variable superimposed over the loss model.

The parameters used in the WI models are shown in Table 6.1. The total path loss
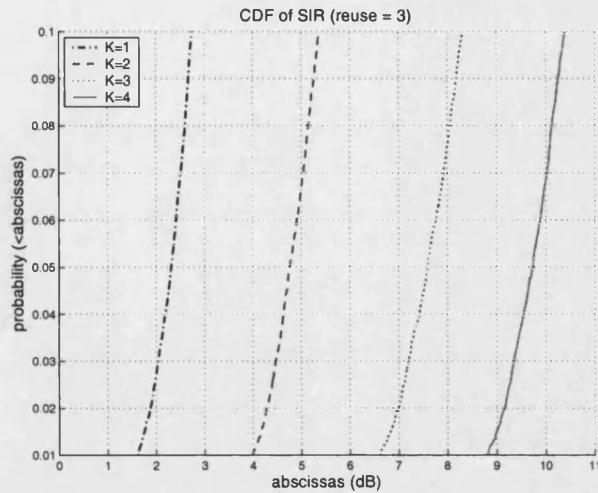
Figure 6.15: CDF of uplink SIR (reuse=3,free space)

consists of two parts, a medium path loss estimated using WI model and a random loss representing shadowing. The variance of the shadowing is determined by the environment.

Table 6.1: WI model parameters

City type	Urban area
Building height	30 m
Building width	35 m
Road width	15 m
Base-station antenna height	5 m
Mobile-station height	1.5 m
Carrier frequency	1 GHz

Here, a constant transmission power is assumed. From Figures 6.16 and 6.17, we can observe that even with highest co-channel interference (for a reuse factor of 1), the distributed antenna can achieve at least 2 dB SIR gain for the 2 antenna unit configuration. When reuse factor increased, the gain also increases. This confirms the analysis presented previously suggesting that the penalty due to the changed antenna position decreases as co-channel distance increases. In the shadowing environment, the advantage is magnified due to the diversity gain obtained from the distributed antenna.

6.4

82
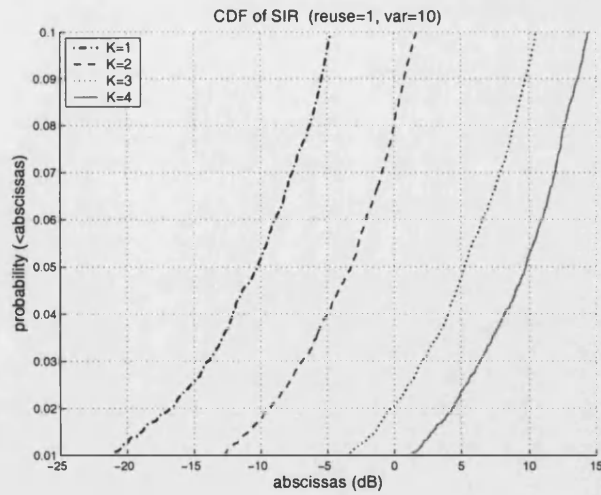
Figure 6.16: CDF of uplink SIR (reuse=1, wim, Var=10 dB)
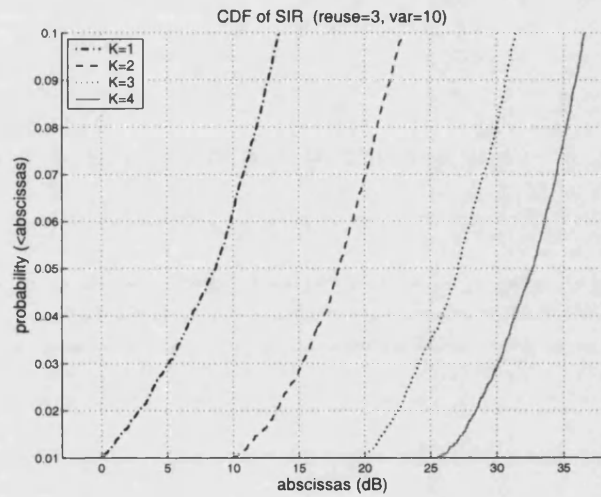
Figure 6.17: CDF of uplink SIR (reuse=3, wim, Var=10 dB)

6.4 Multiple DA cells network

6.4.1 Study method

In the previous sections, we have studied the inter-cell interference characteristics of the distributed antenna and have shown that there are two opposing factors influencing interference level. Reduced transmitted power enables the distributed antenna to tolerate less co-channel isolation. On the other hand, short co-channel distance causes lower interference path loss. Now, we take all factors into consideration to evaluate spectral efficiency. Since the uplink and downlink have different propagation characteristics, we

study them separately.

We still consider one target cell and first tier co-channel cells, but all are now equipped with the distributed antenna system. Spectral efficiency, which is effectively represented by reuse factor, is constrained by the condition that a certain percentage area (90% chosen here) in the cell should have adequate SIR (i.e. more than a given threshold). This SIR threshold, enjoyed by a certain percentage of locations, is called the exceedance SIR. Using snap-shot simulation, we obtain this SIR threshold for each reuse factor configuration. We therefore evaluate the exceedance SIR as a function of reuse factor.

6.4.2 Uplink SIR model

In the uplink, for a particular mobile user, the signal received at the ith base station antenna unit can be expressed as:

$$r_{0i}(t) = \sqrt{p_0}a_{0i,0}e^{j\phi_{0i,0}}s_0(t) + \sum_{m=1}^{6}\sqrt{p_m}a_{0i,m}e^{j\phi_{0i,m}}s_m(t) \qquad (6.4.1)$$

$\sqrt{p_m}a_{0i,m}$ is the amplitude of the signal transmitted from the mobile user in the mth co-channel cell and received at the ith antenna unit in the target cell. p_m is the power allocated to the mobile user of interest in the mth cell. Here, power control is applied as discussed in the previous section. The SIR received at the ith antenna unit is:

$$\gamma_{0i} = \frac{p_0 a_{0i,0}^2}{\sum_{m=1}^{6}p_m a_{0i,m}^2} \qquad (6.4.2)$$

If maximal ratio combining is used across all antenna units, then the resulting SIR is:

$$\gamma_0 = \sum_{i=1}^{K}\gamma_i = \sum_{i=1}^{K}\frac{p_0 a_{0i,0}^2}{\sum_{m=1}^{6}p_m a_{0i,m}^2} \qquad (6.4.3)$$

6.4.3 Uplink performance

In Figures 6.18 and 6.19, the 90% exceedance SIR is plotted as a function of all possible reuse factors (up to 13) for each diversity order (one up to five). These curves show the result for free space and plane earth propagation models, with path loss exponents of 2 and 4 respectively.
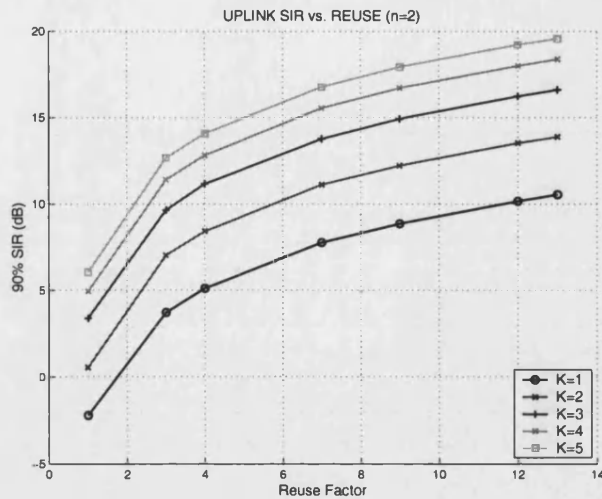
Figure 6.18: 90% exceedance SIR vs. reuse factor (free space, uplink)
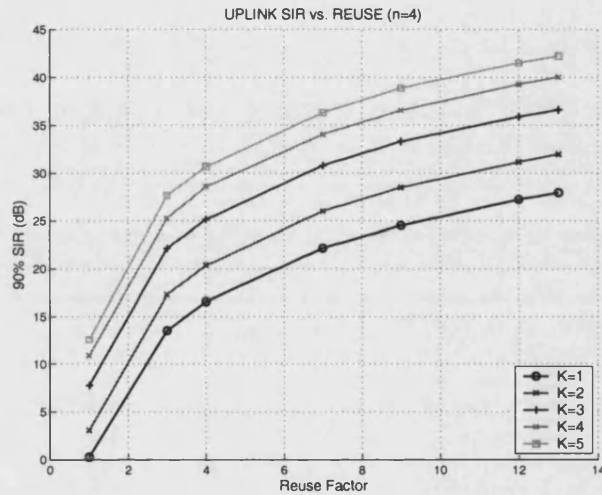
Figure 6.19: 90% exceedance SIR vs. reuse factor (planar Earth earth, uplink)

We can see from these figures that with the same reuse factor, i.e. the same co-channel distance, the distributed antenna can achieve improved SIR. The SIR advantage measured against a conventional antenna is up to 7 dB with 5 antenna units. For two antenna units, the advantage is still approximately 3 dB. As the reuse factor increases, the advantage increases slightly. This is because the penalty due to the edge proximity of the antenna reduces as the co-channel distance increases.

If we compare the cases for a path loss exponent of 2 and 4, we see that the SIR gain achieved by the distributed antenna increases with increasing exponent.

Figure 6.20: 90% exceedance SIR vs. reuse factor (wim, Var=5 dB, uplink)
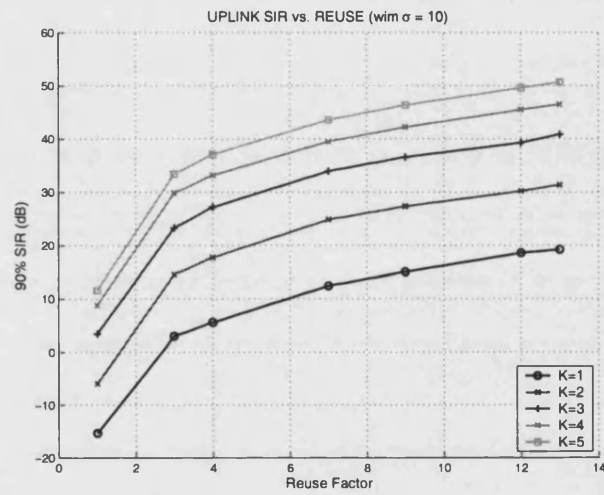
Figure 6.21: 90% exceedance SIR vs. reuse factor (wim, Var=10 dB, uplink)

In Figures 6.20 and 6.21, we show the result for the WI model with superimposed shadowing of variance 5 dB and 10 dB. The effective attenuation factor of this WI model environment is bigger than 4. The gain achieved in the WI model type environment is greater than for a plane earth. Comparing the WI model with different shadowing variance, we notice that for greater shadowing, the distributed antenna achieves greater gain. This is because having independent shadowing, the distributed antenna suffers less shadowing than a conventional antenna and therefore does not need increase transmitted power to overcome shadowing.

Adding shadowing changes the PDF of the path loss stretching the distribution tails at both ends. The 90% point in the CDF is thus shifted downwards. The effect of adding

shadowing to the simulation result is that the entire curve shifts downwards compared to the model without shadowing.

6.4.4 Downlink SIR model

The downlink is different from the uplink. From every co-channel cell, interference comes from multiple antenna units in the distributed antenna case. As the antenna units in the same cell are transmitting the same signal to one specific user, these interfering signal will add vectorially at the victim mobile terminal. The signal at the mobile terminal is therefore:

$$r_0 = \sqrt{p_0} \sum_{i=1}^{K} a_{0i,0} e^{j\phi_{0i,0}} s_0(t) + \sum_{m=1}^{6} \sqrt{p_m} \sum_{i=1}^{K} a_{mi,0} e^{j\phi_{mi,0}} s_m(t) \qquad (6.4.4)$$

and the resulting SIR is:

$$\gamma_0 = \frac{p_0 (\sum_{i=1}^{K} a_{0i,0})^2}{\sum_{m=1}^{6} p_m |\sum_{i=1}^{K} a_{mi,0} e^{j\phi_{mi,0}}|^2} \qquad (6.4.5)$$

where $a_{mi,0}$ and $\phi_{mi,0}$ are the amplitude and phase of the signal transmitted from the ith antenna unit in the mth co-channel cell and received at the target mobile station.

6.4.5 Downlink performance
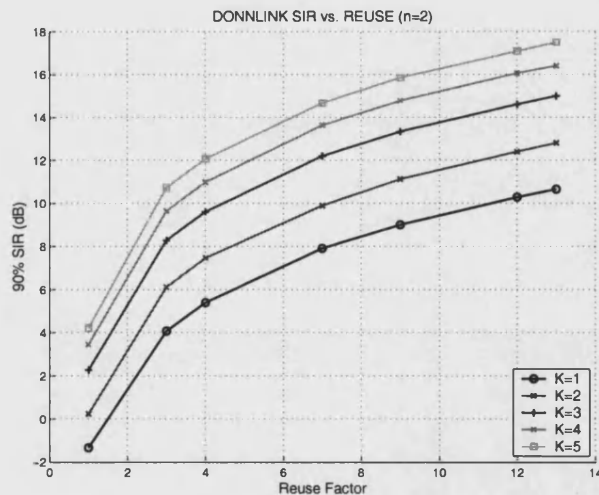
Figure 6.22: 90% exceedance SIR vs. reuse factor (free space, downlink)

We show the results in Figure 6.22 for free space, 6.23 for plane earth, 6.24 and 6.25
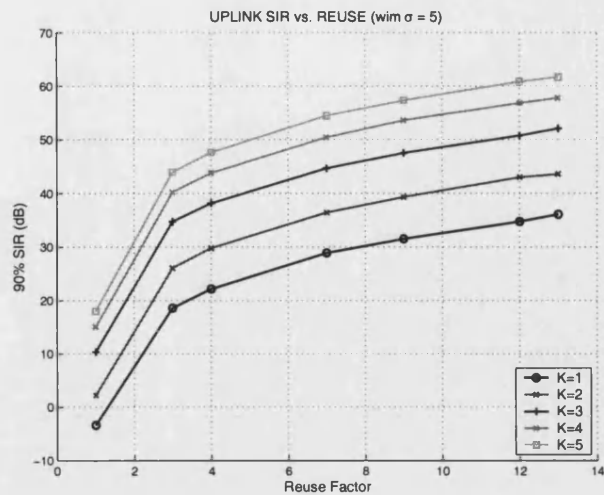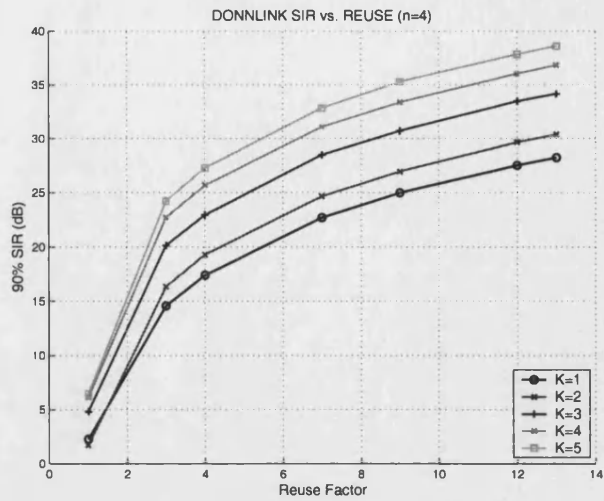
Figure 6.23: 90% exceedance SIR vs. reuse factor (plane earth, downlink)
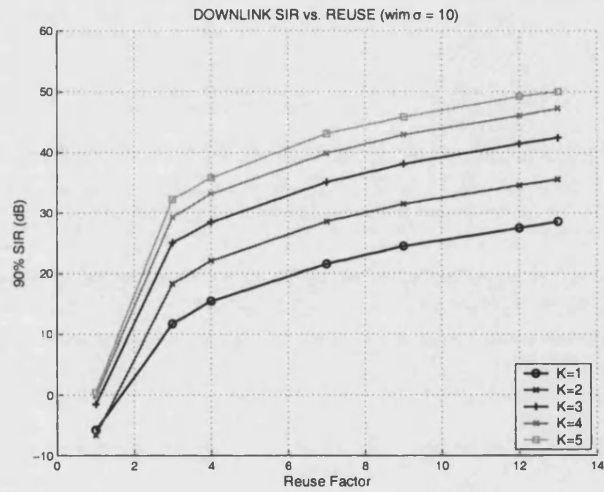
Figure 6.24: 90% exceedance SIR vs. reuse factor (wim, Var=5 dB, downlink)

for WI propagation environments respectively. We can see a similar trend of the SIR vs reuse factor as for the uplink case as well as the relationship between gain and path loss exponent.

There is one difference worth noting, however, which is that for a reuse factor of 1, the two antenna unit configuration has inferior SIR performance compared with the conventional antenna. This penalty exists In all propagation environments and becomes more serious increasing path loss exponent.

This is because the shifted antenna unit is closer to the co-channel cell than the conventional antenna. During the simulation, therefore, when the mobile user is located
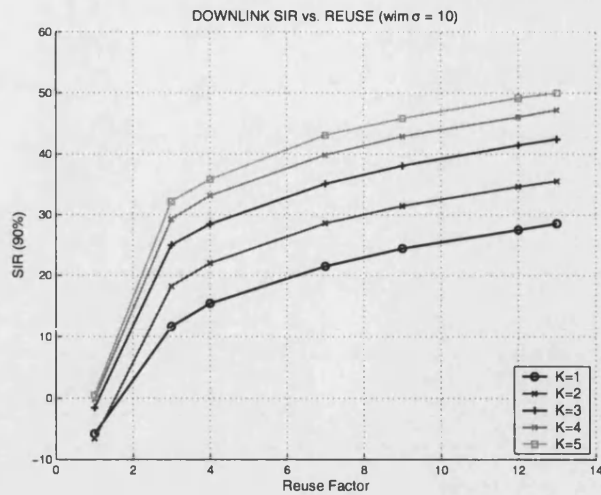
Figure 6.25: 90% exceedance SIR vs. reuse factor (wim, Var=10 dB, downlink)

in an area close to the cell edge, it may be closer to the antenna unit in the co-channel cell than its local antenna. Even worse, if the mobile user in the co-channel cell is also close to the cell edge, the base station in that cell will increase transmitted power. The geometry is shown in Figure 6.26. Both base station antennas have similar transmitted powers, but the co-channel antenna unit may experience less path loss due to the mobile user's location.
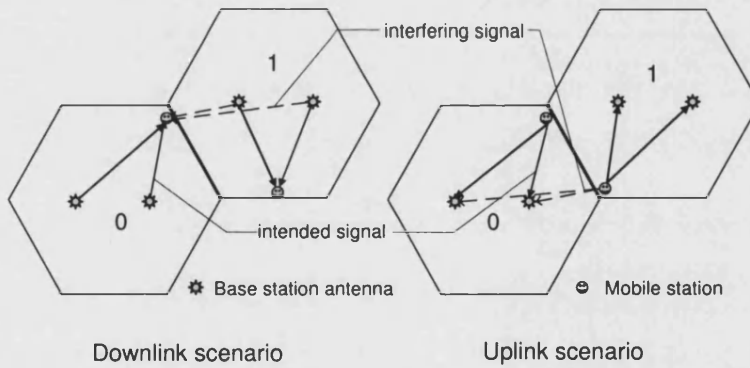
Figure 6.26: Worst case geometry for the two antenna unit distributed antenna

As shown in section 6.1, the dominance of the antenna proximity effect depends on the co-channel distance as well as the path loss exponent. This is why the two antenna case in free space path loss model still has advantage over the conventional antenna while in the plane earth model the conventional antenna has superior performance. As the path loss exponent increases (in WI model), the penalty becomes greater.

6.4

89

This phenomenon does not exist in the uplink case. In the uplink, interference is received at base station antenna unit and the signals received at all antenna units are combined. Normally, when a mobile user is located close to the cell edge, only one antenna unit will suffer from strong interference. The other antenna units contribute a better SIR and compensate this deterioration after the combination.

The last point about this observation is that actually, this phenomena happens only in the simulation. In the simulation, cell is of ideal shape and the mobile user is placed within the cell boundary and the link quality is not considered in the assignment of mobile terminals to a particular cell. In a real network, when the mobile user is located close to the cell edge, the network may trigger a hand-off so that it becomes served by a base station having better link quality.

6.5 Conclusions

The distributed antenna system can improve the cell coverage by efficiently delivering signal power to the mobile users. This benefit can be translated into a spectral efficiency gain if combined with a power control scheme. For the same co-channel separation, a distributed antenna with power control will cause reduced interference.

The fundamental reason for this improvement is explained using the idea of the access distance. When only a pair of cells is considered and transmitted power is controlled to keep received signal power constant, the SIR is proportional to a geometry factor ζ_K, defined as:

$$\zeta_K = \frac{D_{iK}}{D_{aK}} \tag{6.5.1}$$

where the D_{iK} is distance between interfering stations and mobile user and D_{aK} is access distance. Subscript K denotes diversity order, $K = 1$ refereing to the conventional single antenna case. The SIR advantage achieved by the distributed antenna can then be expressed as:

$$G_K = (\frac{\zeta_K}{\zeta_1})^n \tag{6.5.2}$$

where n is the path loss exponent. We have shown that average access distance is significantly decreased for a distributed antenna. If co-channel distance is large enough, the path loss sacrifice due to antenna location can be neglected. D_{iK} can then be assumed constant for all K. G_K is therefore proportional to the access distance raised

to the power n, i.e.

$$G_K = (\frac{D_{aK}}{D_{a1}})^n \tag{6.5.3}$$

We see from equation (6.5.3), the reduction of propagation path loss is the fundamental reason for the improvement of spectral efficiency. When shadowing is considered, there are two points which will influence the above analysis. First, since each antenna unit experiences independent shadowing, a distributed antenna can achieve diversity advantage. This will further increase the gain. Furthermore in the real network shadowing is therefore more likely when access distance is large. The distributed antenna is therefore less likely to suffer from shadowing than the conventional antenna. This suggests that the performance improvement of the distributed antenna in a real environment may be significantly greater than implied by our simulation.

Chapter 7

DISTRIBUTED ANTENNAS IN CDMA SYSTEMS - I

In the previous chapters, we studied the performance of distributed antennas in a narrow-band FDMA or TDMA system. CDMA system requires a new form of diversity scheme. The distributed antenna also raises an important issue - power control. As multiple links are involved in power control, this problem becomes a complicated non-linear problem.

In this chapter, the application of distributed antenna in CDMA systems is discussed. Firstly, a suitable signal model and its properties are reviewed. Based on these properties, a new form of diversity scheme is addressed. Power control, which is critical for achieving the performance, is then addressed. Finally, performance is simulated and the results analyzed.

7.1 Features concerning the distributed antenna

7.1.1 Spread spectrum signal

In CDMA system, the symbol stream is directly modulated onto a PN sequence. The PN sequence used to spread the symbol spectrum has a narrow self-correlation characteristic. One property of the spread spectrum signal that distinguishes it from narrow-band signals is its robustness in frequency selective channels when the chip rate exceeds the coherence bandwidth, i.e. when the delay between multipath replicas is larger than

the time span of a chip. Using a RAKE receiver, the multipath components of the PN sequence spread signal can be resolved and combined in an optimal way. If we assume that the receiver can collect power from all multipath components, then the power of the combining output is the gross power of the multipath profile. We use the gross power to represent the ultimate multipath diversity reception result and use the propagation path loss model to estimate the gross power.

7.1.2 Self-interfering system

In CDMA systems, all users occupy the same frequency band and time slot and are identified by a unique signature PN code. These signature codes have low cross-correlation and in the downlink they are orthogonal. For a L-bit PN sequence, the normalized cross-correlation is:

$$R_x(n) = \begin{cases} 1 & : & n = 0 \\ 1/L & : & n \neq 0 \end{cases} \qquad (7.1.1)$$

In the correlation receiver therefore other users' signals appear as noise. In contrast to FDMA and TDMA systems, in which user capacity is predetermined by the frequency band allocated to the system and the channel width for each user, in CDMA systems each user takes the channel by presenting interference to all other users. The level of interference accumulates as more users are added. The more users in the cell, the greater the interference. When the user's data rate becomes higher, the processing gain achieved with the same chip rate will be reduced. To keep the same link quality (E_b/N_0), a higher transmission power is required. This user will present higher interference to other user. Due to the self-interference feature, interference reduction or power allocation techniques can benefit CDMA systems directly in terms of user capacity per cell.

Since users are located at different distances from the base station and because signals from other users present as interference, users may suffer different uplink SIR. When the distance difference between these two stations is large, the closer station's signal can mask the more distant signal. The solution is power control to equalize SIR.

The result of power control is equalized and just sufficient received power at the receiver. Since the power control is targeting the in-cell users, interferences coming from other cell experience larger propagation loss. Therefore, although signals from users in other cells contribute to interference, the majority of interference in each cell comes from other users in the same cell. To simplify the analysis, therefore, we only consider single cell environment. This simplification will not sacrifice the comparative significance of

this study.

7.2 Uplink signal models

7.2.1 Uplink receiver

Since multiple base station antennas are involved in uplink, a two stage RAKE receiver is used for antenna diversity reception. In the first stage, a conventional RAKE receiver is used for each antenna unit. The outputs of these RAKEs are then combined again across all antenna units. In the second stage, each branch is the output of one antenna unit. The result is the summation of signals from all antennas.
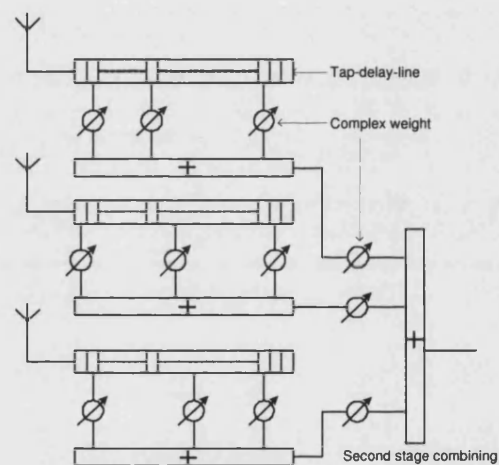
Figure 7.1: Two-stage RAKE receiver

7.2.2 Uplink capacity model

Uplink capacity is determined by the number of users presenting at the base station antenna. Assuming each user requires a SIR Γ_j for acceptable service and denoting the received power for each user by R_j, then for the conventional base station antenna

case:

$$\gamma_1 = \frac{R_1}{\sum_{m=1}^{M} R_m} \geq \Gamma_1$$

$$\gamma_2 = \frac{R_2}{\sum_{m=1}^{M} R_m} \geq \Gamma_2$$

$$\vdots$$

$$\gamma_M = \frac{R_M}{\sum_{m=1}^{M} R_m} \geq \Gamma_M$$

$$(7.2.1)$$

For simplicity, in equation (7.2.1) we include the intended signal power in the interference term. Then we add all conditions together to get:

$$\sum_{j=1}^{M} \gamma_j \geq \sum_{j=1}^{M} \Gamma_i \tag{7.2.2}$$

Since:

$$\sum_{j=1}^{M} \gamma_j = 1$$

The attainable SIR is:

$$\sum_{j=1}^{M} \Gamma_j \leq 1 \tag{7.2.3}$$

Assuming that every user has the same SIR requirement, Γ, then the number of users M must satisfy the condition $M\Gamma \leq 1$.

When there are K antenna units, we denote the received power at the ith unit from the jth mobile user by R_{ji}. The condition is still applied, but expressed as the summation of individual SIR γ_{ji} received at each antenna units, i.e.:

$$\sum_{j=1}^{K} \gamma_{ji} \geq \Gamma_j \tag{7.2.4}$$

and

$$\sum_{j=1}^{M} \gamma_{ji} = 1 \tag{7.2.5}$$

We then sum equation (7.2.4) to get:

$$\sum_{j=1}^{M} \Gamma_j \leq \sum_{j=1}^{M} \sum_{i=1}^{K} \gamma_{ji} \tag{7.2.6}$$

Changing the summation sequence in equation (7.2.6), we get:

$$\sum_{j=1}^{M} \Gamma_j \leq \sum_{i=1}^{K} \sum_{j=1}^{M} \gamma_{ji}$$
$$\sum_{j=1}^{M} \Gamma_j \leq K \tag{7.2.7}$$

This means the distributed antenna can provide K times the total SIR than the conventional antenna. Considering the case when one base station antenna accommodates a certain number of user with a particular SIR requirement, if K antennas are deployed, then assuming uncorrelated interference signals, the combining of K the signals certainly results in K times of the SIR. This SIR gain means K times more users can be accommodated. This is illustrated in Figure 7.2.
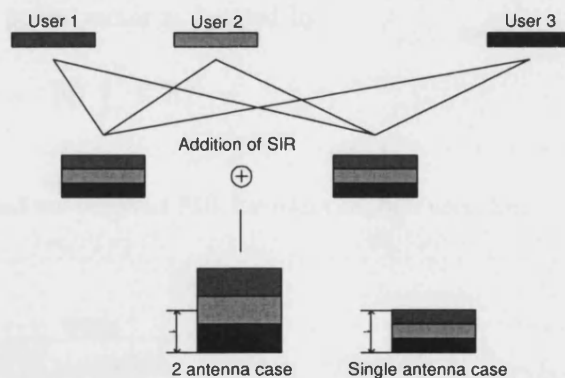
Figure 7.2: Uplink capacity model

7.2.3 Power control problem

Multiple antenna base stations can realize greater SIR than a single antenna. This improvement relies on the implementation of power control. In the single antenna case, if the received power of each mobile user remains constant, then the SIR is equalized. In the distributed antenna case, however this is not true.

A system with M users and K base station antennas can be characterized by a $M \times K$ matrix, G, which describes the transmission loss from every user to every base station antenna unit, and a $K \times 1$ vector P, which specify the transmission power of every user ($\Re_+$ is the set of non-negative real number):

$$G = \begin{bmatrix} g_{11} & \cdots & g_{1K} \\ \vdots & \ddots & \vdots \\ g_{M1} & \cdots & g_{MK} \end{bmatrix} \in \Re_+^{M \times K} \tag{7.2.8}$$

The transmission loss matrix G reflects the propagation path loss including the shadowing condition. Shadowing is assumed to change slowly however and can therefore be assumed to be constant. The variation rate of this matrix therefore determines the power control adaptation rate.

The transmission power vector is denoted by:

$$P = \begin{bmatrix} p_1 & \cdots & p_M \end{bmatrix}^T \in \Re_+^M \tag{7.2.9}$$

Power control equalizes received SIR for every mobile user, i.e.:

$$\begin{aligned} \gamma_j &= \sum_{i=1}^{K} \frac{g_{ji} p_j}{\sum_{m, m \neq i}^{M} g_{mj} p_m} \\ \gamma_j &= \gamma_m, \; \forall j \neq m \end{aligned} \tag{7.2.10}$$

Equation (7.2.10) is non-linear.

7.3 Power control solution and capacity simulation

7.3.1 Power-balance power control

An approximation and simplified solution to the problem is to make the total received power (sum from all antenna units) equal, i.e. to equalize the total received power for each mobile user:

$$p_j \sum_{i=1}^{K} g_{ji} = p_m \sum_{i=1}^{K} g_{mi}, \ \forall j \neq m \tag{7.3.1}$$

This does not however guarantee that the resulting SIRs are equal. If the received total power at all antenna units are equal, i.e.

$$\sum_{j=1}^{K} p_j g_{ji} = P_t, \ \forall j \tag{7.3.2}$$

then the result SIR can be expressed as:

$$\gamma_j = \frac{1}{P_t} \sum_{i=1}^{K} p_j g_{ji} \tag{7.3.3}$$

Applying equation (7.3.2), the SIR for all mobile users is equalized. Summing the SIR of all mobile users, we get:

$$
\begin{aligned}
\sum_{j=1}^{M} \gamma_j &= \sum_{j=1}^{M} \frac{1}{P_t} \sum_{i=1}^{K} p_j g_{ji} \\
&= \frac{1}{P_t} \sum_{i=1}^{K} \sum_{j=1}^{M} p_i g_{ij} \\
&= \frac{1}{P_t} \sum_{i=1}^{K} P_t \\
&= K
\end{aligned}
\tag{7.3.4}
$$

Because γ_i is equalized, we obtain:

$$\gamma_j = K/M \tag{7.3.5}$$

In the ideal case, the equalized SIR is K/M, K times that for a conventional antenna.

In Figure 7.3, we show the CDF of the SIR after applying power control for 16 users located at random positions. Reading SIR at, for example, the 10% probability (90% exceedance) in the figure, we can observe that distributed antenna achieves a higher SIR. The CDF has finite slope, which suggests that this power control scheme may not completely equalize SIR.
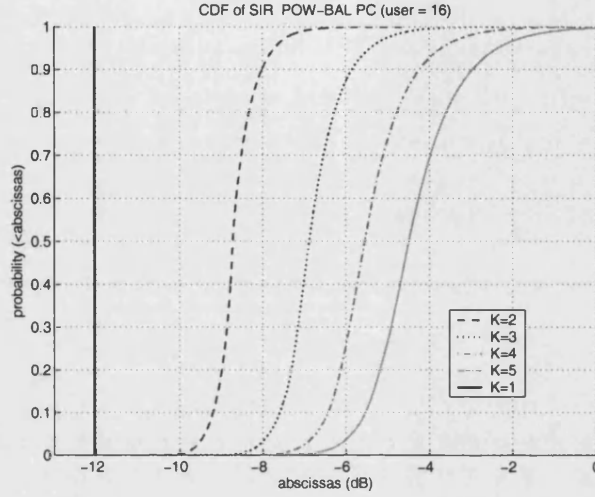
Figure 7.3: CDF of uplink SIR (User=16, POW-BAL PC)

7.3.2 SIR-balanced solution

The power-balanced solution has finite slope in its the CDF. In [24], it is shown that there must be a solution to this problem. Although it is difficult to get closed-form expression for the power control problem, we can use iterative computation to get a solution [84].

The iterative solution is straightforward. We adapt user 1 as a reference. An initial value for P is set to power-balanced solution. In each iteration, all transmitted powers are updated to achieve the same SIR as that f the user 1.

$$\gamma^*(n+1) = p_1(n) \sum_{i=1}^{K} \frac{g_{ji}}{\sum_{m,m\neq j}^{M} p_m(n)g_{mi}} \tag{7.3.6}$$

$$p_j(n+1) = \gamma^*(n+1)(\sum_{i=1}^{K} \frac{g_{ji}}{\sum_{m,m\neq j}^{M} p_m(n)g_{mi}})^{-1}, j \neq 1 \tag{7.3.7}$$

Since mobile user 1 is taken as the reference its transmission power is kept unchanged. This is counter-intuition, but considering that in terms of self-interference, the relative power is critical to performance. When thermal noise is taken into consideration, the absolute transmitted power will be determined by the thermal noise power.
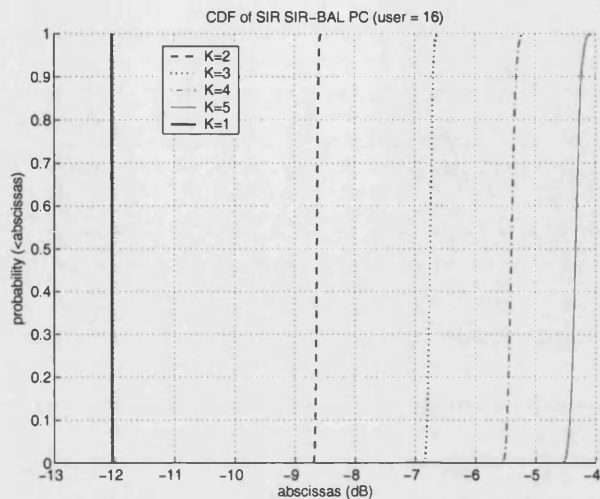
Figure 7.4: CDF of uplink SIR (User=16, SIR-BAL PC)

From Figure 7.4, we see SIR CDF for SIR-BAL power control scheme. The slope of the CDF is greater than that for the POW-BAL power control scheme. This suggests that SIR-BAL scheme can achieve more equalized SIR.

7.4   Capacity gain

For a distributed antenna, providing that the interference received at each antenna unit is independent, capacity gain is linearly proportional to the number of antenna units [24].

We now calculate the capacity gain of the distributed antenna using the POW-BAL and SIR-BAL power control. The result shown in Figures 7.5 and 7.6.

We can see that in both cases, for a given acceptable SIR, the number of users the system can accommodate increases as the number of antenna units increases. It is also clear that the SIR-BAL scheme achieves better SIR performance. The gain from one to two antenna units is about 3 dB and a further 2 dB more for three antenna units. The results suggest an approximately linear increase of SIR with number of antenna
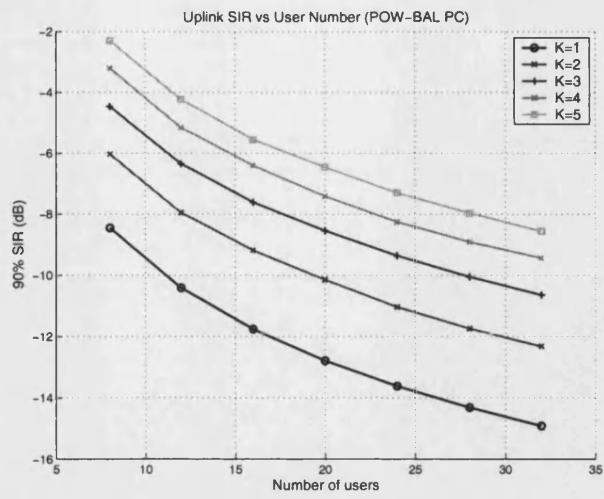
Figure 7.5: 90% exceedance SIR vs. user capacity (POW-BAL PC, uplink)
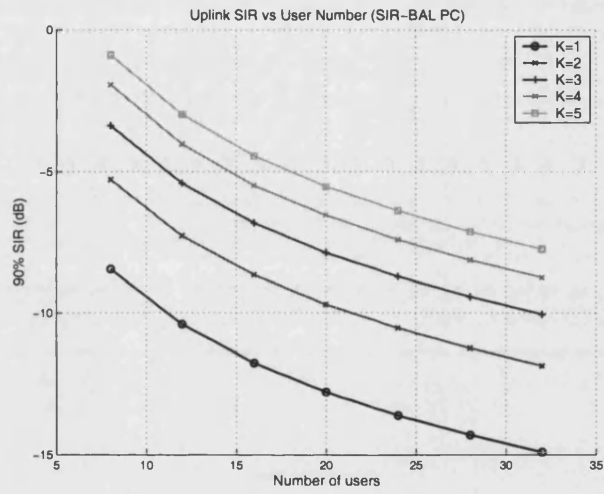
Figure 7.6: 90% exceedance SIR vs. user capacity (SIR-BAL PC, uplink)

units.

Chapter 8

DISTRIBUTED ANTENNAS IN CDMA SYSTEMS - II

In the downlink, due to multiple-input-single-output antenna configuration, all signal branches cannot be received separately as in the uplink. This has been addressed in the Chapter 5 where two different approaches were proposed, i.e. multipath antenna diversity and co-phasing transmission diversity. For different transmission diversity schemes, the SIR analysis will be correspondingly different.

This chapter addresses for the downlink diversity scheme and its SIR performance analysis. Firstly, the signal model is discussed in the context of its broadcasting nature. It is then demonstrated that selective transmission can provide SIR gain only if the power-wise summation diversity is used. Whilst co-phasing diversity can provide SIR gain directly. Simulations of both these schemes are described and the results show that,due to improvement in SIR, distributed antenna base stations can accommodate more users than the conventional based-statistic single antenna.

8.1 Downlink signal model

8.1.1 Single antenna case

In the downlink, the base station antenna broadcasts the signal for all mobile stations. The signals for all mobile station are multiplexed before transmission, each mobile station within a single cell,receives a signal multiplex including its own signal. Importantly

all signals within the multiplex experience the same propagation path:

$$r_j(t) = a_j(\sum_{m=1}^{M} \sqrt{p_m} s_j(t) + \sqrt{p_0} s_0(t))$$
(8.1.1)

$s_j(t)$ is the signal targeting mobile user j and p_j is the power allocated to that user. In the downlink, there is a common pilot channel $s_0(t)$, used for channel estimation by the mobile receiver. It can be viewed on as a special user, to which the base station continuously transmits signal. In our analysis, we treat it as a normal user.

The signals in the multiplex are spread using orthogonal codes. Under the condition of timing alignment, these signals will not cause interference to each other. In the real propagation environment, however the multipath phenomena will cause the inter-user interference, the level of which is denoted by α. α is a factor reflecting the correlation between different signature code symbol synchronization lost. Then, if we ignore thermal noise, the SIR at each mobile station is:

$$\gamma_j = \frac{p_j}{\alpha(\sum_{m,m\neq j}^{M} p_m)}$$
(8.1.2)

For comparative study, we neglect the factor α in our analysis for simplicity. From equation (8.1.2), we see that if SIR for all users is determined by the power allocation in the base station antenna, it is only necessary to allocate power equally to all users and to achieve equalized SIR. The resulting SIR is then $1/(M-1)$.

8.1.2 Distributed antennas case

In the case of a distributed antenna base station, the signal received by mobile users depends on the transmission diversity scheme. One scheme, discussed in Chapter 5, is multipath antenna diversity in which the transmitted signal power from each antenna unit is added power-wise at the mobile user. The composition of received power composition at every mobile users can then be expressed as

$$R_j = \sum_{i=1}^{K} g_{ji}(\sum_{m=1}^{M} p_{mi})$$
(8.1.3)

and SIR can be expressed as:

$$\gamma_j = \frac{\sum_{i=1}^{K} g_{ji} p_{ji}}{\sum_{i=1}^{K} g_{ji} \sum_{m,m\neq j}^{M} p_{mj}}$$
(8.1.4)

If, for each mobile user, the base station antenna units transmit with the same power, then all base station antenna units transmit the same composite signal and we have $p_{mj} = p$, $\forall m, j$.

Equation (8.1.4) can be arranged to give:

$$
\begin{aligned}
\gamma_j &= \frac{p \sum_{i=1}^{K} g_{ji}}{(M-1)p \sum_{i=1}^{K} g_{ji}} \\
&= \frac{1}{M-1}
\end{aligned}
\qquad (8.1.5)
$$

The result is the same as for the conventional single antenna. When power-wise diversity and equal power for all antenna units are adapted, there is no SIR gain for the distributed antenna. This can be explained by the fact that whilst multiple antenna units transmit useful signal to the target user, they also transmit to it the same amount of interference.

8.2 Optimum power allocation

8.2.1 Optimization formulation
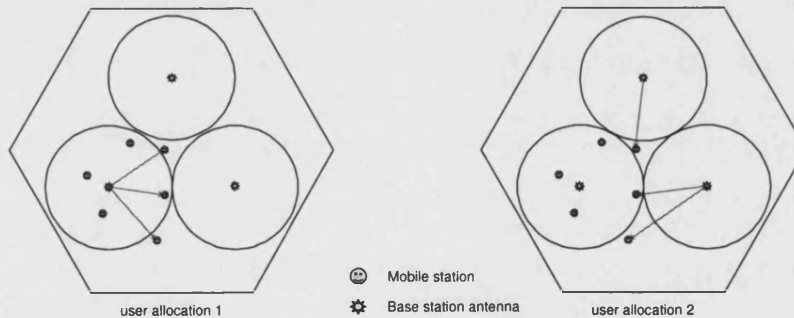
Figure 8.1: Downlink capacity model for distributed antenna

For the distributed antenna, the downlink diversity scheme is not only a signaling problem, but also a resource optimization problem. One way to realize the advantage of the distributed antenna is to transmit users' signals from different antenna units. Each antenna unit transmits a different group users' signals. For a particular mobile user, we call the antenna unit which transmits the signal to that user the serving antenna unit. Part of the interference signals are transmitted from other antenna units, and it is likely

to have propagated a longer distance. Compared to the conventional antenna, in which all interferences propagate the same distance, this scheme will reduce interference level. This can be seen from the example shown in the Figure 8.1. In user allocation scheme 1, every antenna unit transmits signals to all mobile users. In scheme 2, each unit transmits the signal only to one specific user. The interference may then come from the units further away than its own serving antenna unit.

For convenience of matrix manipulation the transmission gain matrix Γ is re-defined by transposing the matrix (7.2.8) as follows:

$$
\begin{aligned}
\Gamma &= \begin{bmatrix} g_{11} & \cdots & g_{1M} \\ \vdots & \ddots & \vdots \\ g_{K1} & \cdots & g_{KM} \end{bmatrix}_{K \times M} \\
&= \begin{bmatrix} \xi_1 & \xi_2 & \cdots & \xi_M \end{bmatrix}_M
\end{aligned}
\tag{8.2.1}
$$

To formulate the problem, we define an allocation matrix Q, which describes the allocation of the power for a particular mobile user among all antenna units, i.e.:

$$
\begin{aligned}
Q &= \begin{bmatrix} q_{11} & \cdots & q_{1K} \\ \vdots & \ddots & \vdots \\ q_{M1} & \cdots & q_{MK} \end{bmatrix}_{M \times K} \\
&= \begin{bmatrix} \Theta_1 \\ \Theta_2 \\ \vdots \\ \Theta_M \end{bmatrix}_M
\end{aligned}
\tag{8.2.2}
$$

$$
\|\Theta_i\|_1 = \sum_{i=1}^{K} q_{ji} = 1, \ q_{ji} \in \Re_+
\tag{8.2.3}
$$

where:

$$
\|\Theta_i\|_1 = \sum_{i=1}^{K} q_{ji} = 1, \ q_{ji} \in \Re_+
\tag{8.2.4}
$$

Q determines the power allocation between antenna units for a particular user. Each component of Θ_i is a fraction of the total power allocated in the ith antenna unit. The transmission power vector P is defined as:

$$P = \begin{bmatrix} p_1 & p_2 & \cdots & p_M \end{bmatrix}, p_j \in \Re_+ \tag{8.2.5}$$

The optimization objective is to determine the matrix Q that maximizes equation The optimization objective is to determine the matrix Q that maximizes equation (8.1.4).

$$Q^* = \arg \max_Q \gamma_j, \; \forall j \tag{8.2.6}$$

This is a non-linear multiple-objective optimization problem.

8.2.2   Determination of transmission power

In the conventional antenna system, when the power assigned to each user is equalized, the resulting SIR will be equalized too. In the distributed antenna system, since different users' signals may be transmitted from different antenna unit, equalizing transmission power can not assure equal received SIR [17, 22, 56, 72]. The received SIR can be re-written into following form

$$
\begin{aligned}
\gamma_j &= \frac{p_j \sum_{i=1}^K q_{ji} g_{ij}}{\sum_{m,m \neq j}^M p_m \sum_{i=1}^K q_{mi} g_{ij}} \\
&= \frac{p_j z_{jj}}{\sum_{m,m \neq j}^M p_m z_{mj}} \\
&= \gamma^*, \; \forall j
\end{aligned}
\tag{8.2.7}
$$

We define a matrix Z to facilitate the development as following:

$$
\begin{aligned}
Z &= Q \times \Gamma \\
&= \begin{bmatrix} z_{11} & \cdots & z_{1M} \\ \vdots & \ddots & \vdots \\ z_{M1} & \cdots & z_{MM} \end{bmatrix}_{M \times M} \\
z_{jm} &= \sum_{i=1}^K q_{ji} g_{im}
\end{aligned}
\tag{8.2.8}
$$

z_{jm} is the total power intended for j^{th} mobile user and received at the mth mobile user. z_{jj} is the received power of the target signal. Then the SIR equalization problem, equation (8.2.7) can then be simplified:

$$\frac{1}{\gamma^*} p_i z_{ii} = \sum_{m,m\neq i}^{M} p_m z_{mi} \tag{8.2.9}$$

If we define the following new quantities (Λ is a unit matrix):

$$Z' = Z \times D^{-1} - \Lambda \tag{8.2.10}$$

where:

$$D^{-1} = \begin{bmatrix} z_{11}^{-1} & 0 & \cdots & 0 \\ 0 & z_{22}^{-1} & \vdots & 0 \\ 0 & 0 & \ddots & 0 \\ 0 & 0 & \vdots & z_{MM}^{-1} \end{bmatrix} \tag{8.2.11}$$

The problem (8.2.9) is transformed to the following eigenvalue problem:

$$\lambda^* P^* = P^* \times Z' \tag{8.2.12}$$

Perron's theorem describing the solution of the above eigenvalue problem states:

If A is a positive matrix, there is a unique eigenvalue of A, which has greatest absolute value. This eigenvalue is positive and simple, and its associated eigenvector may be taken to be positive

Z' has several eigenvalues. The expected solution λ^*, as a function of the target SIR must satisfy the following constraints.

1. $\lambda^* > 0$ since the target SIR, γ^*, must positive.

2. P^* associated with λ^* must all be positive.

3. $\lambda^* = \min\{\lambda | \lambda > 0\}$ λ^* is the least valid value to achieve the best SIR result.

8.2.3 Strongest-link selective transmission

An approximation to optimization problem of equation (8.2.5) is to maximize the received signal power. Thus, the multiple-objective optimization problem is changed to multiple, but individually linear, optimization problems:

$$\Theta_j^* = \arg\max_{\Theta_j} \sum_{i=1}^{K} q_{ji}g_{ij}, \ \forall j \tag{8.2.13}$$

The solution for this simplified problem is:

$$\begin{aligned} \Theta_{ji}^* &= \begin{cases} 1, i = u \\ 0, i \neq u \end{cases} \\ u &= \arg\max_i g_{ji} \end{aligned} \tag{8.2.14}$$

We call this scheme the strongest-link selection scheme. The physical interpretation of this solution is that the received signal power is maximized given a constant transmission power. The power is efficiently delivered to the target users and therefore the received SIR is approximately maximized. Figures 8.2 and 8.3 present the CDF of downlink SIR using this scheme.
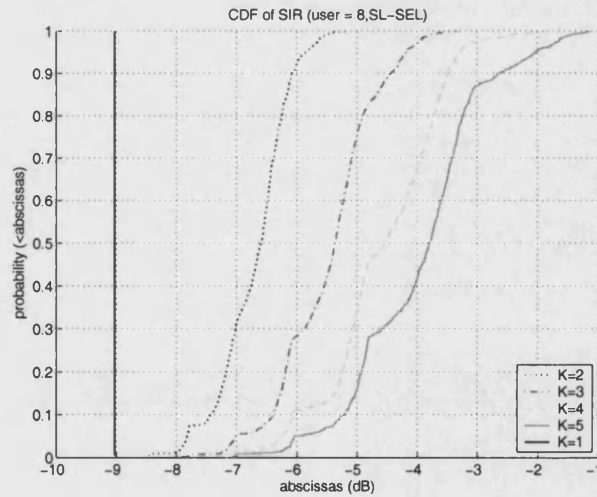
Figure 8.2: CDF of Downlink SIR (8 users, SL-SEL)

We can see from these figures the advantage of the distributed antenna in terms of
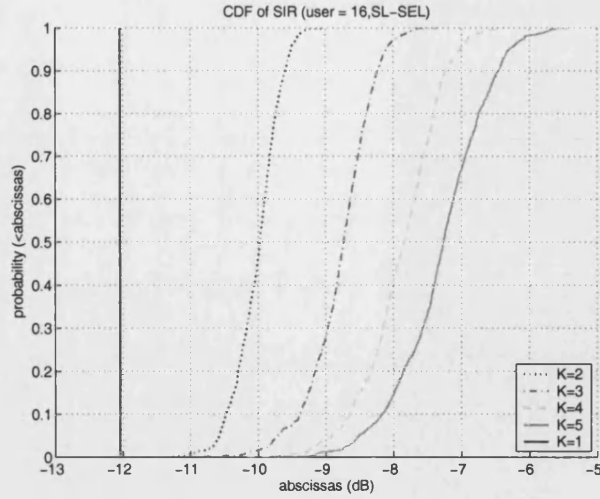
Figure 8.3: CDF of Downlink SIR (16 users, SL-SEL)

downlink SIR. We can also see that the CDF of SIR has finite slope. This is not due to inaccurate power control. It suggests that the equalized SIR achieved for different mobile user distribution is different. When users are clustered evenly around different antenna units, each unit will serve equal numbers of nearby users and each user will received less interference.

8.2.4 Least-interference selective transmission

Another approximation considers the total interference experienced by all other users. We define a new vector Ψ_j, each element of which is the ratio between the total power transmitted from the ith antenna and received at other users to the power received by the jth user.

$$\Psi_j = \begin{bmatrix} \zeta_{1j} \\ \zeta_{2j} \\ \vdots \\ \zeta_{Kj} \end{bmatrix}_K$$

$$\zeta_{ij} = \sum_{m=1}^{M} \frac{g_{im}}{g_{ij}} - 1 \qquad (8.2.15)$$

The total interference caused by transmitting the jth mobile user's signal is:

$$\beta_j = \Theta_j \times \Psi_j \qquad (8.2.16)$$

The approximate optimization problem then is transformed to:

$$\Theta_j^* = \arg\max_{\Theta_j} \beta_j \qquad (8.2.17)$$

This has the same form as equation (8.2.6). The solution is:

$$
\begin{aligned}
q_{ji}^* &= \begin{cases} 1, i = u \\ 0, i \neq u \end{cases} \\
u &= \arg\max_i \zeta_{ij}
\end{aligned}
\qquad (8.2.18)
$$

The essential objective here is to minimize the total interference power experienced by other mobile user while keeping a constant received power for the target user. We call this scheme least-interference selection transmission. The CDF of the downlink SIR using this scheme is shown in Figures 8.4 and 8.5.
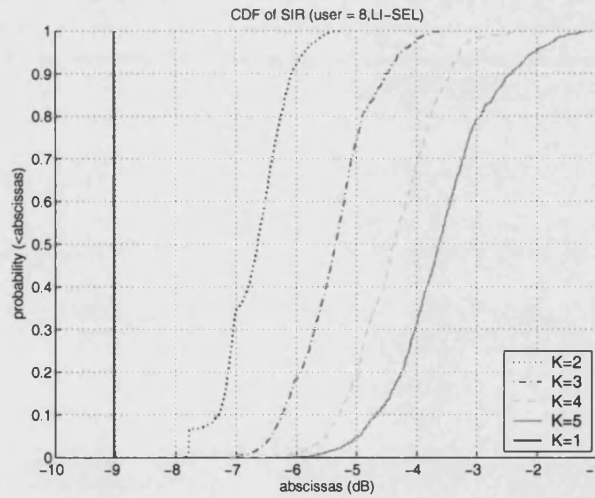
Figure 8.4: CDF of Downlink SIR (8 User, LI-SEL)

It can be seen that SIR gain and CDF shape are similar to those for strongest-link selective scheme.
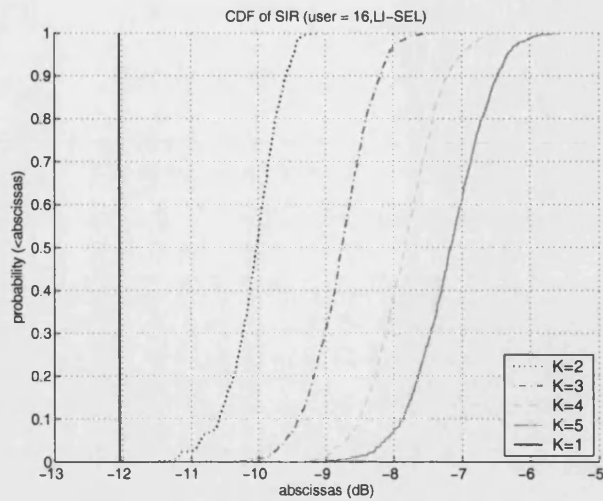
Figure 8.5: CDF of Downlink SIR (16 User, LI-SEL)

8.2.5 Capacity improvement

We have evaluate 90% SIR as function of user number for the downlink selective schemes. Figure 8.6 shows the results for strongest-link selective scheme and Figure 8.7 shows the results for the least-interference selective scheme.
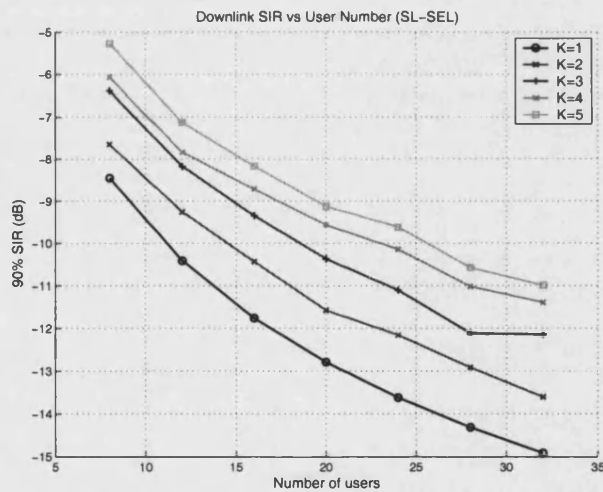
Figure 8.6: 90% exceedance SIR vs. user number (SL-SEL, downlink)

In these figures, we can see the SIR gain of the distributed antenna downlink selective schemes. The two schemes give similar results. Compared to the uplink case, the gain is smaller. We compare the two schemes by plotting 90% SIR difference between LI-SEL and SL-SEL against number of users in Figure 8.8 99% SIR different in Figure
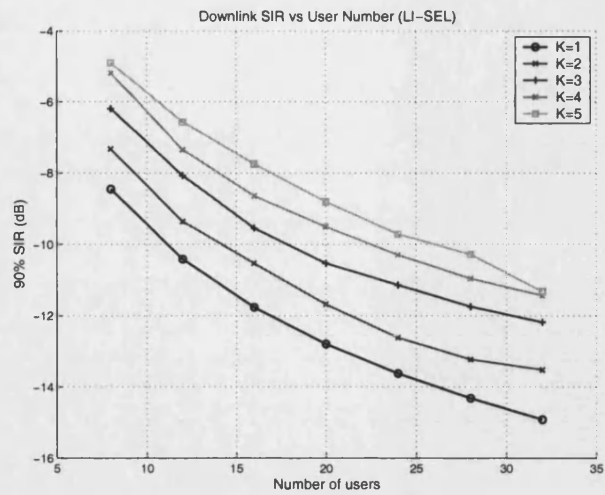
Figure 8.7: 90% exceedance SIR vs. user number (LI-SEL, downlink)

8.9. We see that the least-interference scheme achieves marginally better performance than the strongest-link scheme when the number of users per antenna unit is low (8 and 12 users for 4 and 5 antenna units).
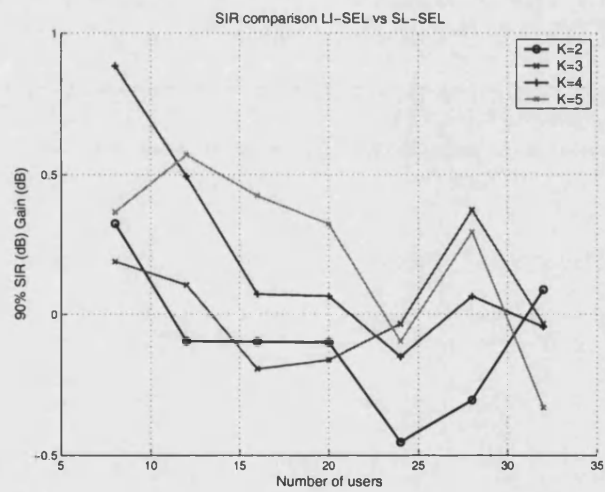
Figure 8.8: 90% exceedance SIR difference vs user number (LI-SEL vs SL-SEL)

The capacity gain achieved by using the selective scheme comes from matching between mobile users' spatial distribution and the position of the antenna units. Each antenna unit then forms a virtual cell. In the vicinity of an antenna unit the intended signal thus experiences less loss than the interference arriving from antenna units further away. This is analogous to the spatial division gain achieved by cell splitting.
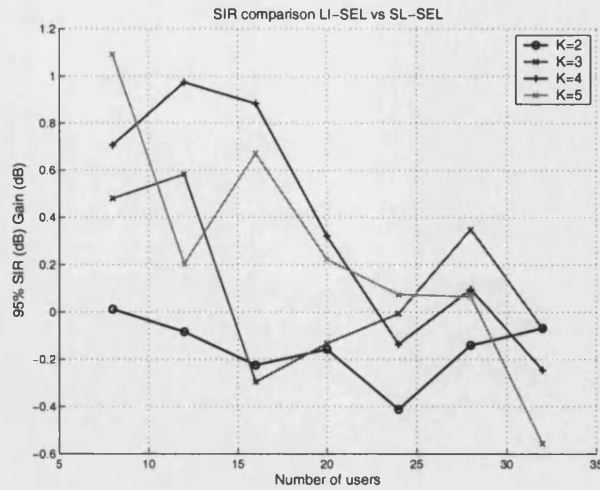
Figure 8.9: 95% exceedance SIR difference vs user number (LI-SEL vs SL-SEL)

8.3 Co-phasing transmission diversity

8.3.1 Signal model

The SIR received at each mobile user can be increased taking the advantage of user distribution and the extra attenuation of interference. As selective diversity uses only one channel at each time, however, this scheme is inferior in terms of fade mitigation to a diversity scheme which combines all channel signals. In Chapter 5, we have already shown that using co-phasing diversity can achieve better SIR.

The feature of this scheme is that for each target user, the signals from all channels are summed in amplitude (voltage-wise), while interference is summed power-wise. If, for each user, we allocate power in proportion to the transmission gain of each channel, we get a power allocation matrix as follows:

$$
Q = \left[\begin{array}{ccc} g_{11} & \cdots & g_{K1} \\ \vdots & \ddots & \vdots \\ g_{1M} & \cdots & g_{KM} \end{array} \right]_{M \times K}
\tag{8.3.1}
$$

Q is not a valid power allocation matrix because 1-norm of each column vector does not equal to one. This does not change the ultimate result, however, because the same factor will be reflected in the transmission power in the eigenvalue solution. The SIR

for each user is therefore expressed as:

$$\gamma_j = \frac{p_j(\sum_{i=1}^{K} g_{ij})^2}{\sum_{m,m\neq j}^{M} p_m \sum_{i=1}^{K} g_{im} g_{ij}}$$

(8.3.2)

8.3.2 Equalization of SIR

The received SIR is equalized using the same process as in the previous schemes, but the Z matrix has a different value, i.e.:

$$Z' = (Q \times \Gamma - \Lambda) \times D^{-1}$$

(8.3.3)

Here Λ and D^{-1} are diagonal matrices with values:

$$D = \begin{bmatrix} (\sum_{i=1}^{K} g_{i1})^2 & \cdots & 0 \\ \vdots & \ddots & \vdots \\ 0 & \cdots & (\sum_{i=1}^{K} g_{iM})^2 \end{bmatrix}_{M \times M}$$

(8.3.4)

$$\Lambda = \begin{bmatrix} \sum_{i=1}^{K} g_{i1}^2 & \cdots & 0 \\ \vdots & \ddots & \vdots \\ 0 & \cdots & \sum_{i=1}^{K} g_{iM}^2 \end{bmatrix}_{M \times M}$$

(8.3.5)

(8.3.6)

Figures 8.10 and 8.11 show CDF of SIR for 8 and 16 users using for this co-phasing transmission scheme.

We can see that using the co-phasing scheme, the CDF of downlink SIR is still uneven for different spatial distributions. Similar to the selective case, the slope of the CDF is related to the number of antenna units. The more antenna units, the smaller the slope. This can be explained by the observation that when there are more antenna units, the ways of clustering the mobile users around these units increases, and this influences the resulting SIR.
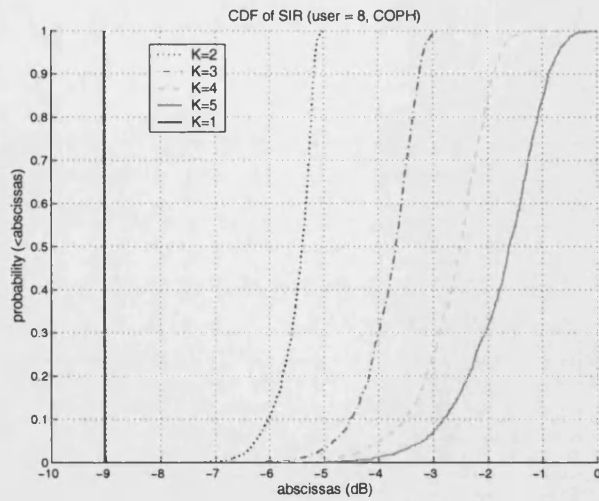
Figure 8.10: CDF of Downlink SIR (8 User, COPH)
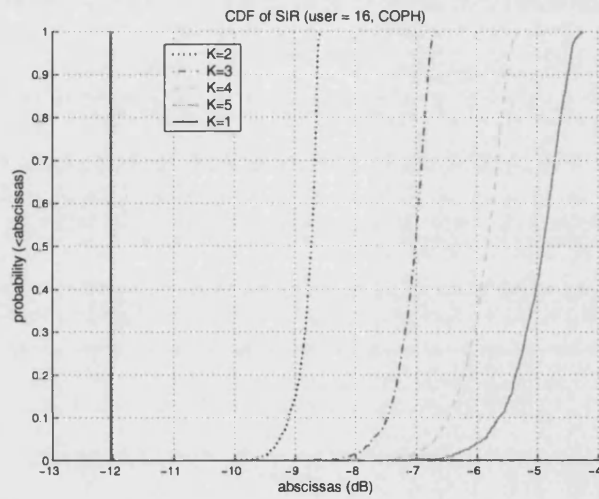
Figure 8.11: CDF of Downlink SIR (16 User, COPH)

8.3.3 Capacity improvement

Figure 8.12 shows the 90% SIR as a function of user number for the co-phasing scheme. Compared to the selective schemes, this scheme achieves higher SIR gain. This improvement comes from the increased signal strength after co-phase combining.
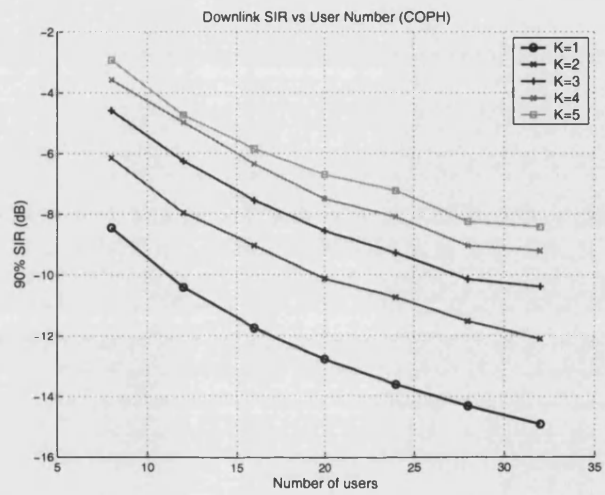
Figure 8.12: 90% exceedance SIR vs user number (COPH, downlink)

Chapter 9

CONCLUSIONS AND FUTURE WORK

In this chapter, we summarize the results obtained from the project. The results are on four aspects: radio coverage, wide-band transmission diversity, network spectral efficiency and user capacity in CDMA system. In each of these aspects, some directions of future work are suggested to either make the study more thorough or enable the practical usage.

9.1 Conclusions

The following conclusions are drawn from the study of the distributed antenna system.

9.1.1 Improved coverage

Distributed antennas improve radio coverage significantly especially for high carrier frequencies, since propagation loss and shadowing are more serious than for lower frequency carriers. The evaluation of coverage of the distributed antenna system has been performed in outdoor and indoor environments, using ray tracing and on-site measurement methods respectively. Both the first-order moment statistical metrics and CDF curves show that the distributed antenna base station has a dramatic advantage over a conventional antenna base station.

9.1.2 Transmission diversity

Due to the single antenna nature of the mobile station, transmission diversity is a critical technique to realize the advantage of the distributed antenna system. In the narrow-band system, as the time dispersion caused by multipath propagation is neglected, co-phasing transmission is possible. In the wideband system, it is not trivial to achieve a combining gain when the arriving signal is dispersed in time. Based on the on-site measurement, we propose a wideband co-phasing transmission diversity scheme. The evaluation of the diversity performance in terms of the gross power after combining shows that it has an advantage over another scheme – multipath antenna diversity.

9.1.3 Inter-cell interference and spectral efficiency

The deployment of the distributed antenna system results two new characteristics: reduced transmission power and closer interfering distance. These two effects have opposing effects on the inter-cell interference. A simulation of a pair interfering cells shows that the distributed antenna system increases the inter-cell interference marginally when a constant total transmitted power is assumed. When the power control technique is used with the distributed antenna, the advantage of the efficient delivery of signal can be translated into a dramatic decrease in inter-cell interference.

A multiple-cell simulation shows that when the distributed antenna system is deployed in several neighbouring cells, the spectral efficiency can be improved significantly. The use of the distributed antenna system can release the capacity demand in the hot spot.

9.1.4 The distributed antenna system in a CDMA system

Because of the spread-spectrum nature of the CDMA system, the distributed antenna system has new features when it is used in the CDMA system. In the uplink, because of the SIR gain achieved by combined reception, the distributed antenna can provide more user capacity.

In the downlink, to realize the advantage of the distributed antenna, an optimal power allocation is needed. For the power-wise summation diversity, a selective transmission is optimal in terms of the resulting received SIR. When wideband co-phasing diversity is used, the power allocation is proportional to the transmission gain of each channel, which is the same principle as maximal ratio combining. This scheme achieves better

SIR than the selective transmission scheme.

9.2 Future work

The distributed antenna system is a complex system with many details to be investigated before it can be put into practical usage.

9.2.1 Study of co-phasing transmission

Co-phased transmission is a critical constituent technique in the distributed antenna system. In the performance analysis presented in this thesis, we neglect the implementation details of this technique assuming a perfect co-phasing transmission. But in a real system and propagation environment, there is some work to be done to achieve co-phasing transmission.

Characterizing the channel's phase response

Knowledge of the temporal variation characteristics of the channel response, particularly the phase response, is crucial for the implementation of the co-phase transmission. The temporal variation characteristic determines the tracking loop bandwidth and the necessary update rate of the channel information.

Investigation of the frequency correlation could facilitate the design of the channel estimation scheme for FDD duplex mode.

Channel estimation

The co-phasing transmission is based on a complete knowledge of the downlink channel. The first task is to investigate the channel estimation, especially the phase information. For the TDD mode duplex operation, the downlink channel information can be obtained from the channel estimation of the reciprocal uplink [42].

But for the FDD mode, the reciprocity does not apply any more since different frequencies are used in uplink and downlink. There are two options available. One is using a

reverse signaling channel to transmit the channel information measured at the mobile-station back to the base station. An obvious disadvantage is that this scheme will sacrifice channel utilization due to the signaling overhead. Then there will be a trade-off between signaling data rate and channel information accuracy. The transmission and coding/decoding channel information will inevitably introduce delay in applying the channel information to the co-phasing process. Another choice is to utilize the correlation between the uplink and downlink channels to derive the downlink channel information from the uplink channel [31]. Due to the complexity of the multipath propagation, this scheme may not have the required accuracy.

Performance evaluation of co-phasing implementation

Evaluating the performance of the co-phasing implementation conversely aids the design of the co-phasing transmission. The sensitivity of the performance against the phase information accuracy determines the requirements on the selection of the channel estimation algorithm and the estimation rate. In the case that the channel information is to be transmitted, this also determines the word-length of the phase information.

9.2.2 Study of wideband transmission diversity

The transmission diversity scheme for wideband signals studied in this thesis is based on a measurement in an indoor environment. But the outdoor environment configuration can be more complex than indoor environment. Building material is of more types and building height is of greater range. Because of an open nature and rich scattering, the delay profile in outdoor area has larger rms delay. This may cause the phase response in the delay profile to vary at a higher rate. These factors disable results obtained in this thesis from being applied in an outdoor environment. A separate study, with similar method presented in this thesis, is needed in an outdoor environment.

9.2.3 Downlink performance in the CDMA system

In the CDMA system, because the synchronization is easily maintained, orthogonal codes are used for all users served in one cell. If this chip synchronization is maintained at the receiver, all users' signals can be separated without any inter-user interference. Multipath propagation causes the loss of synchronization resulting in loss of orthogonality, represented by the Orthogonal Factor (OF). The level of inter-user interference

is proportional to OF, which is in the interval $[0, 1]$ [54]. 0 is for the orthogonal case and 1 for the non-orthogonal spreading code [28, 18].

In the distributed antenna system, for the selection transmission schemes, as different users' signals may be transmitted from different antenna units, it's difficult to maintain the synchronization at every receiver. Each antenna unit can be seen as a scatter causing one multipath component. In the study presented in this thesis, we assume that the loss of orthogonality in the distributed antenna system is similar to the case of a traditional antenna.

Study of orthogonal factor

A study of the orthogonal factor in the distributed antenna system is needed to evaluate the inter-user interference. The orthogonal factor is a random variable as a function of the relative arrived time of other users' multipath signals. The study could obtain the statistics of the orthogonal factor [50]. As different transmission diversity schemes have different signal flow pattern, this will result a different orthogonal factor statistics.

Mitigation of loss of synchronization

For the selective transmission scheme, a possible mitigation for the loss synchronization could be to adjust the relative arrived time by pre-delaying the signals at each antenna unit. This may not enable signals arrive at the same time instant, but it can minimize the total time dispersion caused by multiple antenna transmission.

New spreading code

Some researchers use computers to aid searching for 'good' spreading codes, which have low auto- and cross-correlation [13, 15, 41]. New family of spreading codes – complementary codes – is also proposed [16, 9]. It is proved that it has good auto- and cross-correlation characteristics. Downlink performance of the distributed antenna may not be compromised when used with these types of spreading code.

9.2.4 Multi-cell joint power control in CDMA system

In this thesis, the power control is performed among all users in one cell. When the distributed antenna system is adopted in several neighboring cells, as antenna units are spread in the service area and the cell boundary are blurred, it will give a better performance to perform a multi-cell joint power control.

Uplink case

In the uplink, as all users are using non-orthogonal spreading codes, the intra-cell and inter-cell interference has the same correlation character. It is very easy to extend the distributed antenna power control to the multi-cell case. The transmission gain matrix is extended to included all base station and mobile antennas in all cells involved. The only concern is the computation load of finding the eigenvalue.

Downlink case

In the downlink, as the intra-cell and inter-cell interferences have different correlation characteristic. The extension of the transmission gain matrix from single cell to multi-cell is not trivial. The element in the matrix may have a different weight depending on the orthogonal factor. The intra-cell interference has a less than 1 OF and inter-cell interference has a largest OF of 1. Apart from this, the difficult of finding the eigenvalue is the same as the uplink case.

References

[1] E. Adair and R. Petersen, "Biological effects of radiofrequency/microwave radiation," *Microwave Theory and Techniques, IEEE Transactions on*, vol. 50, no. 3, pp. 953–962, March 2002.

[2] S. Ariyavisitakul, T. Darcie, L. Greenstein, M. Phillips, and N. Shankaranarayanan, "Performance of simulcast wireless techniques for personal communication systems," *Selected Areas in Communications, IEEE Journal on*, vol. 14, no. 4, pp. 632–643, May 1996.

[3] A. Arredondo, D. Cutrer, J. Georges, and K. Lau, "Techniques for improving in-building radio coverage using fiber-fed distributed antenna networks," in *Vehicular Technology Conference, 1996. 'Mobile Technology for the Human Race'., IEEE 46th*, vol. 3, 28 April-1 May 1996, pp. 1540–1543.

[4] J.-E. Berg, "A recursive method for street microcell path loss calculations," in *Personal, Indoor and Mobile Radio Communications, 1995. PIMRC'95. 'Wireless: Merging onto the Information Superhighway'., Sixth IEEE International Symposium on*, vol. 1, 27-29 Sept. 1995, pp. 140–143.

[5] R. Bernhardt, "Macroscopic diversity in frequency reuse radio systems," *IEEE Journal on Selected Areas in Communications*, vol. 5, no. 5, pp. 862–870, 1987.

[6] N. Blaunstein and M. Levin, "Propagation loss prediction in the urban environment with rectangular grid-plan streets," in *Antennas and Propagation, Tenth International Conference on*, vol. 2, 14-17 April 1997, pp. 178–181.

[7] A. Brandao, L. Lopes, and D. McLernon, "Base station macro-diversity combining merge cells in mobile systems," *Electronics Letters*, vol. 31, no. 1, pp. 12–13, 1995.

[8] K. Bye, "Leaky-feeders for cordless communication in the office," in *Electrotechnics, 1988. Conference Proceedings on Area Communication, EUROCON 88., 8th European Conference on*, 13-17 June 1988, pp. 387–390.

[9] H. Chen, J. Yeh, and N. Suehiro, "A multicarrier CDMA architecture based on orthogonal complementary codes for new generations of wideband wireless communications," *Communications Magazine, IEEE*, vol. 39, no. 10, pp. 126–135, Oct. 2001.

[10] P. Chow, A. Karim, V. Fung, and C. Dietrich, "Performance advantages of distributed antennas in indoor wireless communication systems," in *Vehicular Technology Conference, 1994 IEEE 44th*, vol. 3, 8-10 June 1994, pp. 1522–1526.

[11] T.-S. Chu and M. Gans, "Fiber optic microcellular radio," *Vehicular Technology, IEEE Transactions on*, vol. 40, no. 3, pp. 599–606, Aug. 1991.

[12] COST231, *Urban transmission loss models for mobile radio in the 900- and 1800 MHz bands (Revision 2)*. European commission, 1996.

[13] E. Cruselles, M. Soriano, and J. Melus, "Uncorrelated pn sequences generator for spreading codes in CDMA systems," in *Personal, Indoor and Mobile Radio Communications, 1995. PIMRC'95. 'Wireless: Merging onto the Information Superhighway'., Sixth IEEE International Symposium on*, vol. 3, 27-29 Sept. 1995, p. 1335.

[14] V. Erceg, A. J. Rustako, and R. Roman, "Diffraction around corners and its effects on the microcell coverage area in urban and suburban environments at 900 mhz, 2 ghz, and 4 ghz," *Vehicular Technology, IEEE Transactions on*, vol. 43, no. 3, pp. 762–766, Aug. 1994.

[15] M. Fong, V. Bhargava, and Q. Wang, "Concatenated orthogonal/pn spreading sequences and their application to cellular ds-cdma systems with integrated traffic," *Selected Areas in Communications, IEEE Journal on*, vol. 14, no. 3, pp. 547–558, 1996.

[16] R. Frank, "Polyphase complementary codes," *Information Theory, IEEE Transactions on*, vol. 26, no. 6, pp. 641–647, Nov. 1980.

[17] R. Gejji, "Forward-link-power control in CDMA cellular systems," *Vehicular Technology, IEEE Transactions on*, vol. 41, pp. 532–536, Nov. 1992.

[18] E. Geraniotis and M. Pursley, "Error probability for direct-sequence spread-spectrum multiple-access communications–part ii: Approximations," *Communications, IEEE Transactions on*, vol. 30, no. 5, pp. 985–995, May 1982.

[19] C. Ghobadi, P. Shepherd, and S. Pennock, "2d ray-tracing model for indoor radio propagation at millimetre frequencies, and the study of diversity techniques," *Microwaves, Antennas and Propagation, IEE Proceedings*, vol. 145, no. 4, pp. 349–353, Aug. 1998.

[20] K. Gilhousen, I. Jacobs, R. Padovani, A. Viterbi, L. J. Weaver, and C. I. Wheatley, "On the capacity of a cellular CDMA system," *Vehicular Technology, IEEE Transactions on*, vol. 40, no. 2, pp. 303-312, May 1991.

[21] A. Goldsmith and L. Greenstein, "An empirical model for urban microcells, with applications and extensions," in *Vehicular Technology Conference, 1992 IEEE 42nd*, vol. 1, 10-13 May 1992, pp. 419-422.

[22] S. Grandhi, R. Vijayan, D. Goodman, and J. Zander, "Centralized power control in cellular radio systems," *Vehicular Technology, IEEE Transactions on*, vol. 42, no. 4, pp. 466-468, Nov. 1993.

[23] L. Greenstein, N. Amitay, T.-S. Chu, L. J. Cimini, G. Foschini, M. Gans, I. Chih-Lin, A. J. Rustako, R. Valenzuela, and G. Vannucci, "Microcells in personal communications systems," *Communications Magazine, IEEE*, vol. 30, no. 12, pp. 76-88, Dec. 1992.

[24] S. Hanley, "An algorithm for combined cell-site selection and power control to maximize cellular spread spectrum capacity," *Selected Areas in Communications, IEEE Journal on*, vol. 13, no. 7, pp. 1332-1340, 1995.

[25] ——, "Capacity and power control in spread spectrum macrodiversity radio networks," *Communications, IEEE Transactions on*, vol. 44, no. 2, pp. 247-256, Feb. 1996.

[26] V. Hardman and S. Hailes, *Insights into Mobile multimedia communications*, ser. Signal Processing and its applications. Academic Press, 1999, ch. Mobile multimedia access for the Internet, pp. 111-130.

[27] P. Harley, "Short distance attenuation measurements at 900 mhz and 1.8 ghz using low antenna heights for microcells," *Selected Areas in Communications, IEEE Journal on*, vol. 7, no. 1, pp. 5-11, Jan. 1989.

[28] F. Hemmati and D. Schilling, "Upper bounds on the partial correlation of pn sequences," *Communications, IEEE Transactions on*, vol. 31, no. 7, pp. 917-922, July 1983.

[29] K. Kerpez, "A radio access system with distributed antennas," *Vehicular Technology, IEEE Transactions on*, vol. 45, no. 2, pp. 265-275, May 1996.

[30] A. Klein, B. Steiner, and A. Steil, "Known and novel diversity approaches as a powerful means to enhance the performance of cellular mobile radio systems," *Selected Areas in Communications, IEEE Journal on*, vol. 14, no. 9, pp. 1784-1795, Dec. 1996.

[31] K. Knoche, H. Rinas, and K.-D. Kammeyer, "Channel estimation with linear interpolation and decision feedback for utra fdd downlink," in *Spread Spectrum Techniques and Applications, 2002 IEEE Seventh International Symposium on*, vol. 1, 2002, pp. 54–58.

[32] J. Korhonen, *Introduction to 3G Mobile communications*, 2nd ed. Artech House, 2003, ch. 3G Services, pp. 395–406.

[33] T. Kürner, D. Cichon, and W. Wiesbeck, "The influence of land usage on uhf wave propagation in the receiver near range," *Vehicular Technology, IEEE Transactions on*, vol. 46, no. 3, pp. 739–747, Aug. 1997.

[34] N. Lea-Wilson, J. Webster, and M. McElroy, "Dark fibre and spare copper: cable planning for the new generation of uk access networks," in *Customer Access - the Last 1.6 km, IEE Colloquium on*, 1 Jun 1993, pp. 5/1–5/6.

[35] C.-C. Lee and R. Steele, "Effect of soft and softer handoffs on CDMA system capacity," *Vehicular technology, IEEE Transactions on*, vol. 47, no. 3, pp. 830–842, August 1998.

[36] W. Lee, "Effects on correlation between two mobile radio base-station antennas," *IEEE Trans. Communications*, vol. COM-21, pp. 1214–1224, Nov 1973.

[37] ——, *Mobile communications engineering*, 2nd ed., ser. Wiley series in telecommunications. McGraw-Hill, Inc, 1982, ch. 9, pp. 273–290.

[38] ——, *Mobile cellular telecommunications systems*. McGraw-Hill Book Company, 1990, ch. 12, pp. 337–400.

[39] ——, "Smaller cells for greater performance," *IEEE Communications Magazine*, vol. 29, no. 11, pp. 19–23, 1991.

[40] ——, *Mobile communications design fundamentals*, 2nd ed., ser. Wiley series in telecommunications. John Wiley and Sons, Inc, 1993, ch. 2, pp. 47–100.

[41] X. Lin and K. Chang, "Optimal PN sequence design for quasisynchronous CDMA communication systems," *Communications, IEEE Transactions on*, vol. 45, no. 2, pp. 221–226, Feb. 1997.

[42] Y. Lou, "Channel estimation standard and adaptive blind equalization," *Communications, IEEE Transactions on*, vol. 43, no. 234, pp. 182–186, Feb./March/April 1995.

[43] R. Macario, *Cellular Radio: principles and design*. Macmillan Press Ltd, 1993, ch. 9, pp. 191–228.

[44] Motorola, "Urban canyon, and parameters values for the spatial channel model," 3GPP/3GPP2, Tech. Rep. SCM-067, Oct. 2002.

[45] G. T. R. A. Network, "Base station (BS) radio transmission and reception (FDD)," 3GPP, Tech. Rep., Dec. 2004.

[46] J. Oetting, "Cellular mobile radio," *Communications Magazine, IEEE*, vol. 21, no. 8, pp. 15–18, 1983.

[47] L. Ortigoza-Guerrero and A. Aghvami, *Resource Allocation in Hierarchical Cellular Systems*. Artech House Publishers, 2000.

[48] W. Papen, "Uplink performance of a new macro-diversity cellular mobile radio architecture," in *Personal, Indoor and Mobile Radio Communications, 1995. PIMRC'95. 'Wireless: Merging onto the Information Superhighway'., Sixth IEEE International Symposium on*, vol. 3, 27-29 Sept. 1995, p. 1118.

[49] J. Parsons and J. Gardiner, *Mobile communications systems*, ser. Blackie series in information technology. Blackie and Son Limited, 1989, ch. 6, pp. 190–243.

[50] C. Passerini and G. Falciasecca, "Correlation between delay-spread and orthogonality factor in urban environments," *Electronics Letters*, vol. 37, no. 6, pp. 384–386, 15 March 2001.

[51] A. Paulraj, R. Nabar, and D. Gore, *Introduction to Space-Time Wireless Communications*. Cambridge University Press, 2003.

[52] J. Pereira, J. Schwarz, B. Arroyo-Fernández, B. Barani, and D. Ikonomou, *Insights into Mobile multimedia communications*, ser. Signal Processing and its applications. Academic Press, 1999, ch. From wireless data to mobile multimedia: R&D perspectives in Europe, pp. 143 – 176.

[53] R. Pickholtz, D. Schilling, and L. Milstein, "Theory of spread-spectrum communications - a tutorial," *Communications, IEEE Transactions on*, vol. 30, no. 5, pp. 855 – 884, May 1982.

[54] M. Pursley, D. Sarwate, and W. Stark, "Error probability for direct-sequence spread-spectrum multiple-access communications–part i: Upper and lower bounds," *Communications, IEEE Transactions on*, vol. 30, no. 5, pp. 975–984, May 1982.

[55] T. Rappaport, *Wireless Communications: Principles and Practice*, ser. Prenticd Hall Communications Engineering and Emerging Technologies Series. Prentice Hall PTR, 1996, ch. 4, pp. 143–153.

[56] L. A. D. Rocha and J. Brandao, "General analysis of downlink power control in CDMA systems," in *Telecommunications Symposium, 1998. ITS '98 Proceedings. SBT/IEEE International*, vol. 1, 9-13 Aug. 1998, pp. 172–176.

[57] A. Rustak, Y. Yeh, and R. Murray, "Performance of feedback and switch space diversity 900 mhz fm mobile radio system with rayleigh fading," *Communications, IEEE Transactions on*, vol. 21, pp. 1257 – 1268, 1973.

[58] A. Saleh, A. Rustako, and R. Roman, "Distributed antennas for indoor radio communications," *Communications, IEEE Transactions on*, vol. 35, no. 12, pp. 1245 – 1251, Dec. 1987.

[59] A. Salmasi and K. Gilhousen, "On the system design aspects of code division multiple access (cdma) applied to digital cellular and personal communications networks," in *Vehicular Technology Conference, 1991. 'Gateway to the Future Technology in Motion', 41st IEEE*, 19 - 22 May 1991, pp. 57 – 62.

[60] J. Salz, "Effects of fading correlation on adaptive arrays in digital mobile radio," *Vehicular technology, IEEE Trans. on*, vol. 43, no. 4, pp. 1049 – 1057, Nov 1994.

[61] S. Saunders, *Antennas and propagation for wireless communication systems*. John Wiley & Sons, Ltd, 1999, ch. 11, pp. 235 – 251.

[62] C. Seltzer, "Indoor coverage requirements and solutions," in *Antennas and Propagation for Future Mobile Communications (Ref. No. 1998/219), IEE Colloquium on*, no. 3, 23 Feb. 1998, pp. 1 – 4.

[63] Z. Sienkiewicz, "Biological effects of electromagnetic fields and radiation," in *Electromagnetic Compatibility, 1994. Ninth International Conference on*, 5-7 Sep. 1994, pp. 17 – 21.

[64] P. Smyth, *Mobile and Wireless Communications: Key Technologies and Future Applications*. IEE, 2004, ch. Optical Radio - a Review of a Radical New Technology for Wireless Access Infrastructure, pp. 19 – 35.

[65] E. Sousa, "Antenna architectures for CDMA integrated wireless access networks," in *Personal, Indoor and Mobile Radio Communications, 1995. PIMRC'95. 'Wireless: Merging onto the Information Superhighway'., Sixth IEEE International Symposium on*, vol. 3, 27-29 Sept. 1995, p. 921.

[66] I. Stamopoulos, A. Aragon, and S. Saunders, "Performance comparison of distributed antenna and radiating cable systems for cellular indoor environments in the dcs band," in *Antennas and Propagation, 2003. (ICAP 2003). Twelfth International Conference on (Conf. Publ. No. 491)*, vol. 2, 31 March - 3 April 2003, pp. 771 – 774.

[67] G. Turin, "The characteristics and function of a hermition quadratic form in a complex normal variable," *Biometrika*, vol. 47, pp. 199 – 201, June 1960.

[68] M. VanBlaricum, "Photonic systems for antenna applications," *Antennas and Propagation Magazine, IEEE*, vol. 36, no. 5, pp. 30–38, Oct. 1994.

[69] B. V. Veen and K. Buckley, "Beamforming: a versatile approach to spatial filtering," *IEEE ASSP Magazine*, April 1988.

[70] A. Viterbi, A. Viterbi, K. Gilhousen, and E. Zehavi, "Soft handoff extends CDMA cell coverage and increases reverse link capacity," *Selected Areas in Communications, IEEE Journal on*, vol. 12, no. 8, pp. 1281 – 1288, Oct. 1994.

[71] A. Viterbi, A. Viterbi, and E. Zehavi, "Other-cell interference in cellular power-controlled CDMA," *Communications, IEEE Transactions on*, vol. 42, no. 234, pp. 1501 – 1504, Februray/March/April 1994.

[72] M. Wang and O. Tonguz, "Forward link power control for cellular CDMA networks," *Electronics Letters*, vol. 29, no. 13, pp. 1195–1197, 24 June 1993.

[73] W. Webb, *The future of wireless communications.* Artech House, Inc., 2001.

[74] L. Westbrook, L. Noel, and D. Moodie, "Full-duplex, 25 km analogue fibre transmission at 120 mbit/s with simultaneous modulation and detection in an electroabsorption modulator," *Electronics Letters*, vol. 33, no. 6, pp. 694 – 695, 10 April 1997.

[75] R. Williams, *The Geometrical Foundation of Natural Structure: A Source Book of Design.* New York: Dover, 1979, ch. Circle Packings, Plane Tessellations, and Networks, pp. 34–47.

[76] J. Winters, "On the capacity of radio communication systems with diversity in a rayleigh fading environmet," *Selected Areas Communications, IEEE Journal*, vol. SAC-5, no. 5, pp. 871 – 878, June 1987.

[77] ——, "Optimum combining for indoor radio systems with multiple users," *IEEE Trans. Communications*, vol. COM-35, pp. 1222 – 1230, Nov 1987.

[78] J. Winters, J. Salz, and R. Gitlin, "The capacity of wireless communication systems can be substantially increased by the use of antenna diversity," in *Universal Personal Communications, 1992. ICUPC '92 Proceedings., 1st International Conference on*, vol. 2, no. 1, 29 Sept. - 1 Oct. 1992, pp. 1 – 5.

[79] ——, "The impact of antenna diversity on the capacity of wireless communication systems," *Communications, IEEE Transactions on*, vol. 42, no. 234, pp. 1740 – 1751, Feb/Mar/Apr 1994.

[80] A. Wittneben, "Basestation modulation diversity for digital simulcast," in *Vehicular Technology Conference, 1991. 'Gateway to the Future Technology in Motion', 41st IEEE*, 19-22 May 1991, pp. 848–853.

[81] P. Wolniansky, G. Foschini, G. Golden, and R. Valenzuela, "V-BLAST: an architecture for realizing very high data rates over the rich-scattering wireless channel," in *Signals, Systems, and Electronics, 1998. ISSSE 98. 1998 URSI International Symposium on*, 29 Sept.-2 Oct. 1998, pp. 295 – 300.

[82] H. Yanikomeroglu and E. Sousa, "CDMA distributed antenna system for indoor wireless communications," in *Universal Personal Communications, 1993. 'Personal Communications: Gateway to the 21st Century', 2nd International Conference on*, vol. 2, no. 2, 12-15 Oct. 1993, pp. 990–994.

[83] ——, "CDMA sectorized distributed antenna system," in *Spread Spectrum Techniques and Applications, 1998. Proceedings., 1998 IEEE 5th International Symposium on*, vol. 3, 2-4, Sept 1998, pp. 792–797.

[84] ——, "SIR-balanced macro power control for the reverse link of CDMA sectorized distributed antenna system," in *Personal, Indoor and Mobile Radio Communications, 1998. The Ninth IEEE International Symposium on*, vol. 2, 8-11, Sept 1998, pp. 915–920.

[85] Y. Zhang, "Indoor radiated-mode leaky feeder propagation at 2.0 ghz," *Vehicular Technology, IEEE Transactions on*, vol. 50, no. 2, pp. 536–545, March 2001.

[86] S. Zhou, M. Zhao, X. Xu, J. Wang, and Y. Yao, "Distributed wireless communication system: a new architecture for future public wireless access," *Communications Magazine, IEEE*, vol. 41, no. 3, pp. 108 – 113, March 2003.

[87] S. Zürbes, W. Papen, and W. Schmidt, "A new architecture for mobile radio with macroscopic diversity and overlapping cells," in *Personal, Indoor and Mobile Radio Communications, 1994. Wireless Networks - Catching the Mobile Future. 5th IEEE International Symposium on*, vol. 2, 18-23 Sept. 1994, pp. 640 – 644.

Publications

1. **Tong F.; Glover I.A.; Pennock S.R. and Shepherd P.R.**, "distributed antenna diversity", *URSI national symposium*, Leeds UK, July 2003.

2. **Tong F.; Glover I.A.; Pennock S.R.; Shepherd P.R.; Whinnett N. and Aftelak S.**, "Outage probability comparison of distributed antenna diversity and single site antenna diversity", *High frequency postgraduate student colloquium*, Belfast UK, September 2003.

3. **Tong F.; Glover I.A.; Pennock S.R. and Shepherd P.R.**, "Distributed antenna study (on inter-cell interference)", *URSI national symposium*, Bath UK, July 2004.

4. **Tong F.; Glover I.A.; Pennock S.R. and Shepherd P.R.**, "Uplink performance of the distributed antenna diversity", *International Symposium on antennas and propagation*, Seidai Japn, August 2004.

5. **Tong F.; Glover I.A.; Pennock S.R. and Shepherd P.R.**, "Inter-cell interference using distributed antenna", *European Wireless technologies Conference*, Amsterdam Netherland, October 2004.

6. **Tong F.; Glover I.A.; Pennock S.R. and Shepherd P.R.**, "Optimal transmission scheme for a distributed antenna in CDMA system", *5th IEE International conference on 3G Mobile Communication Technologies*, London UK, October 2004.

7. **Tong F.; Glover I.A.; Pennock S.R.; Shepherd P.R. and Davies N.C.**, "Indoor distributed antenna experiment", *14th IST Mobile and Wireless Communications Summit*, Dresden Germany, June 2005.

8. **Tong F.; Glover I.A.; Pennock S.R. and Shepherd P.R.**, "Co-phase transmission diversity for distributed antenna", *IEEE International Symposium on Antennas and Propagation and USNC/URSI National Radio Science Meeting*, Washington US, July 2005.